# GROWTH FACTORS DIRECT MESENCHYMAL STEM CELL FATE AND THERAPEUTIC POTENTIAL

**By**

**Dr Diarmaid Dominic Houlihan**

**MBChB MRCP BSc**

**A thesis submitted to the University of Birmingham for the degree of DOCTOR OF PHILOSOPHY**

**NIHR Centre for Liver Research**

**School of Immunity and Infection**

**University of Birmingham**

**August 2013**

## ABSTRACT

Murine mesenchymal stem cells (MSCs) isolated by plastic adherence contain contaminating cells and have poor growth and differentiation. I report a detailed protocol outlining the steps to prospectively isolate a pure and potent MSC population from murine bone marrow based on their expression of stem cell antigen-1 (Sca-1) and platelet derived growth factor- alpha (PDGFRα) (PαS cells) using flow cytometry. PαS MSCs have augmented growth potential and robust tri-lineage differentiation compared to plastic adherent cells. They exert potent immunosuppressive effects on proliferating naive $CD4^+$ T cells, which is mediated via the production of nitric oxide (NO). Nevertheless, prolonged culture results in cellular senescence, loss of adipogenic differentiation and reduced immunosuppressive properties. Addition of growth factors to standard media (SM) produced significant genotypic and phenotypic changes. Cells cultured in SM supplemented with basic fibroblast growth factor (bFGF) and platelet derived growth factor-BB (PDGF-BB) were primed towards fat and cartilage, but had reduced immunosuppressive potential. In contrast, cells cultured with transforming growth factor-beta (TGF-β) had reduced tri-lineage potential but potent immunosuppressive properties that endured despite long term culture. I demonstrate using novel tissue engineering techniques that bFGF PαS MSCs generate substantial 3-D cartilage pellets. These data have implications for MSC therapy in humans.

# DEDICATIONS

This thesis is dedicated to my wife Amanda, my daughters Eabha May and Annie Rose, and to my parents, Donnie and Pauline, who believed in me and supported me throughout my PhD and in my career.

# ACKNOWLEDGEMENTS

I would like to thank my supervisors Dr Philip Newsome and Professor Jon Frampton for their help and guidance. I would like particularly like to thank Shankar Suresh who has worked with me over the past 3 years. He has been an outstanding colleague and friend at all times.

I have made friends for life since moving to Birmingham and would like to thank 'Prof' (Ian Rowe), 'Parks' (Richard Parker), 'Doc' (Lorenzo Hopkins), 'Le King' (Andy King), 'The Rubbler' (Barney Stephenson), Chris ('The Aristocrat') Corbett for the crack and intellectual discussions over the years. A special thanks to Matt and Caroline Armstrong for being tremendous friends, a constant source of wisdom and for putting up with me and feeding me during the last 3 weeks of the write up. I don't know how you did it!

I would also like to thank other members of the Liver Research group including Stuart Curbishley and all the technicians (Gene, Gill, Nene and Harriet).

The studies presented were done in close collaboration with the following people: Mary Strachan, Sara Dyer, Mike Griffiths (West Midlands Regional Genetics laboratory), Shang Zhang, Anthony Hollander (University of Bristol), Yo Mabuchi, Prof Yumi Matsuzaki (Tokyo Medical University), Kesley Attridge, Lucy Walker (University College London).

This work was funded by a Clinical Research Training Fellowship from the Medical Research Council. Additional funding was competitively awarded from the Medical Research Council Centenary Fund.

## **ABBREVIATIONS** *(in alphabetical order)*

| | |
|---|---|
| APC | Antigen presenting cells |
| bFGF | Basic fibroblast growth factor |
| BM | Bone marrow |
| BMP | Bone morphogenetic protein |
| CFU-F | Colony-forming unit-fibroblasts |
| DC | Dendritic cells |
| DMB | Dimethyl-methylene blue |
| FRC | Fibroblastic reticular cells |
| HSC | Haematopoietic stem cell |
| HCELL | E-selectin/L-selectin ligand |
| ECM | Extracellular matrix |
| GAG | Glycosaminoglycan |
| GVHD | Graft-versus-host-disease |
| GF | Growth factor |
| HSC | Haematopoietic stem cell |
| HSEC | Hepatic sinusoidal endothelial cells |
| hMSC | Human mesenchymal stem cell |
| IDO | Indolamine 2,3-dioxygenase |
| LNGFR | low affinity nerve growth factor receptor |
| MMP | matrix metalloproteinases |
| MSC | Mesenchymal stem cell |
| mMSC | Murine mesenchymal stem cell |
| NO | Nitric oxide |
| OA | Osteoarthritis |
| OI | Osteogenesis Imperfecta |
| PPARγ | Peroxisome proliferator-activated receptor gamma |
| PDGF | Platelet derived growth factor |
| PGA | Polyglycolic acid |
| PGE2 | Prostaglandin E2 |
| PαS | $PDGFR\alpha^{+}Sca\text{-}1^{+}$ |
| Sca-1 | Stem cell antigen-1 |
| Scf | Stem cell factor |
| SM | Standard media |
| T reg | Regulatory T cells |
| Th | T helper |
| TLR | Toll-like receptor |
| TGF-β | Transforming growth factor-beta |

# BIBLIOGRAPHY

## LIST OF FIGURES

# 1 Introduction

## 1.1 Background

### 1.1.1 Historical perspective

Friedenstein was first to suggest the presence of a population of multipotent stromal cells that reside within the bone marrow (BM) (Friedenstein et al., 1974). These cells are readily characterised by their adherence to plastic, spindle shaped morphology and the ability to generate colonies termed colony-forming unit-fibroblasts (CFU-Fs) when plated as single cells *in vitro* (Friedenstein et al., 1970). He subsequently demonstrated these cells could be readily differentiated into bone *in vitro*. Caplan's early work using chick limb bud mesodermal cells helped support the concept of a BM derived stromal progenitor. He observed that plating these cells at different concentrations *in vitro* affected the fate of the cell (down chondrogenic or osteogenic pathways) (Osdoby and Caplan, 1979). He hypothesised that these cells were multipotent mesenchymal precursors and that their fate was determined by the physiological or pathological conditions imposed upon them. Additional experiments in which bone and cartilage formed on a biological matrix following subcutaneous transplantation in rodents further supported this concept (Sampath and Reddi, 1981, Caplan, 1991). These data suggest the presence of circulating multipotent progenitor stromal cells that originate from a stem niche within the BM.

Caplan later proposed the term mesenchymal stem cell (MSC) to describe these cells and hypothesised 'the mesengenic process' to explain the stromal hierarchy which is highlighted in Figure 1-1 (Caplan, 1994). Additional plasticity of MSCs has been suggested with the demonstration of *in vitro* differentiation to muscle, liver and nervous tissues under defined conditions (Petersen et al., 1999, Pittenger et al., 1999). These data have led some to propose a widespread role for MSCs in the maintenance and repair of a variety of organs during injury and the aging process. There has been intense research interest in MSCs as a putative cellular therapy for tissue regeneration over the past decade.

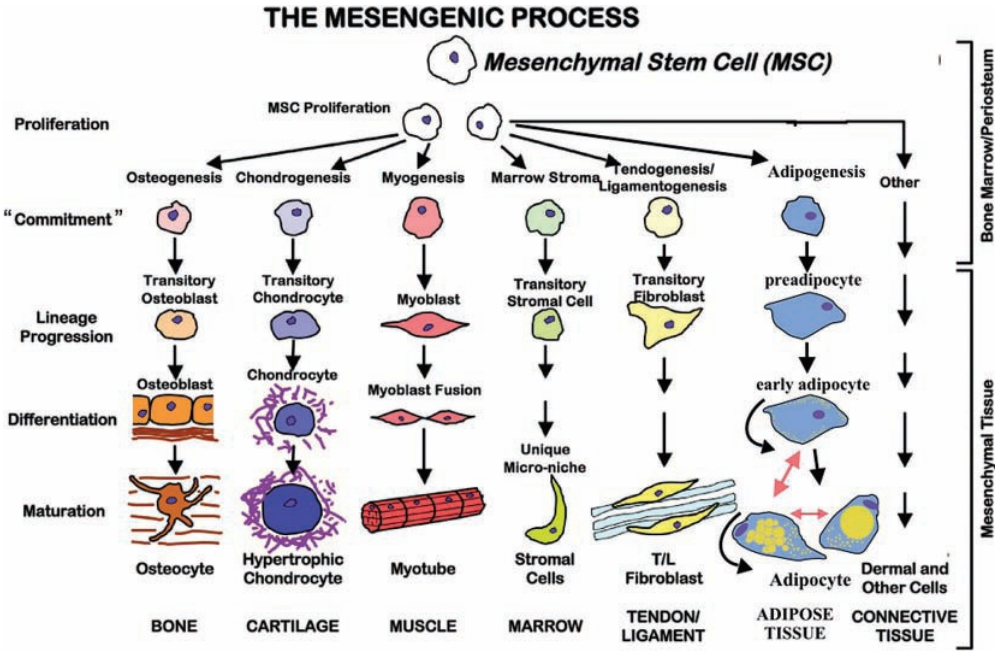


**Figure 1-1 The mesengenic process.**

*This schematic was originally proposed by Caplan and it hypothesises that multipotent MSCs have the ability to self-renew and differentiate down all the mesenchymal lineage pathways depending on the physiological needs of the organism (Caplan, 1994). There are however only limited data available to support the existence of such a cell.*

### 1.1.2 Minimal criteria that define MSCs?

Traditionally, MSCs appear as spindle shaped cells that form CFU-Fs when whole BM is cultured on plastic. The multi-lineage potential of these colonies is examined after a period of culture in defined media that induces cell differentiation to fat, bone and cartilage. Historically, MSCs have therefore been defined by their properties in culture. Although MSCs cultured *in vitro* are probably a heterogeneous population, there is a consensus that they do not express haematopoietic markers. The Tissue Stem Cell Committee of the International Society for Cellular Therapy has proposed minimum criteria that define the human MSCs (hMSCs) (Dominici et al., 2006). The cell must be plastic adherent when cultured under standard conditions and express CD73, CD90 and CD105, without expression of CD45, CD34, CD14 or CD11b, CD79 or CD19 and HLA-DR surface markers. MSCs must also be capable of differentiating into osteoblasts, adipocytes and chondrocytes *in vitro* (Figure 1-2). While this statement clarified somewhat the cellular characteristics of hMSCs, the situation remains unclear for murine MSCs (mMSCs). Until recently specific surface markers for mMSCs have been lacking. Thus mMSCs are still defined by plastic adherence, spindle shaped morphology, and tri-lineage differentiation.

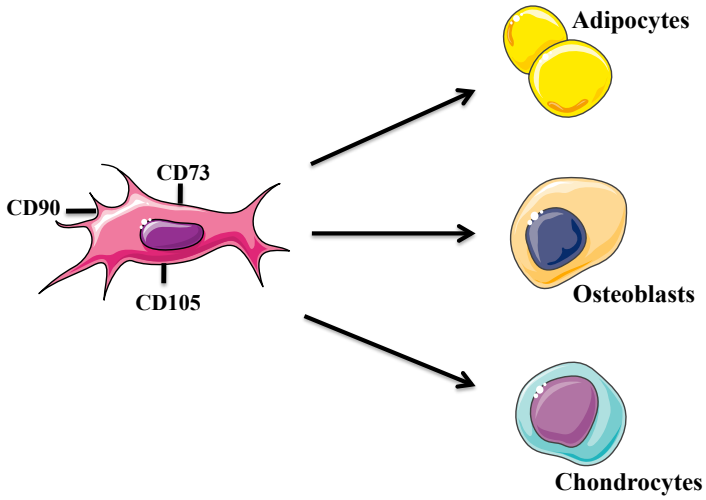


**Figure 1-2 MSCs are characterised by surface marker expression and tri-lineage differentiation**

*hMSC are defined by their spindle morphology when cultured on plastic. They typically express surface markers including CD73, CD90 and CD105 and do not express haematopoietic markers. Additional they must differentiate to fat, bone and cartilage in vitro.*

## 1.2 Tri-lineage differentiation under the microscope

### 1.2.1 Embryological origin of adult MSCs

To understand the genetic regulation and molecular signalling involved in tri-lineage differentiation it is necessary to briefly review some of the early stages in embryological development. Gastrulation occurs during early embryonic development (week 3) and results in the formation of the 3 germ layers known as endoderm, mesoderm and ectoderm. Organogenesis occurs within the germ layers facilitating foetal growth. The mesoderm gives rise to muscle, cartilage, bone, fat, blood vessels and connective tissue. The formation of mesoderm begins with the migration of a

layer of cells between the primitive ectoderm and endoderm. This layer spreads along the anteroposterior and dorsoventral axes of the developing embryo to give rise to the axial, intermediate, lateral plate and paraxial mesoderm. The paraxial mesoderm segments into somites and generates the axial skeleton and muscles of the trunk (discussed in more detail below). The lateral plate mesoderm generates the skeleton and muscles of the limbs. The bones of the skull and face are ectodermal (neural crest) in origin. Caplan's unique hypothesis suggests that each mesoderm-derived organ possesses adult 'MSCs' capable of regenerating and replacing cells during life.

### 1.2.2 Adult cartilage progenitors

Chondrogenesis describes the differentiation of embryonic mesenchyme to cartilage intermediate (Goldring et al., 2006). It is the earliest phase of skeletal development. The first phase of the process involves the recruitment of mesenchymal cells from neural crest (craniofacial development), paraxial mesoderm or somites (axial skeleton) and lateral plate mesoderm (limbs) (Olsen et al., 2000). Following their migration, the mesenchymal cells undergo a process of proliferation and condensation to form chondroprogenitor cells. This process requires defined interactions with overlying ectoderm and is controlled by a variety of differentiation factors and transcription factors highlighted in Figure 1-3. Specific genes involved in early patterning include the homeobox transcription factors encoded by HoxA and HoxD. These factors are required for expression of fibroblast growth factor-8 (FGF-8) and Sonic Hedgehog (Kmita et al., 2005). Hoxd11 and Hoxd13 regulate the proliferation and condensation phase of chondrogenesis while expression of sonic hedgehog is maintained throughout (Tickle, 2003). Sonic hedgehog signalling occurs via its

receptor Patched and the trans-membrane protein Smoothened. The downstream targets of this signalling cascade are Gli3 and Plzf, that act in concert to establish correct spatial and temporal distribution of chondrocytes progenitors within the developing limb (Barna et al., 2005). Bone morphogenetic protein (BMP) receptor, type 1B is required to facilitate such signalling. BMP-2, -4, and -7 signalling regulates patterning of limb elements.

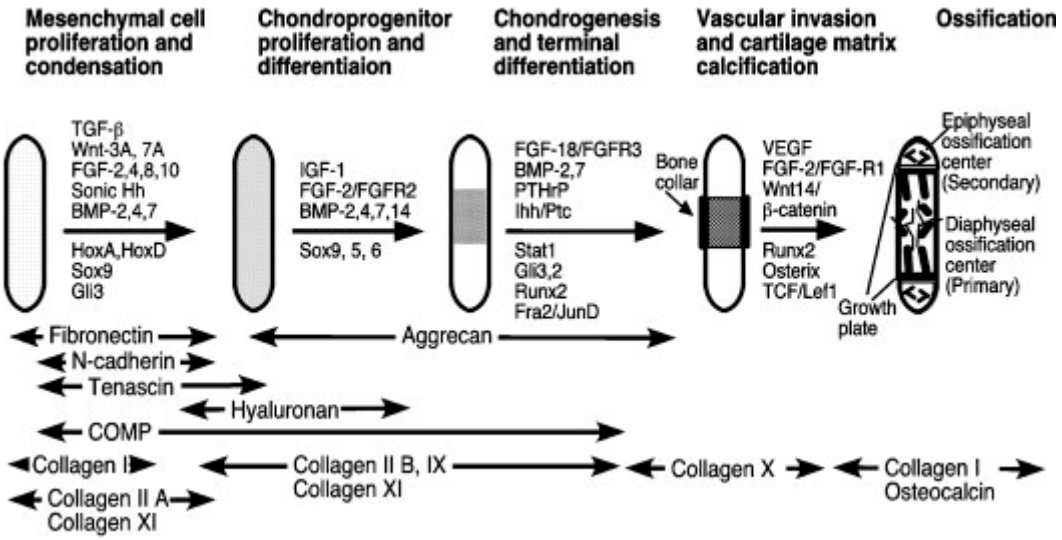


**Figure 1-3 The sequence of events in chondrogenesis during the development of long bones.**

*This figure depicts the sequence of events involved in embryonic chondrogenesis. External cellular stimuli that influence differentiation (above arrows) and important patterning genes (below arrow) are shown. Extra-cellular matrix also exerts a marked effect on chondrogenesis at various time points (Goldring et al., 2006).*

Chondrocyte differentiation from progenitors requires deposition of cartilage matrix collagens including collagen II, IX, and XI and aggrecan. Sox-9 expression is required to promote genes encoding cartilage-specific matrix proteins including

Col2a1, Col11a2 and CD-RAP (Ng et al., 1997). Sox 6 and L-Sox 5 are expressed during chondrocytes differentiation and facilitate expression of Col9a1, aggrecan and Col2a1 (Lefebvre et al., 2001, Lefebvre et al., 1998). The expression of SOX protein depends on BMP signalling via BMPR1A and BMPR1B as described earlier (Yoon et al., 2005). BMP receptor signalling is mediated via the canonical SMAD pathway and involves Smads 1, 5 and 8 and inhibitory Smads 6 and 7 (Wan and Cao, 2005). Activated Smads, complex with Smad 4, translocate to the nucleus and modulate the promoter sites of target genes (Derynck and Zhang, 2003). An alternative signalling pathway during chondrogenesis occurs via TGF-β-activated kinase 1 which activates p38 and JNK cascades. The p38 pathway contributes to condensation and ERK1/2 activation cross-reacts with BMP-2 induced signalling to promote chondrogenesis (Seghatoleslami et al., 2003). Runx2 is also expressed in cartilage sub-types destined to form bone.

### 1.2.3 Fat progenitors

Lineage tracing studies using PPARγ (a transcription factor essential for fat development) expression was initially used to identify adipocyte precursors (Tang et al., 2008). Isolation by FACS of PPARγ-GFP cells demonstrated high expression of the pre-adipocyte markers Pref1, GATA3, Wisp2, Smo and Gli3 (Tontonoz and Spiegelman, 2008). As a demonstration of their potency, transplantation of PPARγ-GFP cells into nude mice resulted in the formation of ectopic $GFP^+$ fat. These studies have also provided insight into the anatomical localisation of fat progenitors. Fat precursors reside within the vascular wall and express a variety of surface markers

including PDGFRβ, SMA and NG2 (Tang et al., 2008). Fat precursors have recently been isolated prospectively based on their surface marker expression: $Lin^-$ /$CD29^+$/$CD34^+$/$Sca\text{-}1^+$/$CD24^+$. Transplantation of 500,000 $Lin^-$/$CD29^+$/$CD34^+$/$Sca\text{-}1^+$/$CD24^+$ GFP labelled into A-Zip lipodystrophic mice resulted normal $GFP^+$ fat deposits (Rodeheffer et al., 2008). Additional pre-adipocyte markers include pre-adipocyte factor 1 (Pref-1 or DLK-1) (Villena et al., 2002), type VI collagen alpha 2 chain (COL6A2) (Ibrahimi et al., 1993) and the Wnt antagonists FRP2/SFRP2 (Hu et al., 1998).

*1.2.3.1 Transcriptional regulation*

The transcriptional cascade responsible for pre-adipocyte development and differentiation is being unravelled. There are 4 stages described including growth arrest, clonal expansion, early differentiation and terminal differentiation. PPARγ is considered a master regulator of this process and is particularly important for the terminal differentiation of adipocytes (Rosen and MacDougald, 2006). The C/EBP family consists of 5 related proteins (C/EBPα, C/EBPβ, C/EBPδ, C/EBPγ and CHOP). These factors are expressed sequentially during adipocyte differentiation. Additional genes that play a role of patterning and development of visceral adipose tissue include HoxA5, HoxA4, HoxC8, Glypican 4(Gpc4) and Nr2f1. Interestingly subcutaneous fat expresses higher levels of HoxA10, HoxC9, Twist1, Tbx15, Shox2 and Sfpr2 (Gesta et al., 2007). These data might suggest a different origin of visceral and subcutaneous adipose tissue.

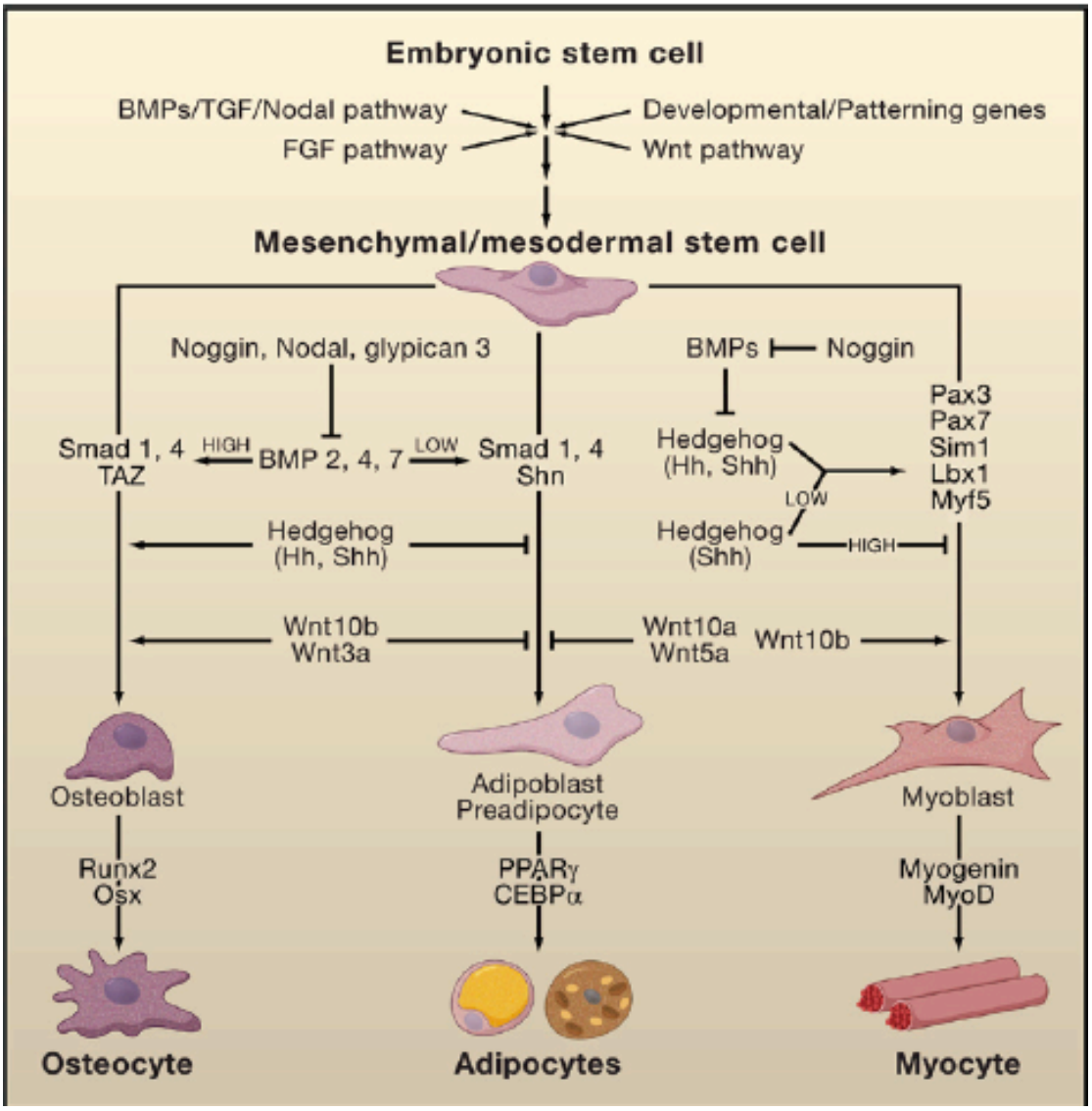


**Figure 1-4 Signalling cascades involved in MSC differentiation to bone, muscle and fat.**

*This cartoon illustrates the different signalling pathways that govern differentiation of MSCs. This figure was adapted from Gesta et al., 2007.*

*1.2.3.2 Signalling during adipose tissue development*

The embryonic patterning and development of fat are controlled by signalling systems involving Nodal, BMP, Wnt and FGFs **(**Figure 1-4**)**. Specifically, BMP-4 has been

shown to stimulate differentiation of MSCs to adipocytes (Tang et al., 2004). Conversely, BMP-2 and BMP-7 promote osteogenic and inhibit adipogenic differentiation (Wang et al., 1993). FGF 1, 10, 16 and 19 have been implicated in adipose development (Gesta et al., 2007). Activation of the Hedgehog pathway by its ligands inhibits adipogenic differentiation of MSCs. Blockade of the Hedgehog using a smoothened receptor antagonist stimulates adipogenesis (Suh et al., 2006). These effects appear to be mediated through intermediate protein signalling GATA-2 and GATA-3, which indirectly results in suppression of the PPARγ promoter region (Tong et al., 2005). Wnt signalling favours osteogenic and myogenic differentiation over adipogenic. Wnt3a pushes MSCs towards osteoblasts whereas blockade of β-catenin promotes adipogenic differentiation (Kennell and MacDougald, 2005, Arango et al., 2005).

### 1.2.4 Bone progenitors

The Runx family is composed of 3 genes Runx1/Cbfa2/Pebp2αB, Runx2/Cbfa1/Pebp2αA, Runx3/Cbfa3/Pebp2αC. Runx2 deletion results in absence of intramembranous and endochondral ossification due to an absence of osteoblasts in mice (Komori et al., 1997). Osterix knockout mice have a complete lack of osteoblasts (Nakashima et al., 2002). Runx2 expression is under the control of Cbfβ and Gata1 (Yoshida et al., 2002). C/EBPβ, C/EBPδ, ETS1, Menin, Smad1 and Smad5 enhance the transcriptional activity of Runx2. Deletions in the Wnt-β-catenin-Lrp5 signalling axis also result in low bone mass, while gain in function experiments result in higher bone mass (Brault et al., 2001, Logan and Nusse, 2004). Indian hedgehog is

crucial for osteoblasts differentiation and double knockout mice lack osteoblasts and endochondral ossification. The signalling events governing MSC differentiation to bone are illustrated below **(**Figure 1-5**)**.

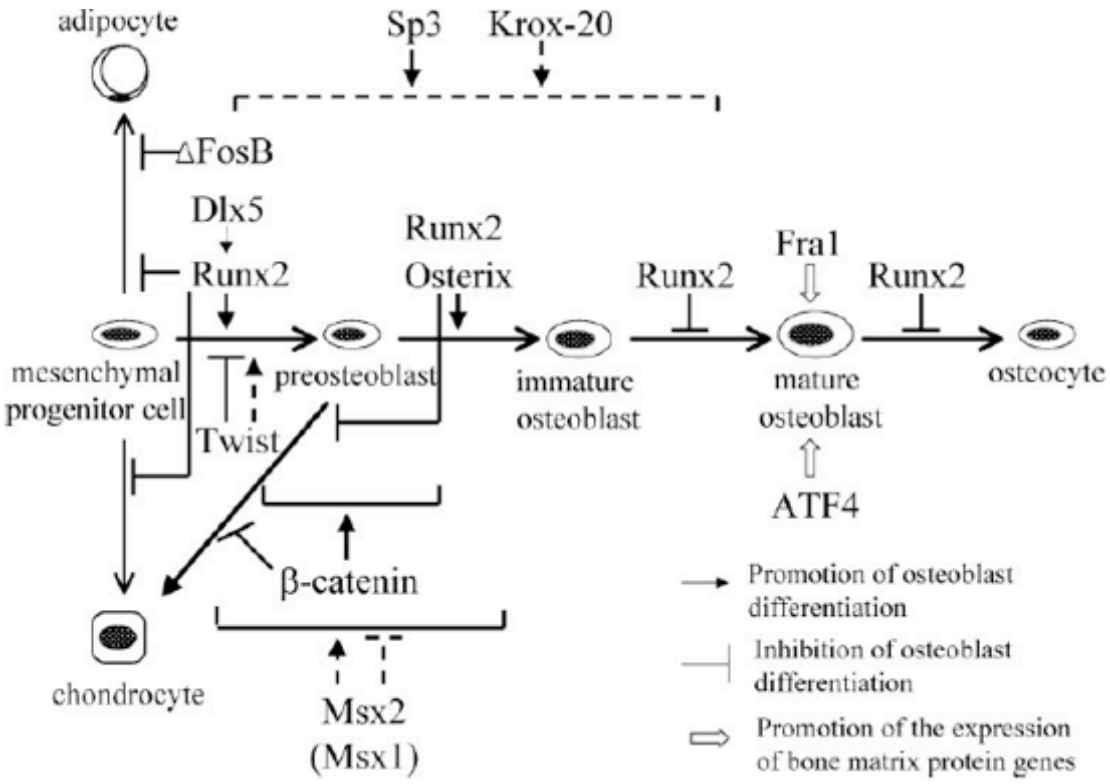


**Figure 1-5 Signalling mechanisms involved in MSC differentiation to bone.**

*This cartoon illustrates the key signalling events that control MSC differentiation to bone. Figure adapted from Komori, 2006.*

Other transcription factors that regulate osteoblasts differentiation include Msx1 and Msx2. Their role is incompletely understood, however $Msx1^{-/-}$ and $Msx2^{-/-}$ mice have severely deficient cranial lobe formation (Satokata et al., 2000). It has been hypothesised that Msx2 promotes osteoblasts maturation (Ishii et al., 2003). Similarly $Dlx5^{-/-}$ and $Dlx6^{-/-}$ mice have abnormal craniofacial bone formation. Interestingly

these genes may also play a role in cartilage development (Robledo et al., 2002). Additional genes that influence osteoblast maturation include Twist-1, Ap1, Krox-20, SP3 and RSK2 (Komori, 2006).

## 1.3 Traditional Isolation of murine MSCs

Various methodologies have been employed to isolate a pure population of potent MSCs. Traditional isolation technique relies on plastic adherence and prolonged culture to exclude contaminating cells. Despite this MSC cultures are frequently contaminated by haematopoietic cells (Pittenger et al., 1999). Prolonged culture on plastic also reduces MSC differentiation and proliferative potential (Wagner et al., 2008). This section describes in more detail MSC isolation methods and attempts to overcome these known limitations.

### 1.3.1 Plastic adherence

Phinney et al. carried out much of the early work isolating MSCs from mice. In an early publication they demonstrated wide variation in the abundance of MSCs obtained from the bone marrow of five commonly used inbred strains of mice (Phinney et al., 1999). Using the traditional CFU-F assay they found that highest and lowest yields were from BALB/c mice ($3 \pm 0.22$ colonies per $10^6$ total cells) and C57Bl/6 mice ($0.3 \pm 0.22$ colonies per $10^6$ total cells) respectively. Culturing cells for 72 hours prior to the removal of non-adherent cells in untreated plastic wells yielded the most favourable growth kinetics. Addition of the growth factors (GFs) bFGF and

Platelet Derived Growth Factor-BB (PDGF-BB) promoted cell growth and inhibited osteogenic differentiation of cells. A major limitation of the isolation was cellular contamination, and using flow cytometry they demonstrate up to 80% of the plastic adherent cells were positive for lymphopoietic markers (CD11b and CD45).

### 1.3.2 Frequent media change

Cellular contamination can be reduced by employing frequent media changes after cell plating (Nadri et al., 2007). In brief, 3-4 hours after plating the BM, non-adherent cells were washed off and fresh media was replaced. This step was repeated every 8 hours for 72 hours. The cells were then washed with phosphate buffer and fresh media was added every 3 - 4 days. When 90% confluent the cells were trypsinised by adding 0.025% trypsin containing 0.02% EDTA for 2 minutes at room temperature. Only the lifted cells at this time were harvested and re-seeded in flasks. This method appeared to be superior to the traditional protocol in which media is changed every 3-4 days and generated 3-fold more CFU-Fs (70±3.4 versus 20±4.2). The authors also report enhanced osteogenic and adipogenic differentiation in cells isolated by frequent media change. The isolated MSCs were stained positively for CD44 and Thy1.2 (CD90) and were negative for haematopoietic markers (Table 1-1).

### 1.3.3 Varying cell density

Cell density also appears to influence purity and potency of MSCs (Eslaminejad et al., 2006). A low-density culture system yielded a more homogeneous population of

fibroblastic looking cells. Some cells from the high-density culture were positive for the haematopoietic and endothelial cell markers CD135, CD34, CD31 and VCAM. Furthermore, cells cultured at lower density also displayed more mineralisation in osteogenic culture when compared to high-density culture cells. Taken together the authors concluded that low-density culture systems yield a purer population of MSC like cells.

### 1.3.4 Magnetic beads

The use of magnetic beads conjugated to CD11b, CD34 and CD45 has been used to remove contaminating cells and obtain a pure population of MSCs (Baddoo et al., 2003). MSCs isolated by this method uniformly expressed CD90, CD29, and CD81 and variable levels of Sca-1, CD44 and CD106. MSCs did not express haematopoietic or endothelial markers. The purified cells also readily differentiated into fat, cartilage and bone *in vitro*. The *in vivo* osteogenic potential of the isolated cells was then assayed by inducing a fracture of the tibia and femur of female mice and infusing 50,000 gender mismatched BrdU labelled cells into the resulting haematoma. 3 weeks post injury the mice were sacrificed and the authors demonstrated new bone formation the infused cells.

Table 1-1 demonstrates the heterogeneity in the published isolation methods and the phenotype of isolated MSCs. There is significant variation in the methodology used to isolate murine MSCs in the listed studies. There is no clear consensus on a panel of surface markers that define these cells. Additionally, many of these papers report cellular contamination of isolated MSC populations. Furthermore, the differentiation

potential and proliferative ability of traditionally isolated MSCs gradually diminishes as the cells mature (Digirolamo et al., 1999). Finally, prolonged culture on plastic changes the surface marker expression of MSCs, making identification of specific makers difficult (Quirici et al., 2002, Boiret et al., 2005). For these reasons, little information exists concerning the *in vivo* identity and biological function of MSCs within the BM niche.

**Table 1-1 Summary of studies describing murine MSC isolation.**

The table highlights the variability in utilised techniques and surface marker expression of isolated cells.

| Paper | Strain | Markers | Technique |
|---|---|---|---|
| Baddoo et al. (Baddoo et al., 2003) | FVB/N + BALB/c | **CD 9,29,44,81**<br>Variable Sca-1, CD44,106 | Immunodepletion with beads<br>FGF2 to augment growth |
| Meirelles LS et al. (Meirelles Lda and Nardi, 2003) | Bl/6 + BALBc | **CD29,44,49e**<br>Moderate Sca-1 | Plastic adherence<br>Multiple passages |
| Jiang et al. (Jiang et al., 2002) | Bl/6 | **CD13, SSEA-1**<br>Weak Sca-1, Flt-1 | Immunodepletion<br>GFs: EGF, PDGF-BB and LIF |
| Nadri et al. (Nadri et al., 2007) | BALB/c | **CD44, 90, Sca-1** | Frequent media changes |
| Peister et al. (Peister et al., 2004) | Bl/6, BALBc, FVB/N, DBA1 | **CD34/Sca-1** | Plastic adherence |

## 1.4 Controversy in the MSC field

### 1.4.1 Are MSCs stem cells?

The term MSC has generated controversy. The classic definition of a stem cell requires that it possess unlimited self-renewal ability and plasticity. Experimentally,

serial transplantation experiments demonstrating that infused stem cells give rise to terminally differentiated daughter tissue cells while maintaining their naive phenotype provide evidence of stemness. Historically such experiments have not been performed with MSCs (Bianco et al., 2008) and many remain sceptical if the title of 'MSC' is a proper and correct term for the cell it now routinely describes.

### 1.4.2 Are MSCs fibroblasts?

The similarities between MSCs and fibroblasts are manifold (Haniffa et al., 2009). To start with fibroblasts and MSCs share surface marker expression including CD73 and CD90. By definition fibroblasts also lack expression of haematopoietic markers CD14, CD34 and CD45 (Ishii et al., 2005). Both fibroblasts and MSCs can be differentiated into bone, cartilage and fat in vitro. The immunosuppressive effects of MSCs are also shared by fibroblasts and many of the underlying mechanisms are similar (including production of soluble factors including prostaglandin E2 (PGE2) and indolamine 2,3-dioxygenase (IDO)) (Lysy et al., 2007). These overlapping features cast doubt on the novelty of much MSC literature and have led some to question their existence.

### 1.4.3 Are cultured MSCs transformed cells?

There are growing concerns that much of the mMSC literature is based on cells that have transformed during prolonged *in vitro* culture. One of the earliest descriptions of this occurred unexpectedly during a series of experiments examining the fate of transfused MSCs (Tolar et al., 2007). Several weeks (between week 12-18) after MSC

(passage 9) infusion the mice started developing tumours. The cancers were donor-cell derived and identified as sarcomas. Further investigation demonstrated that chromosomal atypia readily occurred in cultured mMSCs as early as passage 3 (Zhou et al., 2006). Once again transfusion of these cell resulted in the formation of sarcoma in nude and SCID mice. The exact factors that cause freshly isolated cells to transform in culture are unclear. Several mechanisms including accumulated chromosomal abnormalities, gradual elevation in telomerase activity, and increased c-myc expression have all been hypothesised (Miura et al., 2006). More recently over expression of H19 (a downstream target of c-myc) has been implicated in malignant transformation of murine MSCs (Shoshani et al., 2012). In any case these data have cast a shadow on much of the mMSC field and raised concern about the therapeutic use of hMSCs for clinical indications.

## 1.5 Identification of specific murine MSC markers

### 1.5.1 Defining the need for selective markers

As described previously there are numerous and significant limitations to isolating MSCs by plastic adherence. Exciting progress has recently been made in the identification of specific mMSC and hMSC surface markers allowing their prospective isolation by flow cytometry. Prospective MSC isolation has several advantages compared with the traditional method by plastic adherence (Figure 1-6). Firstly, the isolated population is likely to be more potent as it avoids the prolonged culture period routinely required to select MSC like cells from whole BM. Secondly,

haematopoietic cells can be excluded by using a gating strategy based on lineage markers. Finally, the biology of naive MSCs (unchanged by plastic adherence) can be interrogated immediately following isolation.

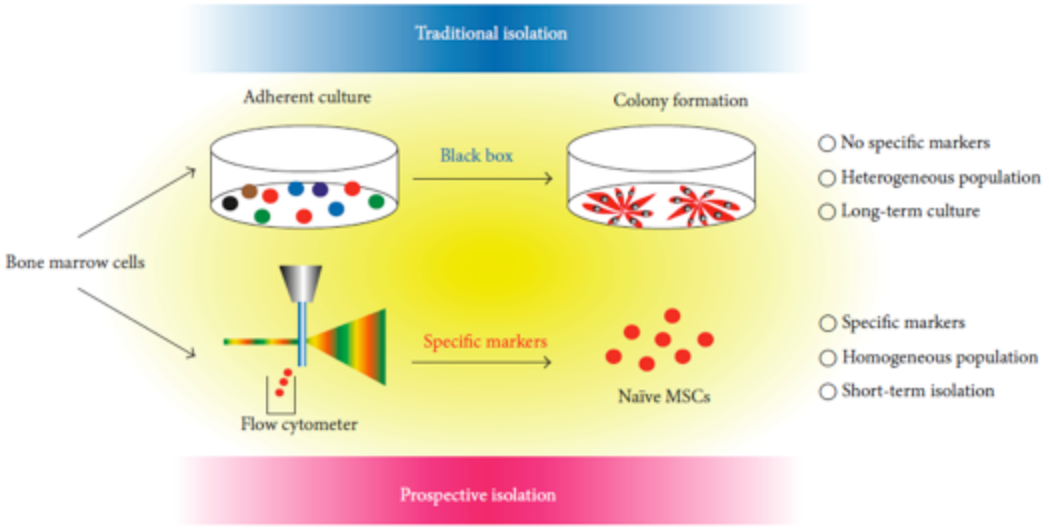


**Figure 1-6 Comparison of prospective and traditional MSC isolation techniques.**

*This figure illustrates the different methods for isolating MSCs from tissue. MSCs isolated by plastic adherence frequently contain contaminating cells. The isolated population are heterogeneous and lack specific surface marker expression. In contrast the prospective isolation of MSCs using defined surface markers over comes these issues and yields a purer population (Mabuchi et al., 2013).*

### 1.5.2 PDGFRα and Sca-1 identify murine MSCs

The identification of specific MSC markers began with the observation that haematopoietic and mesenchymal lineage cells are derived from individual lineage-specific stem cells (Koide et al., 2007). Based on the hypothesis that MSCs most likely resided in the endosteum a detailed screening of candidate surface marked was

performed in BM and collagenase digested bone. The surface markers PDGFRα and Sca-1 were significantly enriched in the digested fraction and dual positive cells were isolated (Houlihan et al., 2012, Morikawa et al., 2009a). PDGFRα$^{+}$Sca-1$^{+}$ (PαS) cells fulfil the basic requirements of the definition of MSCs. They are capable of potent self-renewal and differentiate into osteoblasts, chondrocytes and adipocytes under appropriate conditions *in vitro* (Morikawa et al., 2009a). PαS cells proliferate rapidly when cultured on plastic, yielding more than $10^7$ cells from the original 5000 cells seeded with a doubling time of 50.6 hours. The CFU-F frequency of PαS cells is 120,000-fold higher compared to unfractionated BM mononuclear cells. PαS cells reside in the perivascular space adjacent to vascular smooth muscle. They express Angiopoietin-1 and CXCL12 suggesting that MSCs may play a physiological role in the haematopoietic niche. Transplantation experiments in which $1x10^4$ freshly isolated PαS cells were intravenously injected into lethally irradiated recipient mice demonstrate the stemness of PαS cells. The infused cells homed to their niche in the BM expressing niche factors (Angiopoietin-1 and CXCL12) and also differentiated into osteoblasts and adipocytes in vivo. Sixteen weeks following the transplantation the mice were sacrificed and the isolated PαS cells were capable of forming CFU-Fs and tri-lineage differentiation. The identification of PDGFRα as a selective mMSC marker supports evidence presented in a series of developmental studies demonstrating that a proportion of adult BM MSCs might have a developmental origin in the neural crest (Morikawa et al., 2009b, Takashima et al., 2007).

### 1.5.3 Nestin identifies murine MSCs

More recently the neural marker, Nestin, has successfully been used to identify and prospectively isolate murine MSCs (Mendez-Ferrer et al., 2010). Nestin$^+$ cells represent a small subset of non-haematopoietic stromal cells in BM. These cells are anatomically located in the perivascular space, in close proximity to catecholaminergic nerve fibres and haemopoiteic stem cells (HSCs). In keeping with PαS MSCs, the Nestin$^+$ cells express haematopoietic niche factors and are capable of tri-lineage differentiation *in vitro* and *in vivo*. Nestin$^+$ MSCs also play an important functional role in maintaining the HSC niche. Following depletion of Nestin$^+$ MSCs there is a dramatic reduction in the number and function of HSCs. Additionally, homing of transplanted HSCs back to their BM niche was significantly impaired following irradiation. These data suggest an important role of MSCs in the maintenance of the HSC niche.

These are the first studies to identify specific markers that can be used for prospective isolation and *in vivo* localization of mMSCs. PαS and Nestin$^+$ MSCs have been assayed in the traditional stem cell assays (including serial transplantation assays and clonogenic assays) and their properties of self-renewal and potency confirmed. We have also gained a valuable insight into the importance of these cells in maintaining the HSCs niche. It is not entirely clear if Nestin$^+$ cells are the same as PαS cells. We know that Nestin$^+$ cells largely overlap the PDGFRα$^+$CD51$^+$ population however, this population contains Sca-1 positive and negative cells (Pinho et al., 2013). These data suggest that the Nestin$^+$ population is comprised of PαS and PDGFRα+ cells. Interestingly, investigations using *Nestin-Cherry* and *Nestin-GFP* double transgenic mice demonstrates *Nestin-Cherry* expression around larger vessels but not around sinusoids, while *Nestin-GFP* expression was detected around both (Ding et al., 2012).

Thus, different *Nestin* transgenes seem to be expressed by different subpopulations of perivascular stromal cells. Nonetheless, the identification and prospective isolation of PαS and Nestin$^{+}$ cells will provide an invaluable substrate for on going research into biological function, hierarchical structure and therapeutic potential of MSCs.

## 1.6 Identification of specific hMSCs markers

### 1.6.1 Defining the need for selective markers

Numerous putative hMSCs surface markers including CD49a (Boiret et al., 2005), CD73 (Pittenger et al., 1999), CD105 (Aslan et al., 2006), CD106 (Gronthos et al., 2003), CD271 (Quirici et al., 2002), MSCA-1 (Battula et al., 2009), Stro-1 (Simmons and Torok-Storb, 1991) and SSEA4 (Gang et al., 2007) have been identified. These markers have been used singly or in combination to enrich for CFU-F in human BM and avoid cellular contamination. Unfortunately, many of these markers are widely expressed in stromal cells and lack specificity for MSCs, contributing to the significant heterogeneity seen among clonogenic colonies from single isolations. The lack of specific markers has hindered attempts to uncover the true identity and function of MSCs *in vivo*. Additionally, as in the case of mMSCs the traditional isolation of hMSCs by plastic adherence reduces the differentiation potential and proliferative ability of the CFU-Fs as the cells senesce reducing their therapeutic potential. (Kim et al., 2009). The prospective isolation and culture of such cells (with or without manipulation) may facilitate the development of safer and more effective clinical therapies in the future.

### 1.6.2 CD146 identifies hMSCs in vivo

CD146 has provided valuable insight into the *in vivo* localization and function of hMSCs (Sacchetti et al., 2007). It marks an adventitial reticular cell that resides in the endothelial space in human BM. These cells express typical stromal markers (CD105, CD49a, CD63, CD90, CD140b) and are capable of robust tri-lineage differentiation. Their physiological function was demonstrated by subcutaneous transplantation of $CD146^+$ clonogenic cells on a scaffold into immunodeficient mice. The $CD146^+$ MSCs supported formation of bony ossicles, sinusoidal vasculature and finally established a functioning haematopoietic microenvironment. Immunohistochemical analysis demonstrated a small proportion of the infused cells in the murine HSC niche. These cells expressed supporting factors including Ang-1. The transplanted $CD146^+$ MSCs were re-isolated, cultured and formed CFU-Fs capable of tri-lineage differentiation demonstrating the self-renewal potency of these cells. Traditionally, MSCs were thought to reside only within the BM as the stromal counterpart to HSCs. Interestingly, the utility of CD146 as a prospective marker of hMSCs is not limited to adult BM. Crisan et al. used immunohistochemistry to examine various different tissue types including both adult and foetal human skeletal muscle, pancreas, adipose tissue, and placenta and identified CD146, NG2 and PDGFRα as prospective pericyte markers (Crisan et al., 2008). A pure population of pericytes was prospectively isolated from each tissue type by flow cytometry. These cells were then differentiated into muscle, bone, fat and cartilage using the standard assays used for MSCs. Furthermore, isolated pericytes expressed typical stromal markers including CD73, CD90 and CD105. These data clearly identify CD146 as a specific marker of mesenchymal progenitor cells in a wide range of organs.

### 1.6.3 CD271 identifies hMSCs

CD271 is also known as low affinity nerve growth factor receptor (LNGFR). Isolation of $CD271^+$ MSCs enriches for CFU-F potential and the growth kinetics of this subpopulation greatly exceeds that of plastic adherent cells (Quirici et al., 2002). Additionally the growth and differentiation potential $CD271^+$ cells exceeded that of isolated populations expressing CD146, CD106 and CD166 respectively (Jones and McGonagle, 2008). The therapeutic potency of this cell population has also been confirmed. $CD271^+$ MSCs are more efficient at inhibiting the proliferation of allogeneic T- lymphocytes in mixed lymphocyte reaction assays compared to cells isolated by plastic adherence. Furthermore, in an interesting assay of therapeutic function $CD271^+$ MSCs greatly augmented $CD133^+$ haematopoietic engraftment following sub-lethal irradiation (Kuci et al., 2010). A recent study demonstrated that CFU-Fs were highly enriched in both $lin^-/CD271^+/CD146^+$ and $lin^-/CD271^+/CD146^{low}$ stem cell fractions. The authors demonstrate that CD146 is up regulated in normoxia and down regulated in hypoxia. This information is of physiological significance with $CD146/CD271^+$ reticular cells located in the perivascular space whereas $CD271^+$ MSCs were located adjacent to bone. Interestingly, in both locations the MSCs were flanked by $CD34^+$ haemopoiteic progenitor stem cells (Tormin et al., 2011).

## 1.7 Physiological role of MSCs

### 1.7.1 Hypothesised role of MSCs

The physiological role proposed for MSCs are manifold. The best characterised includes the provision of a suitable microenvironment for haematopoiesis (Friedenstein et al., 1974, Calvi et al., 2003). Following transplantation into NOD-SCID, hMSCs differentiate into pericytes, myofibroblasts, marrow stromal cells, osteocytes, osteoblasts and endothelial cells, all of which are necessary for functional haematopoiesis to occur (Muguruma et al., 2006). MSCs also play an important role in wound healing and provide a constant source of osteogenic and chondrogenic precursors for bone development and growth (Caplan, 1991). There is accumulating evidence that MSCs exert a profound regulatory effect on our immune system (Uccelli et al., 2008). This property has obvious potential for the treatment of a variety of autoimmune and inflammatory diseases.

### 1.7.2 MSCs support haematopoiesis

The HSC niche provides a specialised microenvironment that promotes stem cell maintenance and function. Several cell types including osteoblasts, endothelial cells, and adventitial reticular cells to the niche function are thought to maintain it (Wilson and Trumpp, 2006). A contribution of MSCs to niche function has been proposed, however until recently this has remained unproven. The observation by Morikawa et al. that PαS cells reside in the HSC niche (perivascular space adjacent to HSCs), and express niche factors (Angiopoietin-1 and CXCL12) supports this hypothesis (Morikawa et al., 2009a). Indeed, Nestin$^{+}$ MSCs appear to play a critical role not only the maintenance of HSCs within the niche, but also the homing of transplanted HSCs back to the BM. Interestingly, a significant proportion of perivascular PDGFRα$^{+}$ cells

express Nestin and the exact contribution of each subpopulation to the niche is not entirely clear. Recent data suggest that non-myelinating Schwann cells play an important role in maintaining the HSC niche via modulation of TGF-β (Yamazaki et al., 2011). Interestingly these cells are Nestin$^{+}$ generating some controversy in the field. Recently, Morrison et al. confirmed the importance of perivascular cells in maintaining the HSC niche through production of stem cell factor (Ding et al., 2012). In summary, HSC frequency and function were not affected when stem cell factor was conditionally deleted from hematopoietic cells, osteoblasts, Nestin$^{+}$ cells. However, HSCs were depleted from BM when stem cell factor was deleted from endothelial cells or leptin receptor expressing perivascular stromal cells (also positive for PDGFRα, PDGFRβ, CXCL12 and alkaline phosphatase expression). Clearly much remains unknown in this complex microenvironment, however the data suggest that one or more MSCs subtypes contribute to HSC niche homeostasis.

## 1.8 Therapeutic potential of MSCs

### 1.8.1 MSCs hold significant therapeutic promise

MSCs are defined as non-haematopoietic, plastic adherent self-renewing cells that are capable of *in vitro* tri-lineage differentiation to fat, bone and cartilage (Pittenger et al., 1999). Additional plasticity of MSCs has been suggested by experiments demonstrating their *in vitro* differentiation to myocytes, neuron-like cells and hepatocytes (Drost et al., 2009, Galvin and Jones, 2002, Tao et al., 2009). These multipotent cells are found in various foetal and adult human tissues, including BM,

umbilical cord blood, liver and term placenta (Battula et al., 2007, Erices et al., 2000, Yen et al., 2005, Zvaifler et al., 2000). MSCs are multipotent and have low immunogenicity, and therefore, are considered as potential candidates for a variety of clinical applications (Jung et al., 2012c, Stappenbeck and Miyoshi, 2009). There are currently 276 studies registered on 'ClinicalTrials.gov' investigating MSCs in a variety of different diseases. Examples of such trials include cartilage reconstitution and the treatment of rheumatoid arthritis, acute osteochondral fractures, spinal disk injuries, and inherited diseases such as osteogenesis imperfecta (OI) (Guillot et al., 2008).

### 1.8.2 Regenerative therapy

#### *1.8.2.1 Cartilage*

An amazing demonstration of the regenerative potential of hMSCs was published as a case report in the Lancet in 2008 (Macchiarini et al., 2008). Claudia (30 years of age) suffered from pulmonary TB and following it's eradication developed stricturing tracheitis. Over time the stricturing of her left main bronchus progressed such that she developed significant hypoxia from under ventilation of her left lung. Repeated interventions including surgical resection and stenting made little difference. In 2008, a decision to carry out a cadaveric tracheal transplant was made. In brief, the trachea from a matched donor was decellularised. Epithelial cells and MSCs were then isolated from the patient's endobronchial and BM biopsies respectively. The expanded epithelial cells were then painted onto the inner surface of the decellularised

graft, while chondrocytes derived from BM MSCs were coated on the outer surface. Transplantation of the graft produced dramatic improvements in Claudia's respiratory function. 3 months following the procedure the graft had developed it's own blood supple from vascular co-laterals. Over the past 5 years Claudia has had set backs with recurrent graft stenosis. This has been treated successfully with stents and she continues to live a normal life following her transplant.

*1.8.2.2 Bone Regeneration*

OI is a rare inherited condition of bone metabolism (Sillence et al., 1979). Affected patients develop profound osteopenia, short stature and have recurrent non-traumatic fractures. Bone biopsy reveals a marked paucity of osteoblasts accompanied by a lack of collagen type 1 and structural protein. There is no proven effective treatment for this condition (Glorieux et al., 1998). In 1999, a pioneering study was carried out in which 3 children with OI received matched BM transplants as treatment for their condition. Serial biopsies over the first year following therapy demonstrated greatly increased numbers of donor osteoblasts (4 fold increase compared to the pre-treatment biopsy). In addition the bone was of superior quality with increased mineralisation (range 45 - 77% increase). 2 of the treated children had an 80 – 90% reduction in their fracture rates and this was accompanied by increased growth (Figure1-7).

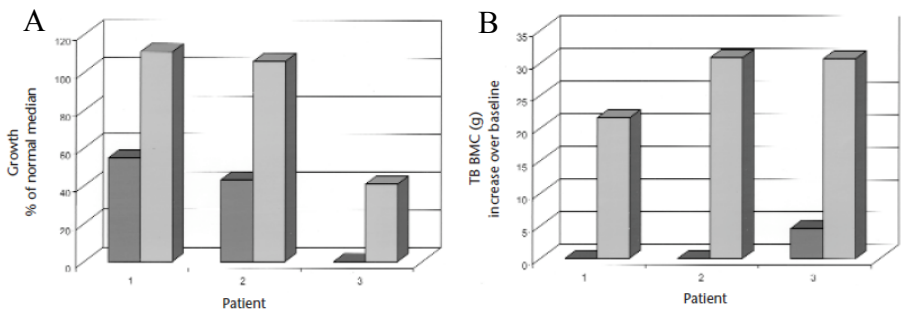


**Figure 1-7 Growth and bone mineral content in each patient before and after therapy is shown.**

*This figure illustrates the growth rates and bone mineral content of 3 patients with OI before and after BM transplantation. Growth was measured over a 6-month period before and after treatment. Bone mineral content was estimated 100 days following BM transplant. The figure illustrates the striking gains in bone quality and growth resulting from the treatment (Horwitz et al., 2001).*

These data provide compelling evidence that MSCs within the donor transplant migrate back to their niche in the BM and differentiate to functional osteoblasts reversing the genetic phenotype of OI. Prolonged follow up (> 2 years) demonstrated that although growth of the children slowed, bone mineralisation continued to increase (Horwitz et al., 2001).

## 1.9 Strategies to optimise the regenerative potential of MSCs

Despite the large number of trials on going worldwide there are several unanswered questions surrounding the use of MSCs in humans including:

1. What is the best MSC isolation method?

2. Do culture conditions including the addition of GFs influence regenerative or immunosuppressive potential?

3. Does the culture flask material impact on MSC therapeutic potential?

This section of the thesis sets about reviewing the literature to address as far as possible these pressing questions.

### 1.9.1 What is the best MSC isolation method?

I have discussed previously recent advances in both mMSC and hMSC isolation methods. A large number of selective markers for the isolation of hMSCs have been proposed. Of these CD146, CD271, Stro-1, VCAM-1, MSCA-1 used alone or in combination appear to be the most selective for hMSC isolation. For example Stro-$1^{+}$VCAM-$1^{+}$ cells are 5000 fold enriched for CFU-F compared to whole BM (Gronthos et al., 2003). Using serial dilution 1 in every 3 Stro-$1^{+}$VCAM-$1^{+}$ cells yield viable colonies. Differing combinations of MSCA-1, CD271, and CD56 have also been used to isolate a pure potent MSC population (Battula et al., 2009). MSCA-1 largely overlaps CD271 bright cells and the CD$271^{+}$/CD$56^{+}$ fraction produces approximately 38 colonies per 500 seeded cells. CD271 has also been used in combination with CD146 and CD$271^{+}$/CD$146^{+}$ cells produce approximately 4 colonies per 100 seeded cells (Tormin et al., 2011). In addition, MSCs selected using these marker combinations have enhanced tri-lineage differentiation compared to conventional MSCs.

A recent publication reports an improved prospective clonal isolation technique. The

combination of three cell surface markers, LNGFR, Thy-1 and VCAM-1, selects highly enriched clonogenic MSCs (one out of three isolated cells) (Mabuchi et al., 2013; In Press). $CD271^{+}/CD90^{+}$ MSCs have higher CFU- F potential compared to $CD271^{+}/CD140^{+}$ and $CD271^{+}/CD146^{+}$ populations. Transplanted $CD271^{+}/CD90^{+}$ MSCs engraft the BM of recipient mice and are capable of tri-lineage differentiation *in vitro* following re-isolation 3 months after infusion. The clonal characterization of $LNGFR^{+}/Thy\text{-}1^{+}$ cells demonstrated significant cellular heterogeneity between the clones. Colonies were designated slowly-, moderately- or rapidly- expanding clones (SECs, MECs and RECs respectively) based of their growth following single cell sorting. RECs exhibited robust multi-lineage differentiation and self-renewal potency, while the others tended to acquire cellular senescence via p16INK4a and exhibited frequent genomic errors. Furthermore, RECs exhibited unique expression of VCAM-1 and higher cellular motility compared to other clones. Collectively, the marker combination $LNGFR^{+}/Thy\text{-}1^{+}/Vcam\text{-}1^{high+}$ (LTVhi) identifies RECs and can be used prospectively to isolate the most potent and genetically stable MSCs described to date.

There is no clear consensus on which MSCs should be used for clinical therapy. Intuitively, a potent population of MSCs that can be easily expanded *in vitro* would suit best for regenerative therapy. For inflammatory disease, the choice is less clear. While bone and cartilage are considered to be immune-privileged sites, fat is a pro-inflammatory tissue. As MSCs have the potential to differentiate down all 3 lineages to seems plausible that osteogenic or chondrogenic primed MSCs may be more immunosuppressive than fat primed or naive MSCs. To my knowledge this

hypothesis has not been tested. Nonetheless, if this is the case, defining conditions that lineage restrict or prime the most potent population of MSCs down required lineages is appropriate.

### 1.9.2 Ex-vivo MSC expansion

#### *1.9.2.1 Growth factors*

Despite the large number of trials on going worldwide there is little or no consensus on how clinical grade MSCs should be isolated or cultured. Ex-vivo expansion (prior to infusion) induces cellular senescence and reduced MSC plasticity (Wagner et al., 2008). Supplementing culture media with GFs is now common to avoid these complications. There are currently 3 commercially available media for the expansion of MSCs including Mesencult-XF (STEMCELL Technologies), StemPro MSC SFM Zeno-Free (Invitrogen) and MSCGM-CD (Lonza). Many of these formulations are supplemented with GFs (FGF, PDGF-BB and TGF-β) and are optimised for the expansion of MSCs and multi-lineage differentiation potential. For example one media, PPRF-msc6, is supplemented with all 3 GFs (Jung et al., 2012a, Jung et al., 2010). There are however little data examining the impact of GF supplemented media on the regenerative and immunosuppressive potential of MSCs. Analysis of the pathways involved in tri-lineage differentiation of MSCs reveals an important role for PDGF, FGF and TGF-β signalling pathways (Ng et al., 2008). Specifically, PDGF signalling was active during adipogenesis and chondrogenesis, TGF-β signalling was active during chondrogenesis, and FGF signalling was active during osteogenesis,

adipogenesis and chondrogenesis. Inhibition of any of the three pathways resulted in an altered differentiation potential and increased population doubling times. These data suggest that many of the commercial MSC media most likely lineage prime or restrict immature MSCs potentially altering their therapeutic potential. Further data are necessary to clarify these complex issues.

*1.9.2.2 Matrix stiffness*

The direct effects of matrix stiffness on MSC differentiation is interesting. In an elegant investigation, Engler et al. utilised a gel system, where controlled cross-linking reactions, predicted the elastic modulus (or stiffness) of the gel (Engler et al., 2006). hMSCs plated on gels of increasing stiffness (1, 11, 34 kPa respectively) were morphologically different and expressed gene patterns in keeping with neuronal, myogenic and osteogenic differentiation respectively. Additionally, following 1 week of culture on soft, moderate and stiff matrix, MSCs expressed key tissue proteins involved in neuronal (P-NFH), muscle (Myo-D) and bone (CBFα1) **(**Figure 1-8**)**.

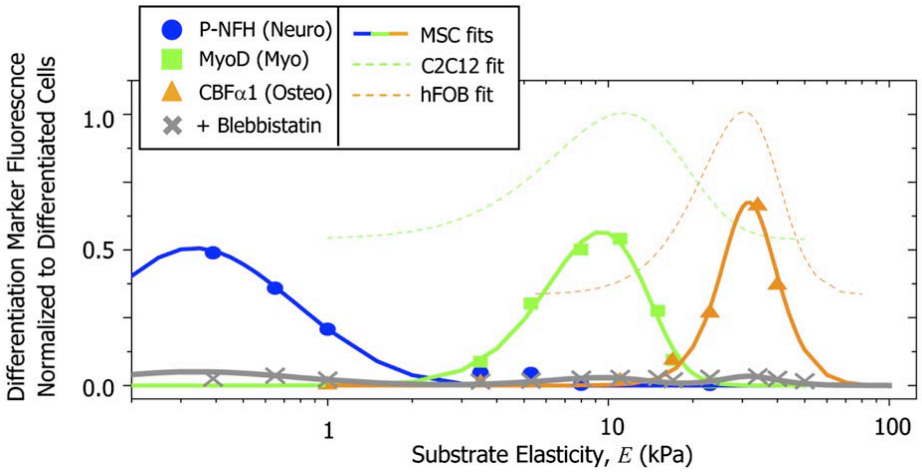


**Figure 1-8 Elasticity-directed protein expression in MSCs cultured on variable stiffness substrates.**

*hMSCs were cultured on substrates with variable stiffness. Cells cultured on the stiff, intermediate and soft matrix expressed osteogenic (CBFα1), myogenic (MyoD) and neurogenic (P-NFH) differentiation markers respectively. The values are normalised using expression of the relevant markers in primary myoblast, osteoblast and neuronal cell lines (Engler et al., 2006).*

Matrix stiffness influences MSC fate by signalling through surface mechanotransducers that translate environmental stimuli into cytoskeletal responses. The non-muscle myosin type II proteins function as mechanotransducers on a wide variety of cells (Kim et al., 2005). A potent inhibitor of this protein family, Blebistatin, effectively inhibited the effects of matrix stiffness on MSCs.

Recent data confirms the profound influence of matrix stiffness on MSCs cultured in 3D matrix (Pek et al., 2010). In brief, MSCs cultured in thixotropic gel of variable rigidity have different lineage specifications. Specifically, increased expression of neurogenic (ENO2), myogenic (MYOG) and Osteogenic (Runx2, OC) transcription factors were seen in MSCs when cultures in gels with tau(y) of 7, 25 and 75Pa

respectively. The RGD active tri-peptide site is a key binding site in ligands that bind integrins (including all 5 αV integrins) (Humphries et al., 2006). MSCs embedded in RGD enriched gels have enhanced proliferation and differentiation suggesting a role of integrins in mechanotransduction. These observations have been confirmed more recently with the demonstration that α5 and αV integrins cluster in response matrix stiffness to bind complementary RGD motifs (Huebsch et al., 2010).

#### *1.9.2.3 Culture in hypoxia*

Hypoxic preconditioning of MSCs has been investigated in detail (Das et al., 2010). MSC cultured at low oxygen tension have accelerated cell division and augmented cell differentiation to both bone and fat (Ren et al., 2006, Hung et al., 2012). In addition, enhanced MSC migration and survival is seen (Liu et al., 2010, Annabi et al., 2003). HIF-1α and AKT dependant up regulation of CXCR4 and CXCR7 may underlie these effects. Therapeutically, MSCs cultured in hypoxic conditions produce increased amounts of pro-angiogenic and pro-survival factors and in a model of cardiac infarction produce superior angiogenesis and functional benefit compared with control MSC infusions (Hu et al., 2008).

### 1.9.3 Enhancing tissue specific MSC migration

Targeted cells therapy requires that the infused cells migrate specifically to diseased tissue to enhance therapeutic efficacy and minimise off target side-effects. Plastic adherent MSCs have poor homing capability (Rombouts and Ploemacher, 2003). It is

therefore of therapeutic interest to modify MSCs to enhance organ specific homing. For example promoting MSC migration to bone is therefore an attractive option for treating diseases such as OI. MSCs do not however express ligands to E-selectin, which is constitutively expressed on the microvasculature of BM capillaries, and is important for haematopoietic cell homing. Sackstein and colleagues report ex-vivo glycosyltransferase-programmed stereo-substitution of CD44 on hMSCs converting it to haematopoietic binding E-selectin/L-selectin ligand (HCELL). Intra-vital microscopy demonstrates that the HCELL modification augments MSC migration to bone by 100 fold. The initial interaction between HCELL and complimentary selectins, triggers VLA-4/VCAM-1 binding between endothelium and hMSCs, that ultimately leads to arrest and transmigration (Thankamony and Sackstein, 2011). Integrins play an important role in hMSC binding to hepatic sinusoidal endothelial cells (HSEC). In an elegant study carried out by Aldridge et al show that rolling of hMSCs on HSEC is regulated by CD29/VCAM-1. CD29/CD44 interactions with VCAM-1, fibronectin, and hyaluronan on HSECs determine firm adhesion in vitro (Aldridge et al., 2012). In the $CCL_4$ induced model of liver injury, hMSC migration was reduced following antibody blockade of CD29 and CD44 demonstrating the functional relevance of these findings.

## 1.10 The Immunosuppressive potential of MSCs

### 1.10.1 MSC suppress inflammation

The immunosuppressive potential of MSCs was highlighted by Bartholomew et al. who showed that MSC infusion prolonged skin-graft survival in primates (Bartholomew et al., 2002). Subsequently, MSCs have been shown to have a beneficial immunosuppressive effect in a variety of inflammatory and immune mediated disease models including encephalitis, stroke, diabetes mellitus, renal disease, rheumatoid arthritis, lung fibrosis, cardiac injury in rodents (Augello et al., 2007, Lee et al., 2006, Li et al., 2002, Orlic et al., 2001, Ortiz et al., 2007, Zappia et al., 2005). These positive results have led to the use of MSCs in human clinical trials in a variety of different settings. Before describing the myriad of mechanisms by which MSCs exert immunosuppressive effects it is necessary to describe individual components of the immune system.

### 1.10.2 Function and structure of the immune system

The human immune system protects the host from infectious diseases including bacteria, viruses, fungi and parasites. It is highly evolved to identify and kill pathogens without causing self-harm. The immune system may be divided into two distinct arms (Chaplin, 2006). The innate immune system is comprised of neutrophils, macrophages, monocytes, cytokines and acute phase proteins. These cells recognise molecular patterns specific to microbes and provide immediate host defence against pathogen. In contrast the adaptive immune system is mediated by T- and B- cells and is highly specific due to the presence of highly conserved antigen receptors on their surface. For effective immunity however there has be close interaction between cells of the innate and adaptive immune systems. This frequently involves antigen presentation by innate immune cells to complimentary T- and B- cells. Lymph nodes

are specially adapted immune organs that facilitate and promote such interactions and may be considered functional organ of immunity. The next section describes how these immune cell interactions occur and how stromal subsets (including mesenchymal cells) within lymph nodes are key orchestrators of this process.

### 1.10.3 Antigen presentation and recognition by T-cells

Naïve T cells (following exit from the thymus and BM) move in a continuous fashion between lymph nodes and other secondary lymphoid structures in search of their respective antigen. These cells recognise antigen only when presented with self-structures termed antigenic-peptide binding MHC molecules. Antigen can be loaded onto MHC in two ways (Parkin and Cohen, 2001). Firstly the antigen may be processed within a tissue cell (as occurs during viral infection) and then presented on the surface of the cell in association with MHC class I. Alternatively, exogenous antigen is endocytosed by antigen presenting cells (APCs), which may then be processed and presented in association with MHC class II molecules. CD4 lymphocytes respond to antigen presented with MHC class II, while CD8 cells respond to co-stimulation with MHC class I. CD8 responses are therefore generally targeted towards infected or transformed host cells while CD4 activation occurs in response to microbial infection.

### 1.10.4 T-cell receptor signalling

Antigen binding to the T-cell receptor embedded in the CD3 complex results in phosphorylation of tyrosine residues and activation of a second messenger cascade

resulting in gene transcription and cell proliferation (Brownlie and Zamoyska, 2013). Lymphocyte activation requires the activation of co-receptors including CD80, CD86 and CD40 that bind CD28, CTLA-4 and CD40 ligand respectively. T cell receptor activation in the absence of co-stimulation results in cell anergy or apoptosis. Once activated single lymphocytes can undergo up to 10 population doublings. The lymphocyte clone acquires the necessary receptors to exit the lymph node and traffic to the disease where they will mount a cytotoxic attack or initiate an inflammatory response. Some T cells will remain in the node as memory cells and will mount an accelerated response following re-exposure to the same antigen.

### 1.10.5 Effector T cells (CD4+ T helper and cytotoxic T cells)

CD4+ T helper (Th) cells effectively organise and activate other cells of the immune system in response to antigen. Precursor Th0 cells (following appropriate stimulation) differentiate into Th1 or Th2 cells. Th1 responses essentially control intracellular pathogen infection. They are characterised by interlukin-2 and Interferon-γ production which serves to increase the proliferation and activation of lymphocytes and macrophages (Sallusto et al., 1999). Interferon-γ also stimulates Th0 precursor cells to differentiate into Th1 cells and inhibits Th2 differentiation. Activated macrophages produce IL-12 which also promotes a Th1 response. Th2 response is characterised by IL-4, IL-5, IL-6 and IL-10 production, which favour antibody mediated responses and have been implicated in allergic disease. IL-4 favours IgE production by B cells and also feeds back to support Th2 and inhibit Th1 responses. IL-5 promotes the growth of eosinophils.

### 1.10.6 Cytotoxic T ($CD8^+$) cells

Following activation, cytotoxic T cells kill host cells that express specific antigen (Barry and Bleackley, 2002). Mechanistically the cytotoxic T cell binds to the host cell, inserts perforins into its cell membrane through which granzymes are infused into the cytoplasm of the cell inducing DNA fragmentation and apoptosis. Cytotoxic T cell binding also trigger apoptosis by activating target cell surface Fas molecules by their Fas ligand. These mechanisms play a critical role in controlling virally infected cells that cannot be targeted by the innate immune surveillance.

### 1.10.7 B lymphocytes

B cells produce antibodies including IgM, IgG and IgA (Mauri and Bosma, 2012). The function of antibody is manifold and includes neutralising toxin, preventing organism adherence to the mucosal surface, complement activation, opsonisation and sensitising infected cells and tumour cells for antibody dependant cytotoxic attack by killer cells. All B cells produce IgM initially following antigenic stimulation. Antibody class switching, is mediated by the binding of CD40 on B cells to CD40 ligand on T cells and occurs later if the immune response is augmented. Naive B cells can process antigen (via the B cell receptor) and function as an APC for T cell activation. In this way B cells can facilitate elements of the innate and adaptive immune systems. B cells reside and traffic between mucosal associated lymphoid tissues in the gut, lung and genitourinary tract where they provide first line protection from environmental pathogens. The marginal zone of the spleen also contains a large compliment of B cells that have a particular role in protection from encapsulated

pathogens (including haemophilus, pneumococcus and meningococcus). B cells can be activated when bound to free antigen in the lymph nodes. Alternatively in cases of re-infection follicular dendritic cells (DCs), which bear Fc and complement receptors can activate the B-cell response in an accelerated fashion.

### 1.10.8 Autoimmune responses

The development of T and B cells is tightly regulated to prevent the generation of auto-reactive cells (Rioux and Abbas, 2005). Specifically, activation of immature cells in the BM or thymus triggers cell death by apoptosis and clonal death. This process occurs when antigen is detected in the absence of co-stimulation or supporting cytokines. Indeed the vast majority of thymocytes die in the thymus following negative and positive screening process (frequently involving exposure to auto-antigen). Additional mechanisms to prevent autoimmunity include receptor editing of auto-reactive antibody on B cells and the production of neutralising antibody that recognises auto-antigen.

### 1.10.9 The lymphatic and lymphoid systems

The circulatory system is specially adapted to allow nutrient rich plasma escape from capillary beds facilitating the delivery of essential metabolites to tissue and the removal of cellular waste. The majority of this plasma is reabsorbed back into venules and returns to the systemic circulation. The remainder is collected by a network of conduits called lymphatic vessels (Schmid-Schonbein, 1990). These vessels collect into larger lymphatics that eventually flow back into the systemic blood circulation.

Lymph nodes are secondary lymphoid structures, through which lymph passes on it's way back to the blood stream. The nodes act as they act as site-specific filters and are ideally positioned to receive foreign antigen (unbound or APC- bound) and facilitate interactions required for effective acquired immunity. Naive lymphocytes enter the nodes via high endothelial venules. Lymphocytes that do not encounter cognate antigen re-enter the systemic circulation within a few days. In contrast activated lymphocytes under go clonal expansion and acquire effector function (as described above) facilitating elimination of the pathogen or foreign antigen (Malhotra et al., 2013).

*1.10.9.1 Structure*

The lymph node is comprised 2 sections – the cortex and the medulla. The cortex is subdivided into the T-cell (paracortex) and B-cell areas (Katakai et al., 2004). The medulla is comprised of a network of lymph draining sinuses and contains large numbers of immune cells including plasma cells, macrophages, and memory T cells. The microstructure of lymph nodes is specially adapted for immune cell interaction (von Andrian and Mempel, 2003). The paracortex is arranged into paracortical cords that originate between B cell follicles and extend into the medulla. These cords are bordered by lymph filled sinuses and are permeated by reticular fibres. Interstitial fluid and migratory dendritic cells percolate through these channels facilitating antigen detection be innate immune cells. At the centre of each paracortical cord is a high endothelial venule that is surrounded by layers of pericytes known as fibroblastic reticular cells (FRCs). The space between the FRCs and endothelium is termed the

'perivenular channel' and this receives lymph from the FRC conduit (Figure 1-9b). Functionally naive lymphocytes gain access to the node through the high endothelial venule. The FRCs directly communicate with trafficking lymphocytes and provide a reticular structure upon which lymphocytes can interface with antigen loaded dendritic cells.

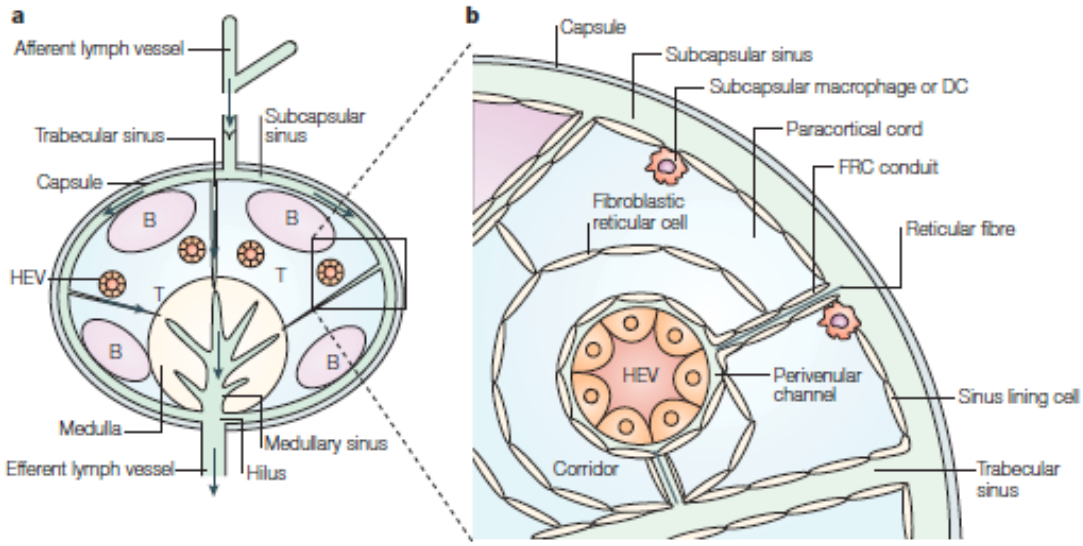


**Figure 1-9 Lymph-node architecture**

*This schematic diagram shows the major structural components of a lymph node. Lymph (carrying free antigen and APC bound antigen) enters through the afferent lymph vessel and percolates through the subcapsular sinus, the trabecular sinuses and along FRC conduits towards the medulla (Figure 1-9a). Figure 1-9b shows a paracortical cord. This structure allows lymph to flow through a fine network of channels comprised of reticular fibres and FRCs and facilitates close interaction between APCs and lymphocytes in the perivenular channel (von Andrian and Mempel, 2003).*

*1.10.9.2 Function*

Lymph nodes provide a scaffold to facilitate effective adaptive immune responses. Given the low frequency of antigen specific T cells, one critical function of the node is to attract antigen (either bound or unbound) into it. There are several mechanisms that help achieve this. Firstly, tissue –resident dendritic cells can migrate to draining lymph nodes via lymphatics. The lymphatic vessels also express numerous adhesion molecules that facilitate the migration of DCs into the node (Johnson et al., 2006). Secondly, the lymph node is specially designed to detect and sample antigen as it passes through it. For example, the FRC lymph channels are enclosed in mannose receptor-expressing endothelial cells, macrophages and CD11b+ DCs, which sample the lymph and remove microorganisms and debris within it. These cells function as APCs and can under appropriate circumstances activate T-cells and B-cells. Thirdly, afferent lymphatics facilitate the flow of antigen and immune cells into the node while efferent vessels regulate their release (Cyster and Schwab, 2012). During active inflammation leukocyte recruitment to the lymph node is increased dramatically while their exit is blocked. These changes occur as a result of alteration in levels of chemokines, cytokines and adhesion molecules and ultimately increase the chances of antigen – T-cell interaction. Activated T-cells can leave lymph nodes via cortical sinuses and efferent lymphatics. This process is tightly regulated by lymphatic endothelial cells that produce sphingosine 1-phosphate allowing egress of the activated cells.

*1.10.9.3 Stroma and Lymph nodes*

FRCs ($CD38^+/CD31^-/CD140a^+/VCAM\text{-}1^+$) are one of the main stromal populations identified in lymph nodes (Fletcher et al., 2010). FRCs provide the reticular scaffold for lymph nodes. In addition, FRCs regulate immune cell trafficking within the lymph node. The FRC conduits regulate immune cell migration by ensuring that low molecular weight lymph borne signals, particularly chemokines, are transported from subcapsular sinuses to the high endothelial venules (Malhotra et al., 2013). In this way FRCs facilitate direct communication between lymph and blood and directly determine leukocyte migration from systemic circulation to the node. FRCs also play an important role in T cell homeostasis. They promote the survival of naïve T cells by production of IL-7 and CCL19 (Link et al., 2007). On the other hand the presentation of peripheral tissue antigen on these stromal cells represents a key mechanism for tolerising autoreactive CD8+ T cells (Lee et al., 2007). Interestingly FRCs showed reduced stimulation of T cells after Toll-like receptor 3 ligation (Fletcher et al., 2010). In addition it has been proposed that the inhibitory effects of FRCs on the immune system extends beyond the induction of peripheral tolerance. In an elegant experiment FRCs exerted potent anti-proliferative effects on stimulated T cells. This effect was IFN-γ dependant and was mediated via increased NOS2 expression and NO production (Lukacs-Kornek et al., 2011). These studies illustrate the complex role of FRCs in promoting and modulating adaptive immune responses. These data provide mechanistic and physiological insights into the interactions between mesenchymal cells and the immune system that are described in the next section.

## 1.11 MSCs suppress cells of the immune system in vitro

### 1.11.1 MSCs and the innate immune system

An overview of the immunosuppressive effects of MSCs on the immune system is shown in Figure 1-10. DCs have a critical role in antigen presentation to naive T cells. Maturation of DCs is accompanied by expression of co-stimulatory molecules (CD80 and CD86) and up-regulation of MHC class I and class II molecules. Secretion of IL-6 and $PGE_2$ by activated hMSCs inhibits the maturation and function of monocyte-derived DCs, impairing their ability to function as APCs (Nauta et al., 2006). MSCs can potently inhibit cytokine production by mature DCs in vitro in particular reducing IL-12 secretion (Jiang et al., 2005, Nauta et al., 2006). In addition, co-culture of DCs and plasmacytoid DCs with MSCs reduces TNFα and IFNγ production and increases production of the regulatory cytokine IL-10 (Aggarwal and Pittenger, 2005). MSCs also inhibit cytotoxic effects of NK cells by down regulation of NKp30 and NKG2D. Activation and INFγ production by activated NK cells is completely abrogated by co-culture with MSCs (Moretta et al., 2001, Spaggiari et al., 2006). The effects of MSCs on neutrophils are complex. MCSs can inhibit the respiratory burst of neutrophils. They also appear to prolong neutrophil life span (via IL-6 production) by inhibiting cellular apoptosis (Raffaghello et al., 2008).

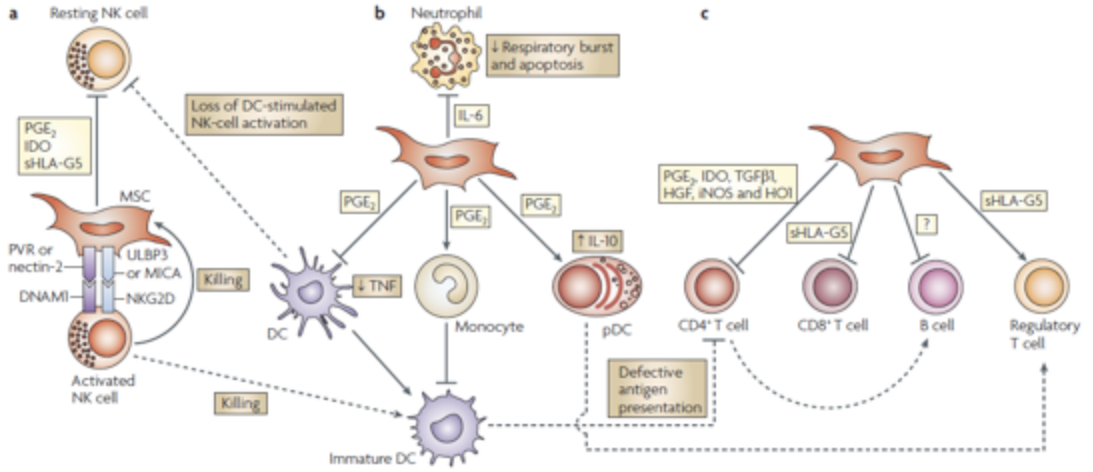


**Figure 1-10 MSCs suppress innate and adaptive immune cells via a variety of different mechanisms.**

*This figure illustrates the effects MSCs exert on cells of the innate and adaptive immune system. MSCs have potent immunosuppressive effects mediated by both direct contact and the production of soluble factors. These effects are described in detail in the text. Figure adapted from Uccelli et al., 2008.*

### 1.11.2 MSCs and the adaptive immune system

T cell proliferation in vitro may be induced by a variety of different mechanisms including addition of polyclonal mitogen, allogeneic cells or addition of specific antigen. There are countless published manuscripts demonstrating inhibition of T cell proliferation by MSC co-culture (Uccelli et al., 2008). Although the mechanisms of suppression vary, induction of cell cycle arrest in the $G_0/G_1$ phase appears to be a common final pathway (Sato et al., 2007, Benvenuto et al., 2007). In addition MSCs alter the cytokine profile, changing a pro-inflammatory IFN-γ rich milieu into an anti-inflammatory IL-4 producing state (Zappia et al., 2005). Co-culture experiments also demonstrate that MSCs can prevent the formation of cytotoxic T cells (Rasmusson et al., 2003). In addition to dampening or inhibiting components of the adaptive

immune, MSCs can also induce a regulatory phenotype. As described above MSC can induce plasmacytoid DC to produce IL-10 that triggers the generation of regulatory T cells (T-regs) (Beyth et al., 2005, Aggarwal and Pittenger, 2005). MSCs can also specifically stimulate T-regs to proliferate in response to HLA-G5 (Selmani et al., 2008). There are significant data to support a suppressive effect of MSCs on B cells (Corcione et al., 2006). As outlined above B cell proliferation and activation occurs as a consequence of T cell activation. As the latter is largely suppressed by MSCs it is logical to assume that B cell activation will also.

### 1.11.3 Mechanisms of immune suppression

There are numerous mechanisms documented by which MSCs exert their immunosuppressive effects. Broadly speaking immunosuppressive mechanisms can be divided into contact dependant and independent. Some studies clearly demonstrate that inhibition of T-cell proliferation requires close contact with MSCs facilitating Programmed Death 1–ligand interaction leading to T cell exhaustion (Augello et al., 2005). Direct cell-cell contact also induces IL-10 production (Selmani et al., 2008). IL-10 is an anti-inflammatory cytokine that that regulates inflammation and induces T reg formation. IL-10 has also been linked with HLA-G5 production by MSCs, which suppresses T-cell proliferation as well as NK cell and T-cell cytotoxicity. On the other hand MSCs can produce soluble factors that inhibit immune activation. NO and IDO are produced by stimulated MSCs act to induce cell cycle arrest in proliferating lymphocytes directly (via NO) or indirectly by depleting tryptophan (via IDO) (Krampera et al., 2006, Ryan et al., 2007). Additional mechanisms include the production of TGF-$\beta_1$ and hepatocyte growth factor that suppress T cell proliferation

in MLRs using allogeneic DCs or peripheral blood lymphocytes for antigen presentation (Di Nicola et al., 2002). Other soluble immunosuppressive factors that are produced by MSCs include IL-6, IL-10 and PGE2. Production of PGE2 by transplanted MSCs conferred a significant survival advantage over untreated mice in the 'caecal ligation and perforation' sepsis model (Nemeth et al., 2009). Interestingly, in this model stimulated MSCs (TNFα and/or lipopolysaccharide) produce $PGE_2$, which acts on local macrophages to induce a regulatory phenotype secreting the anti-inflammatory cytokine IL-10. The effects of IL-6 are diverse and include inhibition of the respiratory burst by neutrophils and monocyte maturation (Djouad et al., 2007, Raffaghello et al., 2008). An additional mechanism of interest is matrix metalloproteinase production (MMP) by MSCs that cleaves CD25 (Il-2 receptor) on responding T cells. In fact MSC infusion significantly reduced delayed-type hypersensitivity responses to allogeneic antigen and markedly prolonged survival of fully allogeneic islet grafts in transplant recipients by MMP-2 and MMP-9 production (Ding et al., 2009).

## 1.12 MSC therapy in GVHD

### 1.12.1 Overview

Graft-versus-host-disease (GVHD) occurs in patients following an allogeneic tissue transplant and commonly occurs in patients receiving a BM transplant. Essentially donor immune cells (T cells) in the graft recognise recipient antigen as foreign. T cell activation is accompanied by release of inflammatory cytokines including TNFα and

Interferon-γ, both of which prompt a severe immune attack in the recipient. The most commonly affected organs are skin, gastrointestinal tract and liver. The mucous membranes are also commonly affected causing severe discomfort to patients. There are 2 different forms of GVHD. Acute GVHD occurs within 100 days of transplantation and a major cause of morbidity and mortality following BM transplantation (Goker et al., 2001). Chronic GVHD (>100 days following transplantation) carries a more benign prognosis however, can result in pre-mature death (Lee et al., 2003). Experimentally, GVDH can be induced in rodents by carrying out strain mis-matched BM transplants (Schroeder and DiPersio, 2011). This allows for the investigation of potential therapeutic compounds.

### 1.12.2 Rodent data

Ren et al have published elegant data demonstrating the efficacy of MSCs for the therapy of GVHD (Ren et al., 2008). In summary (C57BL/6 x C3H) F1 mice (genetically uniform and heterozygous for all the genes for which the two parental strains differ) were lethally irradiated (13Gy) and after 24 hours were reconstituted with nucleated bone marrow cells ($5 \times 10^6$) and splenocytes ($5 \times 10^6$) isolated from C57BL/6 mice. These positive control mice develop extensive GVHD 2 – 3 weeks following the infusion resulting universally in death of the recipients, while negative controls receiving syngeneic BM transplant and were unaffected. The authors demonstrated that MSC treated rodents had a survival advantage if treated with MSCs ($0.5 \times 10^5$ cells via tail vein infusion). The therapeutic effect could be significantly diminished by blockade of NO and/or interferon γ signalling **(**Figure 1-11**)**.

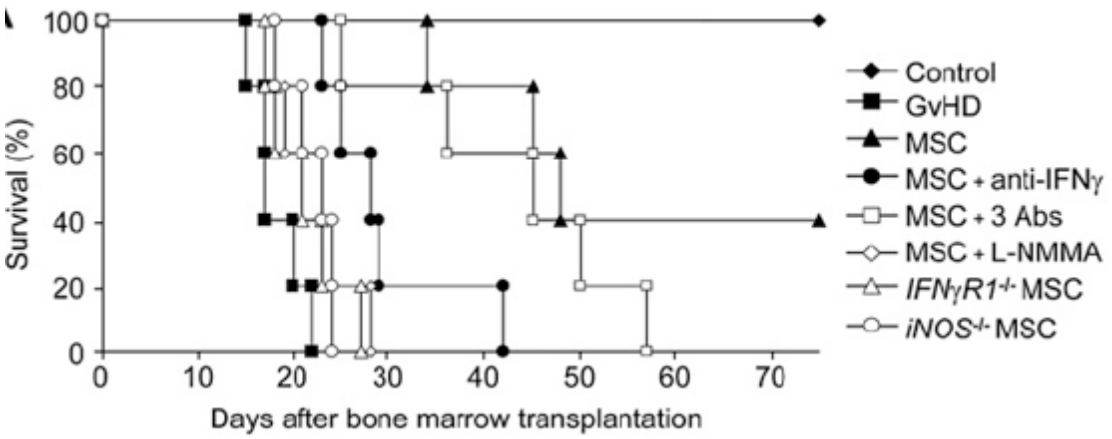


**Figure 1-11 Survival curves for MSC treated mice with GVHD.**

*This figure shows the survival curves of mice with GVHD with and without MSCs MSc treatment. MSC therapy clearly improved survival overall survival. In order to identify important signalling mechanisms involved in this effect, additional experiments were performed blocking antibodies (including anti-Interferon-γ or a combination of anti-TNFα, IL-1α, and IL-1β) and MSCs isolated from iNOS and Interferon-γ knockout mice. Notably, blockade of NO signalling (L-NNMA) and interferon-γ dramatically reduced the benefit of MSC infusion.*

Interestingly, the authors also demonstrate that the immunosuppressive effect is dependant on MSC chemokine production. Activated MSCs produce a variety of leukocyte chemo-attractants that draw activated immune cells into close proximity for NO-mediated immunosuppression to function effectively.

### 1.12.3 MSC efficacy in humans with GVHD

Le Blanc and colleagues published the first demonstration of the efficacy of MSCs for the treatment of acute GVHD. In a particularly striking case report, peripheral venous

MSC infusions were used to treat refractory GVHD in a 9-year-old boy with acute lyphoblastic leukaemia (Le Blanc et al., 2004). This boy received 2 infusions of MSCs at 60 days and 180 days following his stem cell transplant and enjoyed a full clinical response to this therapy 1 year following the transplant **(**Figure 1-12**)**.

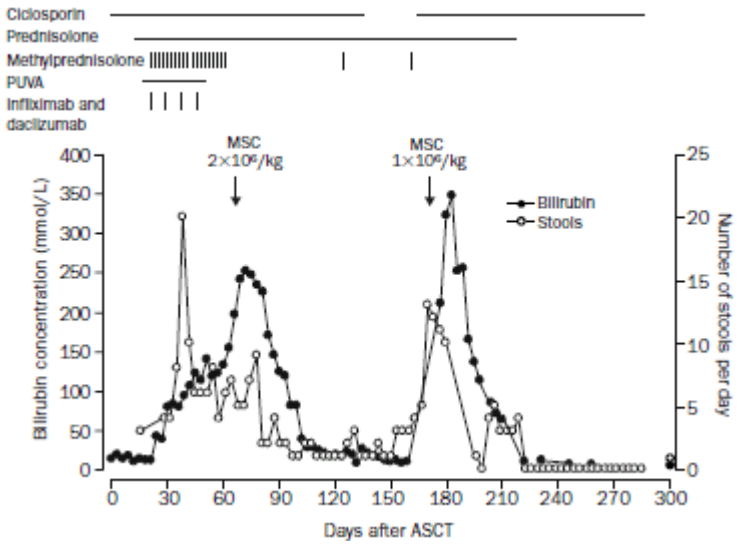


**Figure 1-12 Response of refractory GVHD to autologous MSC therapy.**

*This figure illustrates the clinic course of a 9-year-old boy with refractory GVHD treated with MSC infusions. The bilirubin and number of stools per day reflect the severity of liver and bowel involvement. The figure highlights the dramatic response to repeated MSCs infusions as evidenced by a return to baseline of liver and bowel function (Le Blanc et al., 2004).*

### 1.12.4 MSCs are licensed for GVHD

The excitement surrounding the therapeutic potential of MSCs has in part been justified this year when Prochymal (MSCs derived from unrelated volunteer donors) was the first stem cell therapy to be approved for use in humans. Prochymal has been approved for the treatment of acute GVHD in children in Canada. The landmark

phase 3 trial responsible for this randomised patients (2:1 ratio) with steroid resistant GVHD to receive 8 infusions of 2 x $10^6$ MSC/kg over 4 weeks (an equivalent volume of placebo) with an additional 4 infusions administered weekly after day 28 to those patients that had a partial response. The primary end point was attainment of a durable complete response. 244 patients were enrolled in the study. Although there was no significant difference between the groups regarding the primary endpoint (35 versus 30% in MSC and placebo groups respectively in the ITT population), there were important differences between the groups in the secondary endpoints. Notably patients with more severe GVHD (liver, skin and gastrointestinal involvement) had a 63% response compared to no response in the placebo arm. Additionally patients treated with MSCs had less progression of GVHD at weeks 2 and 4 respectively (32% versus 59% (P=0.05) and 37 versus 67% (P=0.05) respectively (Martin et al., 2010). These data formed the basis of a successful campaign to license MSC therapy for the treatment of severe GVHD by an internationally recognised regulatory authority. Prochymal is now approved in Canada, New Zealand and is currently available in several other countries including the USA under the expanded access program.

## 1.13 Enhancing the immunosuppressive potential MSC

### 1.13.1 Non-adherent culture

Culture of cells as 3D spheroids affects the immunosuppressive potential of MSCs (Bartosh et al., 2010). Spheroid-derived MSCs are capable of tri-lineage differentiation and express typical MSC markers including CD73, CD90 and CD105.

They have higher expression of the anti-inflammatory molecule, TNFα stimulates gene/protein 6 (TSG6). hMSC spheroids also exerted enhanced anti-inflammatory effects on LPS-stimulated macrophages compared to monoculture MSCs. When infused into the rodent model of zymogen induced model of peritonitis, spheroid derived cells were more anti-inflammatory than monoculture derived cells as evidenced by lower levels of TNFα, IL-1β, $PGE_2$ and myeloperoxidase in the lavage fluid.

### 1.13.2 Modulating Toll-like receptor expression

The anti-inflammatory phenotype of MSCs is well described and is a key factor for their use in on-going clinical trials (Le Blanc and Mougiakakos, 2012). We now know that the *in vivo* immune-regulatory phenotype of MSCs, once thought of as constitutively active, is carefully regulated and affected by factors such as infusion time and dose (Auletta et al., 2012, Shi et al., 2012). This complexity is reflected in a few studies that show although MSCs could suppress T cell proliferation *in vitro*, they failed to elicit clinical improvements *in vivo* (Inoue et al., 2006, Sajic et al., 2012, Sudres et al., 2006). An emerging field in MSC biology involves studying the effect of Toll-like receptor (TLR) stimulation and its effect on the immunosuppressive capacity of MSCs (Keating, 2012). TLRs consist of a family of proteins expressed on innate immune cells that recognise danger signals. Activation of these receptors initiates a variety of defence mechanisms geared towards eliminating pathogenic microorganisms and restoring homeostasis (Takeda et al., 2003).

Of the 10 known TLR family members, TLR 1-6 expression has been detected in both mMSCs and hMSCs (DelaRosa and Lombardo, 2010). Early work by Liotta and colleagues showed that activation of TLR3 and TLR4 on hMSCs inhibited their ability to supress T cell proliferation *in vitro* (Liotta et al., 2008). This effect was mediated by TLR-mediated down regulation of Jagged-1 on MSCs, resulting in impaired signalling to Notch receptors on T cells. Tomchuck *et al*. report that TLR4-activated MSCs secrete pro-inflammatory cytokines such as TNFα, IL6 and IL1β. Conversely, TLR3 activation results in the secretion of anti-inflammatory cytokines such as IL10 and IL12 (Tomchuck et al., 2008). More recently, Waterman *et al*. report that short-term priming with TLR3 or TLR4 agonists can polarise MSCs towards an immunosuppressive (TLR3-primed) or pro-inflammatory (TLR4-primed) phenotype (Waterman et al., 2010). Addition of TLR3-primed MSCs to stimulated lymphocyte cultures prevented T cell activation and proliferation by up to 90%. However, addition of TLR4-primed MSCs had the opposite effect, and promoted lymphocyte proliferation compared to control samples.

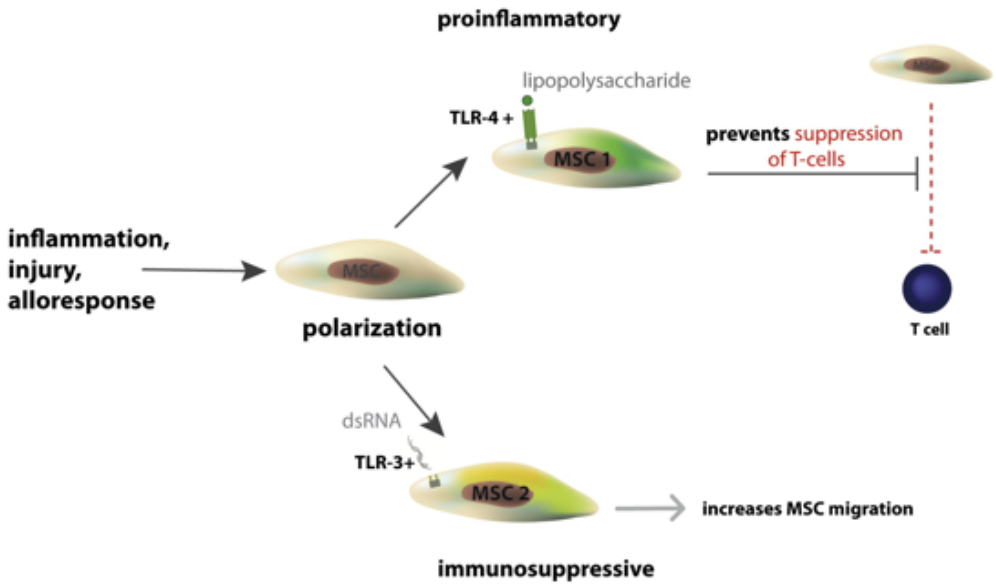


**Figure 1-13 TLR-primed polarisation of MSCs towards a pro-inflammatory or anti-inflammatory phenotype.**

*Lipopolysaccharide, a ligand for TLR-4, primes MSCs towards a pro-inflammatory phenotype in which they lose their ability to suppress immune cells. Conversely, TLR-3 activation primes MSCs towards a more suppressive phenotype (Keating, 2012).*

The physiological relevance of TLR priming of MSCs is only beginning to be unravelled (Auletta et al., 2012). The current hypothesis suggests that MSCs can both promote (TLR4-primed) the immune response during the early stages of tissue injury as well as suppress (TLR3-primed) the response during resolution **(**Figure 1-13**)**. Although these early findings raise interesting questions about the role of MSCs in injury and repair, future work should concentrate on studying the role of TLR-priming *in vivo*. In addition there may be ways to enhance MSC immunosuppressive potential by modulating TLR3 signalling.

## 1.14 Avoiding complications of therapy

### 1.14.1 Can MSCs contribute to scar formation?

There has been considerable interest in the use of BM-derived stem cells for the therapy of liver cirrhosis and numerous clinical trials have been performed (Houlihan and Newsome, 2008). Reports suggest that BM-derived cells, can differentiate into hepatic stellate cells, myofibroblasts and fibrocytes and can directly contribute to liver scar tissue formation (Forbes et al., 2004, Russo et al., 2006). Using sex mismatched BM transplants, Russo et al. demonstrated a contribution of donor BM cells to scar tissue (stellate and myofibroblasts cells) during $CCL_4$ injury. In order to determine which BM cell was giving rise to hepatic myofibroblasts, BM transplants were enriched with either MSCs or HSCs prior to infusion. In female mice that received BM enriched for male MSCs, 53% of hepatic myofibroblasts contained the Y chromosome unlike female recipients that received BM enriched for male HSCs, in which only 8.2% of hepatic myofibroblasts contained the Y chromosome. These data suggest that BM-derived MSCs may contribute to scar formation. Li et al. demonstrate that MSCs migrate to the chronically injured liver along a concentration gradient of sphingosine 1-phosphate and make a contribution to scar tissue formation (Li et al., 2009). In their study infused MSCs marked with GFP comprised over 80% of total liver myofibroblasts (Li et al., 2009). These studies are also in agreement with a number of other studies that demonstrate a contribution of BM derived cells to scar tissue producing cells in a variety of other tissues (Hashimoto et al., 2004, Li et al., 2007). These data have generated a nervous air in the setting of on going clinical trials

investigation the effects MSCs cells in patients with advanced liver injury and other chromic scarring diseases.

### 1.14.2 MSCs and cancer

There is a growing body of evidence to show that embryonic and induced pluripotent stem cells acquire chromosomal abnormality in culture (Mayshar et al., 2010). This has led to suggestions that cellular therapy of either type may be accompanied by risk of tumourigenesis (Ben-David and Benvenisty, 2011). The first clinical case of brain tumour associated with cell therapy occurred in a boy (13years od) with cerebellar ataxia. He had been treated with multiple infusions of foetal neural stem cells 4 years earlier and presented with headache from multifocal brain tumours derived from infused cells from at least 2 donors (Amariglio et al., 2009). Until recently, hMSCs (unlike murine MSCs) were considered genetically stable during in vitro expansion, however some evidence to contrary has recently emerged (Rosland et al., 2009). These preliminary data prompted a large scale analysis of 144 MSC samples (mostly BM derived) for chromosomal abnormality (Ben-David et al., 2011). The analysis detected chromosomal abnormality in approximately 4% of samples studied. Specifically, two monosomies of chromosome 13, four monosomies of chromosome 6q as well as gains of chromosomes 7q and 17q and trisomy 19 were identified. The clinical relevance of these mutations is not known, however in an independent analysis of stromal tumours (lipomas, as well as chondrosarcomas and osteosarcomas) demonstrated monosomy 13 as a common occurrence. These data are of concern with the high number of clinical trials proceeding worldwide. In addition to these data, studies have suggested that co-infusion of MSCs with cancer cell lines accelerate

metastatic tumour spread. It is thought that tumour associated MSCs allow the cancer to evade immunesurviellance which would otherwise kill the cancerous cells (Karnoub et al., 2007). Finally, the first randomised study addressing the benefits of MSC infusion in the context of HSC infusion was published in 2008 (Ning et al., 2008). In total 30 patients (most with acute myeloid leukaemia) received a standard therapy (HSC infusion) alone or in combination with culture expanded MSCs at a dose of 0.3 – 15.3 x 105 cells per Kg. They found that only 1 out of 10 patients in the MSC treatment group developed grade II GVHD compared with 8 out of 15 patients in the non-MSC group. Notably, there was a dramatic increase relapse of the primary disease in the MSC arm (60% versus 20%) raising the possibility that MSCs also suppress the beneficial effects of graft versus leukaemia.

### 1.15 Aims

The therapeutic potential of MSCs holds great promise for a variety of diseases. Traditionally, rodent-based experiments have provided a critical step in bridging the gap between the scientific bench and the clinician's surgery. Limitations of isolation methods, malignant transformation of cultured MSCs and variability in published data have significantly weakened the translational relevance of MSC data from animal studies. Therefore the first objective of this thesis is to isolate and characterise a pure population of mMSCs. Secondly, I will vary culture conditions in an attempt to lineage prime or restrict MSCs at both a genotypic and phenotypic level. Finally, I will assess the different MSCs groups in well-described cartilage assays in an attempt to improve regenerative potential of these cells.

# 2 Methods

## 2.1 Prospective Isolation of Murine MSCs

### 2.1.1 Cell isolation from compact bone

C57BL/6 mice at 8-10 weeks old (3 or more) were sacrificed by cervical dislocation. The carcass was sprayed liberally with 70% ethanol. A wide pelvic incision on the torso of the mouse was made and a forceps was inserted through the exposed knee joint. The skin and hair covering the leg was retracted towards the ankle joint. The ankle joint was cut using a scissors, freeing the limb from overlying skin and hair. The tibia was then dissected free from adherent muscle by blunt dissection. The muscle was then cut away from the limb and the knee joint severed. The tibia was then carefully cleaned using tissue paper and all non-adherent tissue removed. The bone was stored in ice-cold PBS. The femur was dissected free from adherent muscle in a similar fashion. Gentle pressure dislocated the femur from the hip joint and the bone was then cut free from the torso. It was cleaned and stored as previously described.

The bones were then washed 3 times by vigorously shaking them in fresh PBS. The washed bones were then crushed gently using a sterile pestle and mortar achieving 1 fracture per bone. The bone fragments were then cut with sterile scissors into tiny fragments for approximately 5 minutes. Bones and fragments were collected into

50ml container and incubated in 20mls of pre-heated DMEM (Invitrogen, cat. no. 11960085) + 0.2% (40mg) collagenase (Wako, cat. no. 034-10533). This was done in a temperature-regulated (pre-heated) shaker at 110 rpm and 37°C for 1 hour.

The cell suspension was then placed on ice (to quench collagenase activity) and filtered through a 70μm sterile filter (BD Falcon, cat. no. 352350). The remaining bony fragments including those in the filter were collected and placed in the mortar. The bony fragments were then suspended in 2.5mls HBSS+ (Hanks-balanced salt solution (Invitrogen, cat. no. 14170112) supplemented with 2% FBS (Invitrogen, cat. no. 10500064), 10mM Hepes (Sigma, cat. no. H3375), and 1% penicillin/streptomycin (Sigma, cat. no. G6784)) and crushed by gently tapping with the pestle 50 times. A further 5 mls of HBSS+ was then added and using the pipette, the liberated cells were washed out of the bone into solution. The liquid suspension was then aspirated, filtered and added to the filtrate from step 8 and kept on ice. This step was repeated up to 6 times, such that, the total volume of cell suspension became 50 mls.

The cell suspension was then spun in a pre-cooled centrifuged at 280g for 7 minutes at 4°C. The supernatant was discarded and the pellet resuspended by taping the container vigorously until the cell suspension is homogenous and the pellet fully dispersed. The red blood cells in the suspension were lysed by adding ice cold sterile $H_2O$ (1ml) for 5 seconds. This was quickly followed by adding double strength PBS + 4% FBS to quench the reaction. I them made the total volume up to 15 mls with HBSS+ immediately after. The cell suspension was then filtered as before and the

cells are collected by centrifugation at 280g at 4°C for 5 minutes. The resulting pellet was resuspended in 1ml HBSS+ and is ready for staining.

### 2.1.2 Cell staining

I set up additional tubes for compensation during flow cytometry including: negative control, positive control-PE, positive control-FITC, positive control-APC. To each of these cuvettes I added 100μl of HBSS+. 3-5 μl of the cell suspension is then added to each tube. The main sample can be stained in the 50ml container on ice. 1μl (1:100 dilution) CD45-PE (eBioscience, cat no.12-0451-81), Sca-1-FITC (eBioscience, cat no. 11-5981-81) and PDGFRα-APC (eBioscience, cat no. 17-1401-81) was added to the appropriate labelled tube and incubate on ice in the dark for 30 minutes. I aimed to stain approximately 100,000 -500,000 cells in 100μl of HBSS+. For the main sample, 1μl per mouse of each of the above antibodies and Ter-119-PE (eBioscience, cat no. 12-5921-81) was added and the cells stained in a total volume of 1ml. Once completed, all samples were vortexed and incubate on ice in the dark for 30 minutes. The compensation samples are then washed by adding 1 ml HBSS+ to each of the compensation tubes and 10mls HBSS+ to the main sample. The main sample is was collected by centrifugation at 280g at 4°C for 5 minutes. Each pellet was then re-suspended in 2μg/ml PI staining solution (Sigma, cat. no. P4170) and filtered through a sterile 35μm filter into sterile cuvettes and stored on ice in the dark.

### 2.1.3 Cell sorting

The cell sorter should be set up in accordance with the manufacturing specifications. 488nm and 647nm lasers are required for antibody detection. The negative control was run to ensure that the voltages were set appropriately and the cell population is clearly discernible in all channels. Each single colour (PE, FITC and APC) was run and compensated against the other channels. After creating a live gate (PI negative), I selected lineage negative cells (PE-negative) and examined for expression of PDGFRα and Sca-1. I placed a gate around the brightest PαS cell population and these cells were sorted into α-MEM media supplemented with 10% FCS.

## 2.2 Cell culture and differentiation

### 2.2.1 Standard cell culture

The sorted cells were cultured in α-MEM media with GlutaMAX (Invitrogen, cat. no. 325710280), supplemented with 10% FBS and penicillin/streptomycin. I used a minimum density of 5,000 cells per $cm^2$. The media was changed every 3 days and the cells were split when they became confluent. In brief, cells were washed with PBS to remove all serum and Tryplee (trypsin + EDTA) was then added to the culture dish and incubated at 37°C for 3 minutes. Gentle tapping of the culture dish freed any remaining adherent cells. The trypsin was neutralized by adding an equal volume α-MEM media supplemented with 10% FCS. The cells were collected by centrifugation and re-seeded in a bigger well.

### 2.2.2 Clonogenic assays and growth curves

To perform CFU-F assays 2000 cells were seeded in a 10cm plastic dish. The cells were incubated in 10 mls α-MEM media supplemented with 10% FCS for 14 days. I removed half (5 mls) the culture media and replaced it with fresh after 1 week. Adherent cell clusters of greater than 50 cells were counted as a single colony on day 14.

### 2.2.3 Adipocyte differentiation

Once confluent, I commenced culture in adipogenic induction media (Lonza, hMSC Adipogenic BulletKit; PT3004) for 4 days. The media was replaced with adipogenic maintenance media for 4 days. One cycle of this was sufficient to induce robust fat differentiation. I stained for fat using Oil red O as follows: Adipogenic cells were fixed by adding 4% PFA. 60% 2-propanol was then added for 1 minute after which pre-filtered Oil red O solution (Oil red O: Water = 3:2) was added to the cells for 30 minutes. Following removal of the staining solution, I added 60% 2-propanol for 1 minute. The wells were washed three times with water and then counter stained by adding Mayer's haematoxylin for 30 seconds. Finally, the wells were washed by adding an excess of water 3 times.

### 2.2.4 Osteogenic differentiation

Sub-confluent (approximately 60-70%) cells were cultured with osteogenic media (Lonza, hMSC Osteogenic BulletKit; PT-3924) for a period of 2 weeks. The media

was changed every 3 days. I confirm osteoblast differentiation by performing alkaline phosphatase staining and demonstrate calcium deposition using alizarin red staining solution. The alkaline phosphatase staining was performed using Histofine assay kit (NICHIREI BIOSCOENCE INC.). In brief the osteogenic cells were fixed using 4% PFA. The cells were washed three times (10 minutes each) with PBS. Alkaline phosphatase staining solution was then added and the cells were incubated at room temperature (25°C) for 30 minutes. Excess solution was then removed and the cells were washed three times (5 minutes each) with water. The well was counter stained by adding Mayer's haematoxylin for 30 seconds and then washed with water 3 times. The alizarin red staining and quantification was performed using an Osteogenic assay kit (Millipore). In brief the osteogenic cells were fixed using 10% formaldehyde. The cells must be washed three times (10 minutes each) with distilled water. The alizarin red staining solution was then added and the cells incubated at room temperature (25°C) for 20 minutes. Following this the excess dye was removed and the cells were washed four times (5 minutes each) with deionized water. At this point I imaged the well. For alizarin red quantification, 10% acetic acid was added to the stained well for 30 minutes. The suspension along with any adherent cells was transferred to a 1.5ml microcentrifuge tube. The tube was vigorously vortexed and then heated to 85°C for 10 minutes. The resulting slurry was centrifuged at 20,000g for 15 minutes. I neutralise the pH with 10% Ammonium hydroxide. Finally the samples and standards were added to a 96-well plate and read the sample at $OD_{405}$. The alizarin red concentration of the sample was measured against the standard curve.

### 2.2.5 Chondrogenic differentiation

I harvested cultured cells by trypinisation as described above. 2.5 x $10^5$ cells were transferred to a 15ml conical tube and washed in αMEM + glutaMAX. The tube was centrifuged at 150g for 5 minutes at 25°C. The supernatant was discarded and the pellet was resuspended in 1ml Differentiation Basal Medium Chondrogenic, with supplements from the Chondrogenic SingleQuots kit and TGF-$\beta_3$ (10ng/ml, Lonza) and BMP-6 (500ng/ml; R&D Systems). The cells were centrifuged again at 150g for 5 minutes at 25°C. After discarding the supernatant and the cell pellet was resuspended in supplemented Differentiation Basal Medium Chondrogenic. The pellet was then cultured in the incubator at 37°C for 21 days. I replaced the supplemented media every 3 days. Following completion of the differentiation protocol the pellet was cryoembeded and sectioned. To prepare the slides the sections were deparaffinised and hydrated in distilled water. The sections were stained in toluidine blue working solution for 30 minutes. The stained sections were then dehydrated quickly once through 95% and twice through of 100% alcohol and cleared in xylene, 3 changes, 10 minutes each. Finally I placed a coverslip with Entellan (resinous mounting medium) (1.07961.0500: MERCK) over the section.

## 2.3 Immunophenotyping of MSCs

In order to identify surface marker expression of PαS MSCs, cultured cells were washed with PBS. The cells were then incubated for 3-5 minutes in cell dissociation buffer. Non-adherent cells were collected by centrifugation and resuspended in 1ml

HBSS+ for counting. 5 x $10^4$ cells were resuspended in 100μl HBSS+ and stained with each of the antibodies listed in Table1. As previously described unstained cells are initially run to ensure visualised on the histogram and a live dead cell gate is constructed. Isotype controls are then run and a gate that identifies positive antibody expression is created. Each sample is then run and an overlay histogram of negative control, matched isotype and related antibody was constructed.

**Table 2-1** List of antibodies used

| Protein and Fluorochrome | eBiosciences No. | Concentration | Clone | Isotype |
|---|---|---|---|---|
| CD45-PE | 12-0451 | 0.2mg/ml | 30-F11 | Rat IgG2b kappa |
| Ter 119-PE | 12-5921 | 0.2mg/ml | Ter-119 | Rat IgG2b kappa |
| Sca-1-FITC | 11-5981 | 0.5mg/ml | D7 | Rat IgG2a kappa |
| PDGFRα-APC | 17-1401 | 0.2mg/ml | APA5 | Rat IgG2a kappa |
| CD44-FITC | 11-0441 | 0.2mg/ml | IM7 | Rat IgG2b kappa |
| CD34-FITC | 11-0341 | 0.5mg/ml | RAM34 | Rat IgG2a kappa |
| CD105-PE | 12-1051 | 0.2mg/ml | MJ7/18 | Rat IgG2a kappa |
| CD49e-PE | 12-0493 | 0.2mg/ml | HMa5-1 | Armenian Hamster IgG |
| CD29-PE | 12-0291 | 0.2mg/ml | HMb1-1 | Armenian Hamster IgG |
| CD 90-PE | 12-0902 | 0.2mg/ml | 53-2.1 | Rat IgG2a kappa |
| Control-FITC | 11-4321 | 0.5mg/ml | - | Rat IgG2a kappa |
| Control-FITC | 11-4031 | 0.5mg/ml | - | Rat IgG2b kappa |
| Control-PE | 12-4321 | 0.2mg/ml | - | Rat IgG2a kappa |
| Control-PE | 12-4031 | 0.2mg/ml | - | Rat IgG2b kappa |
| Control-PE | 12-4888 | 0.2mg/ml | - | Armenian Hamster IgG |
| Control-APC | 17-4321 | 0.2mg/ml | - | Rat IgG2a kappa |

## 2.4 Lymphocyte Proliferation Assay

### 2.4.1 Isolation of CD19+ B cells

Mice were killed by cervical dislocation. The spleen was dissected free from adherent tissue and stored in cold P2 (PBS + 2%FCS) buffer on ice. A single cell suspension was then made by pushing the spleen through a sterile fine mesh for 2-3 minutes, using the rubber end of a 2ml syringe plunger. 3ml of P2 was then added and the suspension was re-suspended with a pipette to collect any loose cells. The cell suspension was transferred into a 15ml falcon tube and spun at 1400rpm for 7 minutes at 4˚C. The resulting pellet was resuspended in 1ml lysis buffer for 60 seconds. 8ml P2 was added to stop the reaction and the sample was centrifuged at 1400rpm, 7mins, at 4˚C. The pellet was resuspended in 3ml P2 buffer and the cells were counted. An aliquot containing about 40 $x10^6$ cells was removed for the bead purification stage and centrifuged again at above speeds. The pellet was resuspended in 90µl cold MACS buffer per $10^7$ cells and 10µl CD19 microbeads per $10^7$ cells was added. The suspension was mixed (brief vortex) and incubated in the dark at 4˚C for 15 minutes. After incubation, the cells were washed with cold MACS buffer (total volume 8mls). The sample was centrifuged at 1400rpm, 7mins, at 4˚C. Meanwhile, the MACS separator and columns were prepared. I used the LS column for positive selection of up to $10^8$ cells. In brief, a 70µm sterile filter (BD Falcon, cat. no. 352350) was placed over the column to ensure debris did not flow through. 3ml of warm MACS buffer was put through the column to prepare it and collected in a waste universal tube. The pellet was resuspended in 500µl warm MACS buffer and added to the column. The follow through was collected in the waste pot. 3x rinse steps using 3ml warm MACS

buffer each were then performed to ensure all cells passed through the column. After finishing the washes, the collected cells are flushed from the column using 4 mls of warm MACS buffer. The sample is centrifuged at the usual speed (1400rpm, 7mins, at 4˚C), and the purified $CD19^+$ B cell population is resuspended in 2ml of complete C10 (RPMI + 10%FCS + 2-mercaptoethanol) medium. This is stored on ice until required. I counted the cells as described previously.

### 2.4.2 Isolation of $CD4^+CD25^-$ T cells

Mice were killed by cervical dislocation. Lymph nodes were removed and placed in cold P2 buffer on ice (Figure 2-1). A single cell suspension was prepared by pressing the nodes through a sterile fine mesh using the rubber end of a 2ml syringe plunger for 2-3 minutes. 3ml of P2 was added and washed up and down to collect any loose cells. The cells were transferred into a 15ml falcon tube and spun at 1400rpm for 7 minutes at 4˚C. The resulting pellet was resuspended in 3ml P2 buffer and counted. The pellet was resuspended at $10^7$ cells in 40µl MACS buffer and 15µl of biotin antibody cocktail per $10^7$ cells (contains antibodies to CD8a, CD11b, CD45R, and Ter-119) was added. The suspension was mixed (brief vortex) and incubated in the dark at 4˚C for 15 minutes. Following incubation, 30µl MACs buffer, 20µl of anti-biotin microbeads and 10µl of CD-PE antibody was added per $10^7$ cells. After mixing well (brief vortex) the sample was incubated in the dark at 4˚C for 15 minutes. The reaction was quenched by adding 10mls cold MACS buffer and centrifuged at the usual settings. The MACS separator and columns were then prepared. The LD was used to remove CD4- negative cells. In brief the column was placed on the magnet

(with a 70μm strainer on top) and 2 x 1ml warm MACS buffer was added to prepare it. The pellet was resuspended in 500μl MACS buffer and allowed to run through the wet column. The unlabelled CD4-positive cells were collected in a fresh sterile container. The column was washed with 2 x 1ml MACS buffer and the collected cells were counted. Following centrifugation, the pellet was resuspended at the following concentration 90μl MACS buffer per $10^7$ cells. 10μl anti-PE microbeads per $10^7$ cells was added. The sample was mixed well (brief vortex) and incubated in the dark at 4˚C for 15 minutes. The reaction was quenched by adding 10mls cold MACS buffer and centrifuged at the usual speed for the same time. The MS column was then used to remove CD25 positive cells. In brief, the column was placed on the magnet (with a 70μm strainer on top) and 500μl warm MACS buffer was added to it. The stained pellet was resuspended in 500μl warm MACS buffer and added to the wet column. The column was washed with 3 x 500μl of warm MACS buffer and the CD4+CD25- T cells were collected. The CD4+ CD25- T cells were resuspended in C10 culture media and placed on ice until required

.

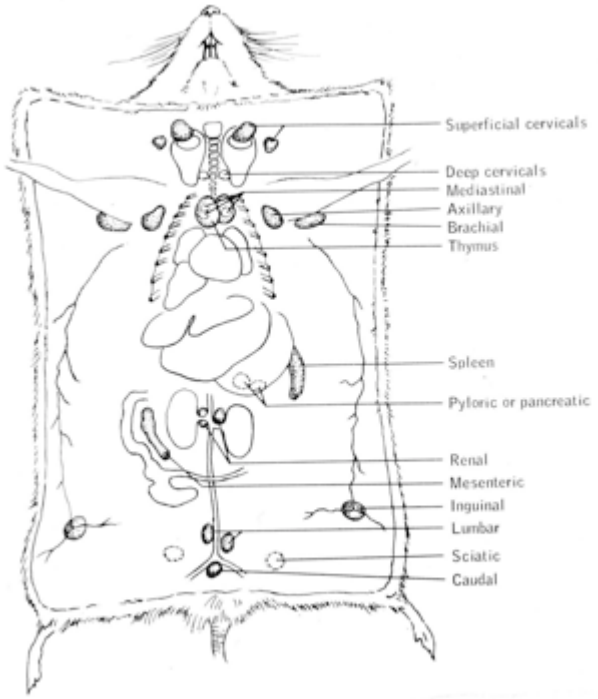


**Figure 2-1 Distribution of mouse lymph nodes.**

*This figure shows the anatomical distribution of mouse lymph nodes. Careful dissection allows the removal of all the named nodes.*

### 2.4.3 Proliferation assay

T cells were cultured in RPMI 1640 supplemented with 10% FCS, 1x P/S/G solution and 50mM 2-mercaptoethanol (β-Me) at a density of 25,000 cells/well in round-bottomed 96-well plates with or without graded numbers of MSCs. 50,000 CD19+ B cells (2:1 ratio) were added for co-stimulation to each well (via CD86-CD28 interaction) and cultures were supplemented with 0.8µg/ml of anti-mouse CD3e (BD Biosciences) to ligate the T cell receptor and stimulate T cell proliferation. Cultures were maintained for 72 hours before staining with anti-CD4 (1/100 dilution; BD

Biosciences) to determine total CD4+ cell number. A pictorial representation of this procedure can be seen in **Figure 2-2**.

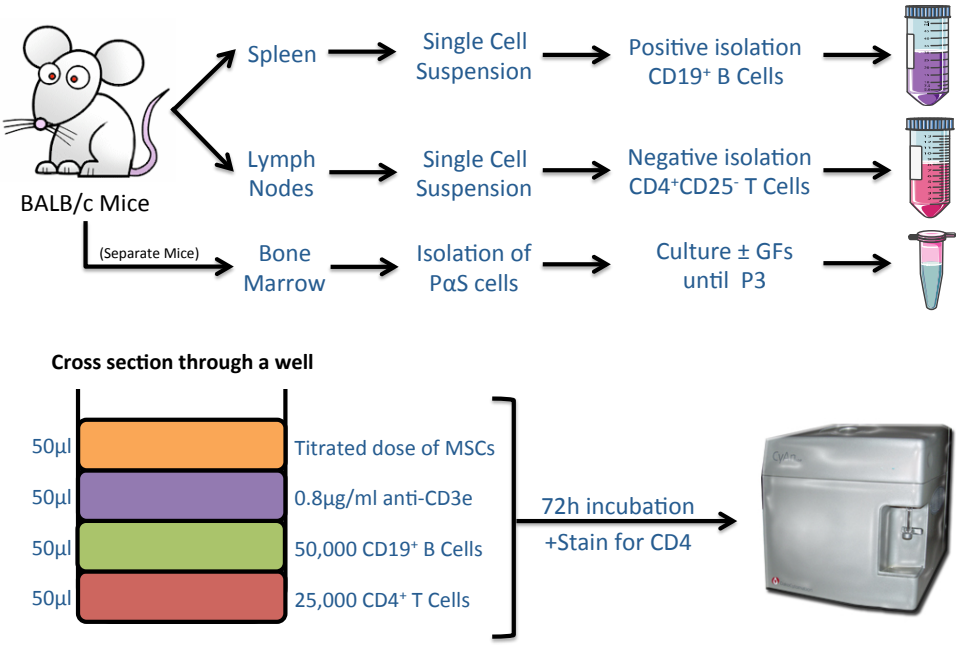


**Figure 2-2 Cartoon demonstrating the steps involved in performing a $CD4^+$ $CD25^-$ proliferation assay.**

*Following lymph node dissection $CD19^+$ B cells and $CD4^+CD25^-$ T cells are isolated using magnetic bead separation as described. The proliferation assay is then performed by titrating the appropriate cell populations into the culture well in the presence or absence of varying MSC concentrations.*

### 2.4.4 Mechanism of MSC mediated immunosuppression

A variety of different mechanisms have been reported to explain the immunosuppressive effects of MSCs. Of these the most commonly reported include: 1. Production of NO 2. Production of $PGE_2$ 3. Production of MMP 2 and 9 and 4. Production of IDO. We sequentially added blockers of each of these pathways at

known physiological concentrations to the assay and calculated their impact on lymphocyte proliferation. The table below shows at blocking compounds and the final tissue bath concentrations used.

**Table 2-2** A list of inhibitors used to determine the mechanism of MSC mediated immunosuppression**.**

| Reagent | Supplier | Solvent used | Final bath concentration |
|---|---|---|---|
| Indomethacin | Sigma | DMSO | 5μM |
| SB-3CT | Sigma | DMSO | 6μM |
| 1-Methyltryptophan | Sigma | Media | 1mM |
| L-NMMA | Sigma | Water | 1mM |

### 2.4.5 Griess Assay

NO release from PαS cells was indirectly quantified using the Griess Assay (Promega). As NO is a volatile agent with a short half-life, the Griess reagent measures the total amount of nitrite ($NO_2$-), a stable breakdown product of NO. Passage 3 MSCs were seeded at a density of 15,000 cells/well in 96 well plates and cultured overnight in RPMI 1640 supplemented with 10% FCS, 1x P/S/G solution, 50mM β-Me, 20ng/ml IFN-γ and 20ng/ml TNF-α (Peprotech) to re-create a pro-inflammatory environment. Following overnight incubation, supernatants were

removed and processed according to manufacturer's instructions. The absorbance was read at 520nm and nitrite values determined by comparison against a standard curve.

## 2.5 Growth factor priming experiments

### 2.5.1 Effects of GFs on MSC traits

To investigate the concept of lineage priming in PαS, freshly isolated cells were cultured in SM alone or supplemented with bFGF, PDGF-BB or transforming growth factor-beta (TGF-β) at a concentration of 10ng/ml respectively. The standard assays including growth potential, tri-lineage differentiation and immunosuppression were performed and compared for each group of cells. In order to identify the signaling pathways responsible for phenotypic changes observed in each group we performed additional experiments in the presence of the following compounds: PDGF-AA, Dasatinib (Src inhibitor), SU5402 (Akt inhibitor) and SB-431542 (TGF-β1 activin receptor like kinase inhibitor).

## 2.6 RNA isolation

### 2.6.1 Preparation

The work area was cleaned with RNAase ZAP and all pipettes, tips, collection tubes and buffers are UV-irradiated prior to use. Samples were kept on ice while processing. DNase I solution (Qiagen 79254) was prepared prior to starting. 10µl of

stock DNase I solution was added to 70µl RDD buffer and mixed gently by inverting (do not vortex) and centrifuged to pool liquid at the bottom. This was enough for one RNA collection column. RLT buffer was prepared by adding 10µl ß-ME (inhibits endogenous RNases) to 1ml of stock in a fume cupboard.

### 2.6.2 Cell lysis

For lysis, we first washed the cells with ice cold PBS multiple times to remove all residual medium. 350µl RLT+ß-ME buffer (<6cm diameter well; 600µl if 6-10cm well) was then added to the culture dish and a pipette tip to lyse cells. The lysate was then collected into an eppendorf tube and mixed using the vortex. I passed the lysate through a 20-gauge needle (0.9mm diameter) at least 5 times to homogenise the sample. An equal volume of 70% ethanol was then added to the sample (i.e. 350µl or 600µl ethanol depending on size of dish or number of cells) and mixed by pipetting.

### 2.6.3 Spin column and DNase digestion

700µl of the sample was transferred into RNeasy spin columns placed over a collection tube. The samples were spun at >8000xg or >10,000rpm for 15 seconds. The flow-through was discarded and the collection tube re-used. 350µl of RW1 buffer is now added to the RNeasy spin column and centrifuged for 15 seconds at max speed to wash the membrane. The flow through was discarded. 80µl of the DNase I incubation mixture (i.e. 10µl DNase I stock to 70µl RDD buffer) was added directly

onto the membrane and incubated at room temperature for 15 minutes. The column was washed with 350µl of RW1 buffer by centrifuging at max speed for 15 seconds and the flow through was discarded.

### 2.6.4 RPE wash step

The RNeasy spin column was placed in a new collection tube. 500µl of RPE buffer (should have ethanol added to it) was added to the spin column and centrifuged at max speed for 15 seconds. The flow through was discarded. 500µl RPE buffer was once again added and the sample was centrifuged at max speed for 2 minutes to completely dry the silica capture membrane ensuring no ethanol is carried over. The RNeasy spin column was then transferred into a new collection tube and centrifuge at max speed for 1 minute, eliminating carryover of RPE buffer. Finally, the spin column was transferred into a sterile 1.5ml eppendorf for RNA collection. 30-50µl of RNase-free water was pipetted directly onto the membrane and the sample was centrifuge at max speed for 1 minute to elute the RNA. The RNA was then stored on ice prior to the quantification step using a Nanodrop.

## 2.7 Microarray

### 2.7.1 Sample preparation

PαS cells were isolated and cultured in SM alone or supplemented with one of the following: bFGF, PDGF-BB or TGF-β. Upon reaching confluence the cells were split as described earlier in a 1 to 2 to ratio. Passage 1 cells were cultured until confluent and then lysed in situ for RNA extraction as described above. RNA quality was monitored using a Bioanalyzer 2100 (Agilent, Stockport UK) then prepared for transcriptional profiling on GeneChip Mouse Exon 1.0 ST Arrays (Affymetrix, High Wycombe UK) according to the manufacturer's recommendations. Briefly, 100 ng of RNA was used to transcribe single stranded cDNA using oligo dT primers. A second strand was then synthesised and the double stranded cDNA purified. This double stranded cDNA was used as a template to generate fluorescently labelled cRNA by in vitro transcription, which was purified and fragmented before being hybridised to the microarray chip.

### 2.7.2 Bioinformatic analysis

The gene expression data were generated using quantile normalization and RMA (robust multi-array analysis). Probe level quantile normalization. and robust multi-array analysis on the raw CEL files was performed using the affy package of the Bioconductor (http://www.biocondutor.org) project and custom cdf MOGENE10ST_Mm_ENTREZG (version 17). To generate the heatmaps, gene

expression data from microarray was quantile normalized and then scaled. Gene annotation was based on NCBI gene database downloaded on May 28, 2013.

## 2.8 Karyotyping

### 2.8.1 Cell preparation

The MSC groups were cultured in SM alone or supplemented with either bFGF, PDGF-BB or TGF-β in a 25cm tissue culture flask as described earlier. When the cells were approximately 70% confluent we added B-ONC to the media (final tissue flask concentration) approximately 16 hours before cell harvest. On the day of harvest 0.05ml colcemid was added to the tissue flask and re-incubated for 1 hour. The cells were trypsinised (as described earlier) and pipetted to give a single cell suspension. 8 mls of aqueous 0.025M KCl supplemented with colcemid was added to the cell suspension and the sample was incubated at 37C for 20 minutes. If a previous harvest had shown total failure to rupture the cell membrane then add 8ml plain distilled water to the 2ml of trypsinised cell suspension (and 0.1 ml of 10% Colcemid containing BrdU) as a hypotonic. Again incubate for at least 20 minutes, possibly longer. The cells were collected by centrifugation at 1000 rpm for 5 min. The supernatant was removed and cells resuspended by gently flicking the tube. The cells were then ‘slow fixed’ in 1 mL of fresh Carnoy’s fixative at room temperature and the suspension was topped up to 7 mls with fixative.

### 2.8.2 Chromosome spreads

The slides were prepared by cleaning them in a mixture of absolute ethanol and concentrated HCl (1:1). To make chromosome spreads on these slides, three drops of the cell suspension was added from a prepared Pasteur pipette (~0.2-mL capacity, drawn to deliver 10-µL drops), and allowed to spread to their maximum size. Once dry, the slides were inspected under low-power phase-contrast microscopy (final magnification 160X). Before G banding, the slides were "aged" for between 3 and 21 d by leaving them in a closed box at room temperature.

### 2.8.3 G banding

The next step is G banding. The prepared slides were placed in 2X SSC in a Coplin staining jar with a lid in a water bath at 60°C-65°C for 1.5 h. The slides were cooled by running tap water over the closed jar and then transferred to 0.85% (w/v) NaCl at room temperature for 5 min. The slides were drained by touching them onto filter paper and then placed on a flat surface. The chamber was flooded with 0.025% trypsin in 0.85% NaCl for 15-20 seconds. The reaction was quenched by placing the slides back into 0.85% NaCl and then the slides were rinsed in phosphate buffer (pH 6.8) and stained in fresh Giemsa stain in 5 mM phosphate buffer (pH 6.8). After 10 minutes in the stain, the wet slides were inspected under low-power, bright-field microscopy (160X) for staining intensity. If necessary, staining was repeated. Slides were examined with a 100X oil-immersion lens and cover sips were applied for storage. The banded slides were than scanned on the 'Metafer system' (which scans the slides and captures metaphases) and then analysed on the 'IKAROS' system.

## 2.9 Additional Cartilage experiments

### 2.9.1 Micromass pellet chondrogenic differentiation (Bristol Method)

ITS basal medium consisting of DMEM (4.5g/liter glucose, Sigma) supplemented with 1mM sodium pyruvate (Sigma), 1% insulin-transferrin-selenium (Invitrogen), Glutamax (1×; Invitrogen) and 1% (v/v) penicillin (100 units/ml)-streptomycin (100 μg/ml) (Invitrogen) was prepared. Culture expanded PαS MSCs were harvested by trypsinisation. $5 \times 10^5$ cells were placed in a 15ml conical tube, washed once in cell expansion medium, and then resuspend in chondrogenic differentiation medium (ITS basal medium freshly supplemented with 50 μg/ml ascorbic acid-2-phosphate (Sigma), 100nM Dexamethasone (Sigma), and 10ng/ml TGF-β3 (R&D System)). The cells were centrifuged at 1,500 rpm for 5 minutes at room temperature to make the cell pellet. The cell pellets were cultured in 1.0 ml chondrogenic differentiation medium per tube. Chondrogenic differentiation medium was changed every 2-3 days. After the first week, the medium was further supplemented with 50 μg/ml insulin (Sigma). The chondrogenic pellets were harvested for further analysis after 21 days.

### 2.9.2 Cartilage tissue engineering

Polyglycolic (PGA) scaffolds were placed in a Petri dish and covered with absolute ethanol for 5 minutes to sterilize it. The ethanol was then removed and the scaffolds were washed three times in sterile PBS. The scaffolds were then inserted into one well of a 12 well plate and covered with 1ml of 100μg/ml fibronectin (aliquots stored at -

20ºC) for 30 minutes. The scaffolds were removed and placed alone in each well and left to dry in the hood overnight (with the lid on). A 1% (w/v) solution of agarose in distilled water was prepared and sterilized in the autoclave. The agarose was microwaved until molten and then used to coat the bottoms of the wells in 24-well tissue culture plates (500µl agarose per well). Only use the central two rows of the plate. The plates were left in the hood with the lids off until the agarose solidified. One fibronectin-coated scaffold is then added to each well in the agarose coated plate. The scaffolds were then fully immersed in stem cell medium and left for approximately 30 minutes to re-hydrate. The PαS cells were then harvested and counted as previously described. A cell suspension equivalent to 600,000 cells was then placed in a separate tube for each scaffold to be seeded. The samples were centrifuged at 1500rpm for 5 minutes and the resulting pellets were resuspended in 30µl culture medium. The medium from the wells containing the scaffolds was then removed. A pipette should be used to suck the medium out of the scaffolds until they turn from pink to white. The white scaffold is then placed in the middle of the well and the 30µl cell suspension is slowly added to it. The empty wells in the 24-well plate are filled with sterile water to minimise evaporation and the seeded scaffolds are placed in the incubator over night.

On the next day, the scaffolds are turned over and left in the incubator for another 2 hours. ITS Basal Medium was prepared as previously described. 1ml Differentiation Medium (ITS basal medium freshly supplemented with 50 µg/ml ascorbic acid-2-phosphate (Sigma), 100nM Dexamethasone (Sigma), 10ng/ml TGF-β3 (R&D System) and 100ng/ml BMP-2(R&D System) was then added to each scaffold and the

culture dish was placed on a rotating platform (50rpm) within the incubator. Medium on the scaffolds was changed after day 6 and 8 using fresh Differentiation Medium. After day 10, the chondrogenic differentiation medium was further supplemented with 50 μg/ml insulin (Sigma). The medium was then changed every 2 or 3 days for a total of 35 days (5 weeks).

### 2.9.3 Sample fixation and sectioning

Chondrogenic micromass pellets or tissue engineered cartilage samples were frozen in O.C.T. embedding matrix (BDH). Full-depth sections (thickness, 12μm) were cut with a cryostat (Leica), fixed in 4% (w/v) paraformaldehyde (sigma) in PBS, pH 7.6 for 30 min and washed three times (5 min each time) in PBS.

### 2.9.4 Haematoxylin and Eosin staining

A circle was drawn around pre-fixed section using a PAP pen (Sigma) and let dry. Sections were re-hydrated in distilled water for about 5 minutes. Hematoxylin QS (Vector Laboratories, H-3404) was then added to the section for 2 minutes. Excess haematoxylin was removed by dipping briefly in distilled water followed by addition of 1% (v/v; 0.15g / 15ml water) eosin for 2 minutes. The slide was then dipped briefly (for 30 seconds) in 70% ethanol and then 100% ethanol respectively. Finally, the slide was cleared in xylene (Sigma) for 2 minutes and mounted in DPX mounting medium (Fisher scientific) and a cover-slip was added.

### 2.9.5 Safranin O staining

A circle was drawn around pre-fixed sections using a PAP pen and let dry. The pre-fixed slides were hydrated in distilled water for approximately 5 minutes. 0.02% (0.1g/500ml distilled water) FastGreen FCF (Sigma) was added to the sections for 4 minutes and then quickly rinsed off with 1% acetic acid solution for no more than 10 –15 seconds. The slides were stained in 0.1% (0.5g/500ml) Safranin O solution (Sigma) for 5 minutes. Then they were dehydrated and cleared using 95% Ethanol (10 dips), 100% Ethanol (20 dips), 100% Ethanol (2minutes) and Xylene (2 minutes).

### 2.9.6 Immunolocalisation of Types I and II Collagen

A circle was drawn around the pre-fixed section using a PAP pen and let dry. The fixed sections (12μ in thickness) were digested with hyaluronidase (Sigma H-3506) in PBS (0.01 g/ml), at 37ºC for 30 min in a humidified chamber (cover the bottom of a tray with wet paper towels). The solution was tipped off into the tray and sections were washed in PBS for 5 minutes on a shaker. The section was treated with pronase (Boehringer Mannheim 165921) in PBS (0.002 g/ml) at 37ºC for 30 min. It was then washed in PBS, for 5 min, on a shaker. Endogenous peroxidase activity was quenched using a solution of 3% hydrogen peroxidase (Sigma) in water, for 5 minutes (1ml 30% $H_2O_2$ + 9ml distilled water). It was washed again in PBS, for 5 min, on the shaker. Next the section was blocked with 3% BSA (Sigma A-7638; crystalline grade) in TBS/Tween (0.15M (13.15g) NaCl; 0.05M (9.08g) Trizma Base (Sigma T-1503); Tween 20 (0.75ml) made up to 1.5 litres with ultra-pure distilled water and adjust pH to 7.5-7.6), to avoid non-specific background staining, at room temperature for 1 hour

(0.3g BSA in 10ml TBS-Tween). This was washed off 3 times with TBS/Tween for 10 minutes each. The respective antibodies were then made up as follows: goat-anti-type I collagen (Southern Biotech; 0.4mg/ml; 1310-01) and goat-anti-type II collagen (Southern Biotech; 0.4mg/ml; 1320-01) as 1:100 and 1:20 dilution in 1% BSA in TBS/Tween respectively. A negative control was also prepared by diluting normal goat Iggy (Santa Cruz; 0.4mg/ml; SC-2028) 1:20 in 1% BSA in TBS/Tween. The section was incubated with 70µl primary antibody (diluted in glass or screw-top Eppendorf tubes) for 1 hour at room temperature in a humidified chamber. This antibody was washed off for 15 minutes in a high salt wash (HSW: TBS/Tween containing 2.5% NaCl) and twice for 15 min in TBS/Tween. It was then incubated with rabbit anti-goat IgG secondary antibody (Vectastain *Elite* ABC kit; Vector Laboratories PK6105) for 1 hour at room temperature in a humidified chamber (5µl Ab + 15µl normal rabbit serum (NRS) + 1ml Ab diluent). ABC reagent from Vectastain *Elite* ABC kit was then prepared and allowed to stand for 30 minutes before use (2.5ml TBS/Tween + 1 drop Reagent A + 1 drop Reagent B. Mix immediately). The antibody was rinsed for 1 x 15 min in the high salt water and then 2 x 15 min in TBS/Teen. The section was incubated with ABC reagent for 30 min at room temperature after which it was washed for 3 x 10 min with TBS/Tween. DAB substrate was prepared just before use (1 drop ImmPACT DAB chromogen concentrate in 1ml ImmPACT diluent) (ImmPACT DAB peroxidase substrate; SK-4105)). The substrate was added to the slides for 5 min until suitable staining developed. It was then quickly washed in distilled water and then washed for a further 5 minutes in distilled water. A few drops of Hematoxylin QS nuclear counterstain (Vector H3404) were added to each slide for approximately 60 seconds following

which it was dipped briefly in excess water and again for 10 seconds in fresh distilled water. The slide was checked under the microscope and more stain added if required. The sections were then dehydrated in 70, 90 and 100% ethanol for 2 minutes each. The slide was cleared in xylene and using DPX was fixed onto a cover slip.

### 2.9.7 Digesting Samples with Trypsin for Biochemical Assays

The chondrogenic micromass pellet samples or tissue engineered cartilage samples were freeze-dried and then digested. The dry weight of micromass pellet samples or tissue engineering samples was determined after freeze-drying. The following solutions were prepared for sample digestion for measurement of Type 1 and 2 collagen content: 1. 200mM Iodoacatamide (37mg / ml dH2O) 2. 200mM EDTA (76 mg/ ml dH20) 3. 2mg/ml Pepstatin A (2mg / ml 95% ethanol) and 4. 50mM Tris/HCl (0.303g / 50ml dH2O, pH 7.6) (all from Sigma). Additionally trypsin solution at concentration of 2 mg/ml in Tris, containing 3 inhibitors diluted 1/200 from above stock solutions (10mg TPCK-treated trypsin (Sigma T-1426) + 4.925ml Tris + 25µl each inhibitor) was prepared. Half of the final volume of trypsin (125µl) was added to the cartilage sample and incubated overnight at 37ºC. The following morning the remaining volume of freshly prepared trypsin (125 µl) was added and the sample was incubated for 2 - 3 hours at 65ºC, mixing every 10 minutes initially. The sample was then boiled for 15 minutes to denature the trypsin. The supernatant was then collected by centrifugation at maximum speed for 2mins. After removal of the supernatant into freshly labelled tube (stored supernatant at 4ºC until assay) 500µl water was added to remaining undigested pellet. This was then, vortexed briefly and centrifuged at maximum speed for 2 minutes. After discarding the supernatant, freeze dry and weigh

the pellet. The weight of solubilized sample was calculated by subtracting the dry weight of the sample and the dry weight of remaining undigested sample.

### 2.9.8 Glycosaminoglycans (GAGs) Assay

The cationic dye dimethyl-methylene blue (DMB) can be used for the measurement of GAGs. Reaction between the dye and GAG, at acid pH, produces a dye-GAG complex. Absorbance for the complex is optimally measured at 525nm. DBD solution was made by adding 16mg DMB (Sigma 341088), 3.04g glycine and 2.37g NaCl to 900ml water for 2 hours. The mixture was shielded from light. The pH was adjusted to 3.0 with HCl and the volume to 1L. The solution was stored at room temperature in the dark.

**Table 2-3 Chondroitin sulphate standards**

Chondroitin sulphate (stock at 50μg/ml; Sigma C9819) standards are prepared as follows:

| Standard Number | Standard Conc (μg/ml) | Amount of stock CS (μl) | Amount of water (μl) |
|---|---|---|---|
| 1 | 0 | 0 | 300 |
| 2 | 5 | 30 | 270 |
| 3 | 10 | 60 | 240 |
| 4 | 15 | 90 | 210 |
| 5 | 20 | 120 | 180 |
| 6 | 25 | 150 | 150 |
| 7 | 30 | 180 | 120 |
| 8 | 35 | 210 | 90 |
| 9 | 40 | 240 | 60 |
| 10 | 45 | 270 | 30 |
| 11 | 50 | 300 | 0 |

Firstly, samples were diluted as indicated in water. In a 96-well round-bottomed plates (Costar), 20μl water was added to the first column as blanks (wells A1-H1). The standards were added, in duplicate, using 20μl / well (wells A2-F4). Samples (20μl / well) were then added in duplicate (wells G4-H12). 250μl DMB was added to all wells and OD was read immediately at 525nm. The concentrations of GAGs in each sample were read from the standard curve.

### 2.9.9 Preparing Standards for Type I Collagen Assay

0.5mg AH23 peptide (SFLPQPPQ) was dissolved in 2ml 0.8% SDS/Tris and 24µl of this solution was added to 5.976ml 0.8% SDS/Tris to give a concentration of 1000ng/ml. This was the top standard. This was diluted serially with an equal volume (3ml) of 0.8% SDS/Tris to give the remaining 8 standards (500, 250, 125, 62.5, 31.3, 15.6, 7.8 and 3.9 ng/ml). The samples were stored at 4ºC.

### 2.9.10 Coating plates with AH23

Carbonate buffer was made up by adding $Na_2CO_3$ solution (0.212g $Na_2CO_3$ / 20ml $H_2O$) into $NaHCO_3$ solution (0.84g $NaHCO_3$ / 100ml $H_2O$) and adjusted to achieve pH 9.2. AH23 peptide was dissolved in carbonate buffer to a final concentration of 40µg/ml. 50µl of AH23 solution was added to all wells of 96-well Immulon-2 high-binding flat-bottomed plates (Thermo). The plates were tapped to ensure even distribution over bottom of wells, wrapped in cling-film and stored at 4ºC for 3 days. The plates were then washed 3x with PBS-Tween and 60µl PBS-1% BSA was added to each well. The plates were incubated at room temperature for 30 minutes. Plates were then washed 1x with PBS-Tween and dried in the oven for 15 minutes at 50ºC. The plates were stored at 4ºC until use.

### 2.9.11 Type I Collagen Assay

Digested samples were diluted in 0.8% (w/v) SDS in Tris (0.8g SDS in 100 ml Tris). Using 96 well round bottomed plates (Costar), all wells were blocked (except outer wells, to minimise evaporation) with 110µl of 1% BSA-PBS for 30 min at room temperature. The primary antibody (AH23-1319 from Rabbit) was prepared by diluting 1 / 1000 in Tris buffer containing 4% (v/v) Triton-X100. 5 mls was prepared per plate consisting of 4.8 ml Tris buffer, 5µl primary antibody (AH23-1319) and 200µl of Triton-X100. Wash plate once with PBS-Tween washing buffer and dry thoroughly.

Samples were diluted in Tris buffer (50mM Tris/HCl; 0.303g Trizma base in 50ml $dH_2O$, pH 7.6; Sigma) as required. A 96 well plate was set up and included: 1. Blanks (100 µl SDS-Tris buffer); 2. Maximum binding (50 µl of SDS-Tris); 3. Prepared standards at each concentration; 4. Diluted samples (in triplicate). 50µl of primary antibody was added to all wells except the blanks. The plate was sealed with Parafilm and incubated at 37°C overnight. The following day using a multi-channel pipette, 50 µl was transferred from each well to the equivalent well of an AH23-coated flat-bottom plate. This was incubated at room temperature for exactly 30 min. The secondary antibody (AP conjugated goat anti-rabbit; Southern Biotech 4010-04) was prepared by diluting 1/1000 in 1% BSA/PBS containing Tween-20 also diluted 1/1000. After exactly 30 minutes, the plate was washed three times with PBS-Tween and 50µl of secondary antibody was added to all the wells. The plate was wrapped in parafilm and incubated at 37°C for 2 hours. After this the plate was washed 3x with

PBS-Tween and 1x with distilled water to eliminate bubbles. The substrate was prepared by adding 1 alkaline phosphatase substrate tablet (Sigma) to 10ml diethanolamine buffer (0.25mM $MgCl_2$, 8.9mM diethanolamine (sigma), pH9.8). 50µl of substrate solution was added to each well and the plate was allowed to develop (approximately 20 – 30 minutes). The plate was read at 405 nm with the O.D. of the maximum binding wells approximately 0.5. The amount of detected peptide was converted to the amount of type I collagen in the sample by a factor of 146 according to the molecular weight.

### 2.9.12 Preparing Standards for Type II Collagen Assay

The peptide CB11B (CGKVGPSGAP[OH]GEDGRP[OH]GPP[OH]GPQY) was dissolved in PBS to make 7 standards (0.5, 1, 2, 3, 4, 5, 6 ug/ml).

### 2.9.13 Coating plates with heat denatured collagen type II (HDC)

Carbonate buffer was made up as previously described. 2-5 mg bovine tracheal type II collagen (Sigma) was dissolved with 1ml carbonate buffer in a screw top Eppendorf tube. The collagen was heated for 20mins at 80°C. It was mixed continuously while heating. The denatured collagen type II was diluted in carbonate buffer to a concentration of 40µg/ml. 40µl of denatured collagen type II solution was added to the wells (B2-O13) of 384 well high-binding flat bottomed ELISA plates (Corning). The plates were tapped gently to ensure even distribution over bottom of wells. The plates were wrapped in cling-film and stored at 4ºC for 3 days. Prior to use the plates

were washed 3x with PBS-Tween after which 50µl PBS-1% BSA was added to each well. After a 30 minute incubation at room temperature the plates were washed 1x with PBS-Tween and dried in oven for 15min at 50ºC. The plates were stored at 4ºC until needed.

### 2.9.14 Type II Collagen Assay

The samples were diluted in Tris buffer (50mM Tris/HCl; 0.303g Trizma base in 50ml $dH_2O$, pH 7.6; Sigma) as required. A 384 well plate was set up and included: 1. Blanks (20 µl Tris buffer); 2. Maximum binding (10 µl Tris buffer); 3. Prepared standards at each concentration; 4. Diluted samples (in triplicate). 10µl sample was added in triplicate to relevant wells. The primary antibody was prepared by 1 in 600 dilution (5µl COL2-3/4m antibody in 3ml Tris per plate) and 10µl was added to all wells except the blanks (reverse pipetting). The plate was sealed with a plate-seal and incubated overnight at 37°C. 10µl was transferred the following day from each well to the equivalent well heat denatured collagen-coated plate (40µl of 40µg/ml). The plate was incubated at room temperature for exactly 30 minutes and then washed 3 times with PBS-Tween. 10µl of anti-mouse secondary antibody, diluted 1/1000 in PBS-1%BSA-0.1% Tween (3µl antibody + 3µl Tween in 3ml PBS-BSA per plate) was then added to all wells (reverse pipetting). The plate was then sealed and incubated at 37°C for 2 hours. After this the plate was washed 3 times with PBS-Tween and once with distilled water to remove bubbles. 10µl of the substrate was then added to all wells (1 tablet in 10ml diethanolamine buffer) using reverse pipetting and the reaction was allow to develop at room temperature. The plate was read at 405nm. The amount

of detected peptide was converted to the amount of type II collagen in the sample by a factor of 44 according to the molecular weight.

## 2.10 Detection of mRNA using Q-PCR

### 2.10.1 RNA isolation and reverse transcription

RNA was extracted from cell cultures using Norgen Total RNA Purification kit (Norgen Biotek), according to the manufacturer's instructions. Reverse transcription (RT) was carried out using the PrimeScript RT reagent Kit (TAKARA BIO). 1 μg total RNA sample was diluted in 13 μl RNase free distilled water then reverse transcribed with 5× PrimeScript Buffer (4 μl), PrimeScript RT Enzyme Mix I (1 μl), Oligo dT primer (1 μl), and random 6 mers (1 μl) from the kit to make a total 20 μl, at 37°C for 15 minutes, and then subsequently 85°C for 5 seconds.

### 2.10.2 Primer design

Published primers for the housekeeping gene β-actin were used as a reference for normalization in all Q-PCR (Raff et al., 1997). Published primers for mouse collagen type II, collagen type I and Aggrecan were used for Q-PCR (Salvat et al., 2005). A BLAST search against all known sequences confirmed specificity.

β-actin

Forward 5'-GACAGGATGCAGAAGGAGATTACT-3'

Reverse 5'-TGATCCACATCTGCTGGAAGGT-3'

Collagen type II

Forward 5'-CAG GTG AAC CTG GAC GAG AG-3'

Reverse 5'-ACC ACG ATC TCC CTT GAC TC-3'

Collagen type I

Forward 5'-AAC GAG ATC GAG CTC AGA GG-3'

Reverse 5'-GAC TGT CTT GCC CCA AGT TC-3'

Aggrecan

Forward 5'-GTT GGT TAC TTC GCC TCC AG-3'

Reverse 5'-GTC CTC CAA GCT CTG TGA CC-3'

2.10.3 Quantitative real-time RT-PCR

Quantitative RT-PCR was performed in a 12.5 µl reaction volume containing of the Rotor-Gene SYBR Green PCR Master Mix 6.25 µl (Qiagen), 4 µl of DEPC water, 1.25 µl of primers (10mM) diluted in DEPC water and 1 µl cDNA sample from the reverse transcription, using Rotor-Gene-6000 (Qiagen) machine. The amplification program consisted of initial denaturation at 95°C for 5 minutes followed by 40 cycles of 95°C for 5 seconds and annealing at 60°C for 10 seconds. After amplification and 90 seconds waiting pre-melting, melt analysis was performed by heating the reaction mixture from 60°C to 95°C at a rate of 1°C/5 seconds. The threshold cycle ($C_t$) value for each gene of interest was measured for each RT sample. The $C_t$ value for β-actin

was used as housekeeping gene for normalization. Real-time RT-PCR assays were done in triplicate.

### 2.11 Statistical analysis

Continuous laboratory variables are reported as means and standard error as all variables had parametric distribution on D'Agostino and Pearson Omnibus Normality testing. Categorical variables are reported as number and percentages. For comparison of single variables, unpaired Student t-tests were used. Where repeated samples were taken (i.e. MSC concentrations in proliferation assay), repeated-measures of analysis of variance (ANOVA) was used, incorporating the appropriate *post hoc* analysis (i.e. Dunnett's test) for multiple comparisons. The significance level was set at $p < 0.05$ (*$p<0.05$, **$p<0.01$, ***$p<0.001$; unless specified). All analysis was performed using the GraphPad Prism version 5.0 software package.

# 3 The prospective isolation and characterisation of mMSCs

## 3.1 Introduction

### 3.1.1 Limitations of traditional methods

Despite extensive investigation the identification, physiological function and biological properties of MSCs have remained elusive until recently. There are many reasons for this, including the low frequency of these cells in tissue, lack of specific surface markers to identify the cells and inherent limitations of isolating MSCs by plastic adherence as discussed (da Silva Meirelles et al., 2008). MSCs isolated by plastic adherence are heterogeneous cell populations, which are frequently contaminated with hematopoietic cells (Phinney et al., 1999, Peister et al., 2004). Prolonged culture on plastic (necessary to remove contaminants) also reduces their differentiation potential and proliferative ability, as the cells mature and begin to senescence (Wagner et al., 2008). In a recent publication however Morikawa et al. isolated murine MSCs prospectively based on their positive expression of PDGFRα and Sca-1 (Morikawa et al., 2009a). The prospective isolation of PαS cells allow the isolation of a purer and more potent population of MSCs directly from their boney niche. Therefore, PαS cells have the potential to provide valuable insights into the *in vivo* localisation and properties of bone-derived MSCs (Nombela-Arrieta et al., 2011).

### 3.1.2 Modifications to MSC isolation methods

Numerous attempts at improved murine MSC isolation have been published however each has its own limitations. The use of beads (anti-CD11b, CD34 and CD45) (Baddoo et al., 2003), cytotoxic agents (Falla et al., 1993), and frequent media changes (Soleimani and Nadri, 2009) have been used to try to eliminate cellular contamination. These methods however failed to avoid the irreversible changes to native MSC biology that occurred following prolonged growth on plastic. The prospective identification of murine MSCs based on expression of CD34 appeared to enrich for murine MSCs (Nadri and Soleimani, 2007). CD34 is, however, expressed by diverse cell types including haematopoietic cells and endothelial cells, and cellular contamination was therefore still inevitable. While, MSC isolation based on expression of wheat germ agglutinin helped avoids contamination, the isolated cells had reduced clonogenic potential and colony forming potential (Van Vlasselaer et al., 1994). In contrast to these methods, the prospective isolation of MSCs based on expression of PDGFRα and Sca-1 yielded a pure and potent cell population isolated directly from their boney niche.

### 3.1.3 Technical advances

The isolation of PαS cells incorporated many additional steps compared to traditional methods. Collagenase digestion is required similar to that used previously to enrich for MSCs (Zhu et al., 2010). The rationale for this step is based on the observation that PαS cells reside in the endosteum of the bone (Muguruma et al., 2006). The

protocol used lineage specific antibodies (including CD45 and Ter119) that identify haematopoietic cells and hence prevented contamination of the isolated MSCs. Following sample labelling with the appropriate antibodies, the cells were resuspended with Propidium iodide staining solution. The exclusion of dead cells is an important part of the protocol, as cellular debris can interfere with subsequent culture and growth of MSCs. PαS cell isolation also required high-speed cell sorting, making it more challenging than traditional methods that use plastic adherence only.

### 3.1.4 Aims

Nonetheless, successful isolation of PαS cells will allow investigators to interrogate the biology and physiological functions of MSCs, which until recently has proven difficult. To my knowledge the isolation of PαS MSCs has not been successfully achieved outside of Professor Matsuzaki's laboratory. I therefore aimed to develop a detailed protocol that would facilitate the isolation of PαS cells in our laboratory in the University of Birmingham. I wanted to perform detailed characterization of growth potential, tri-lineage differentiation and immunosuppressive properties of PαS MSCs.

## 3.2 Results

### 3.2.1 Representative flow cytometric profiles

Mice aged between 8 – 10 weeks gave the best cellular yield and in total approximately 10,000 PαS cells may be isolated per mouse using the method described here. The total duration of the procedure takes approximately 7 hours, however this depends on the number of mice used in the experiment.

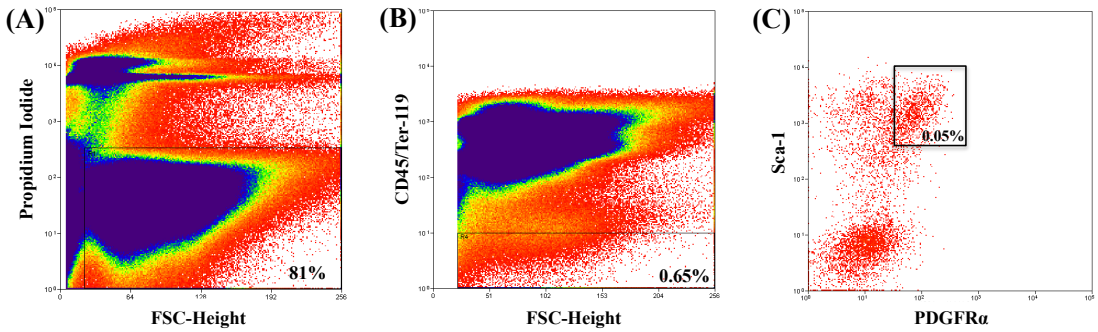


**Figure 3-1 Representative flow cytometric profiles of collagenase-digested bone stained with CD45, Ter-119, PDGFRα and Sca-1.**

*After crushing and washing, the boney fragments were collagenase digested to release the MSCs from their niche. Cells were labelled with CD45, Ter-119, PDGFRα and Sca-1. The cells were then sorted using a sequential gating strategy that allowed for the exclusion of dead cells (propidium iodide positive) on a Beckman Coulter MoFlo XDP high speed cell sorter (*Figure 3-1*A). Haematopoietic cells (CD45/Ter-119-PE) were also excluded (Figure 3-1B). The final gate allowed clear identification of dual positive PαS cells which are then readily sorted in to αMEM + 10%FCS (Figure 3-1C).*

### 3.2.2 Cell morphology and growth

Freshly isolated cells were cultured in αMEM + 10% FCS with media changed every 3 days. Their morphology and growth kinetics are assayed.

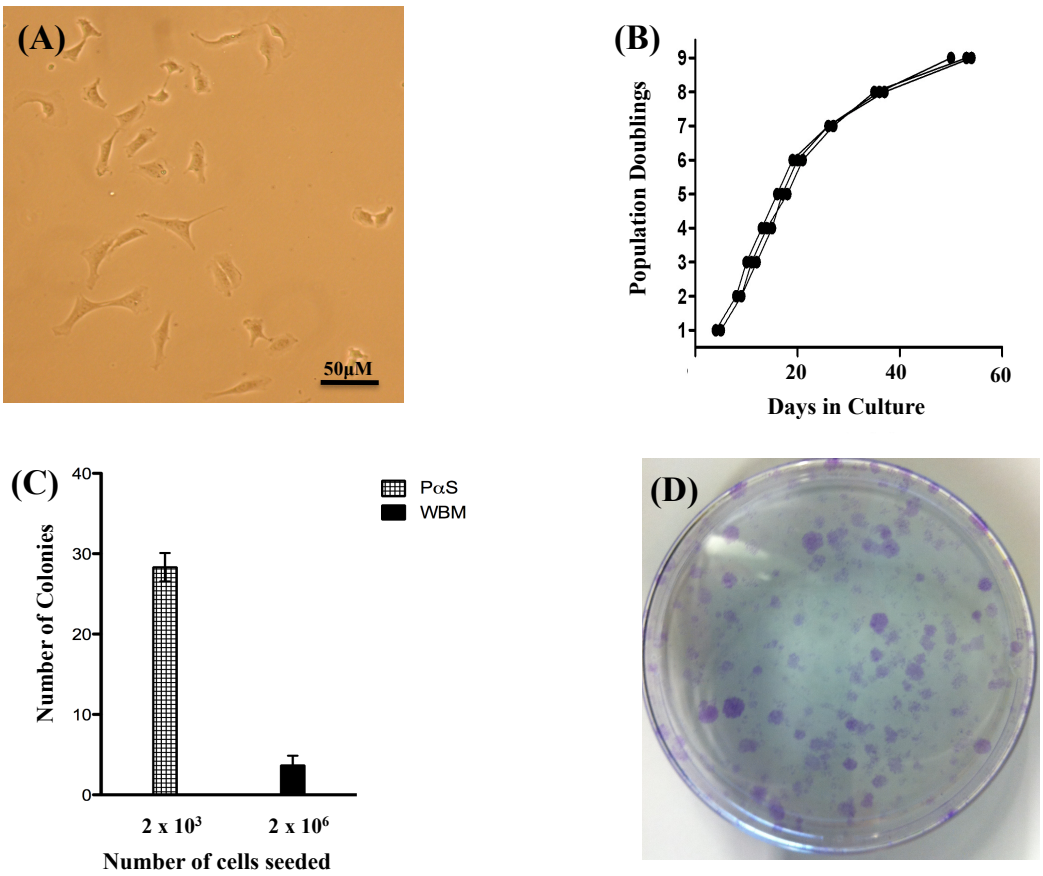


**Figure 3-2 PαS cells have spindle like morphology and robust growth kinetics *in vitro*.**

*PαS MSCs developed a spindle shaped morphology after 3 days in culture (*Figure 3-2*A). When cultured in SM, 5,000 PαS proliferate robustly with almost 9 population doublings over 2 months (*Figure 3-2*B). PαS cells formed far more CFU-Fs compared to whole BM (*Figure 3-2*C&D) demonstrating significant enrichment of MSCs in the PαS fraction.*

### 3.2.3 Surface marker expression

I then examined surface marker expression in cultured PαS MSCs. MSCs were therefore stained with appropriate antibodies for the previously described MSC markers CD29, CD90, CD49e, Sca-1, CD44, CD105 and CD140a and the haematopoietic markers CD45, Ter-119 and CD34.

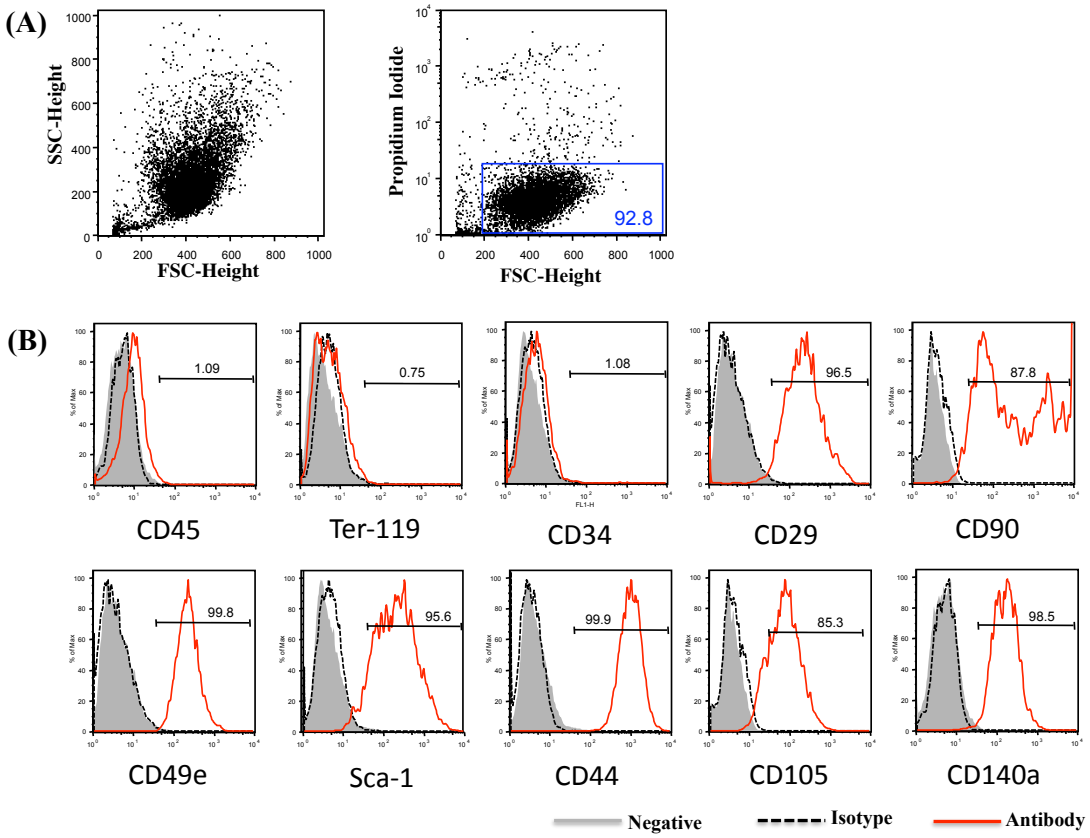


**Figure 3-3 Surface marker expression on PαS MSCs was examined by flow cytometry.**

*Dead cells were excluded by selecting propidium iodide negative cells (*Figure 3-3*A). PαS cells lack expression of haematopoietic markers (CD45, Ter-119, CD34) and possess the MSC markers (CD29, CD90, CD49e, Sca-1, CD44, CD105 and CD140a) (*Figure 3-3*B). Negative and isotype controls are shown.*

### 3.2.4 Tri-lineage differentiation

I then examined tri-lineage differentiation of PαS MSCs to cartilage, fat and bone.

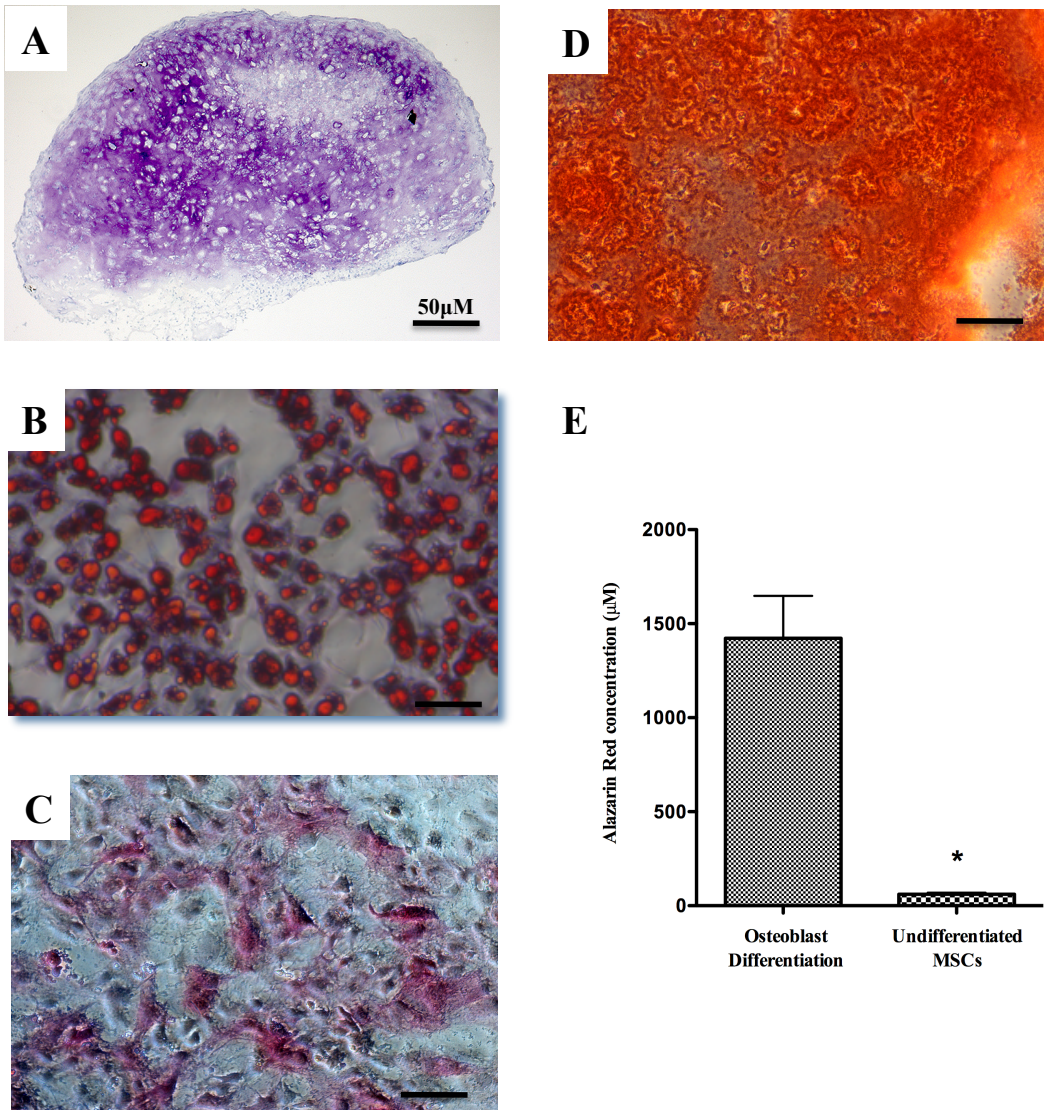


**Figure 3-4 Tri-lineage differentiation of PαS MSCs.**

*Staining with toluidine blue, Oil red O and alkaline phosphatase demonstrate robust differentiation to cartilage, fat and bone (*Figure 3-4 *A, B & C). Alizarin Red staining and quantification confirmed bone mineralisation and was increased compared to undifferentiated cells (*P<0.05) (*Figure 3-4 *D & E*).

### 3.2.5 Immunosuppressive effects of MSCs

The immunosuppressive effects were assayed in a lymphocyte proliferation assay. The assay was performed as described in the methods section. Graded numbers of MSCs were added to the reaction and their effects on $CD4^+$ cell proliferation was assessed.

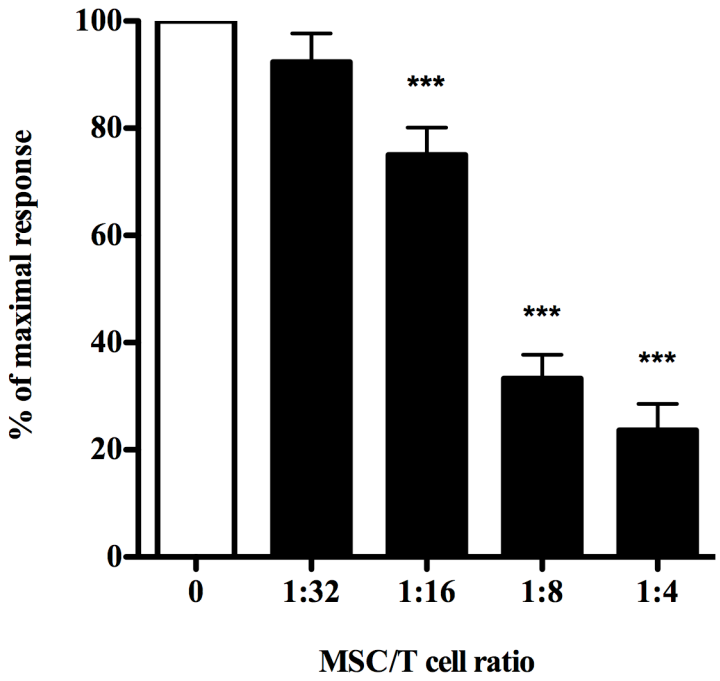


**Figure 3-5 PαS MSCs exert potent immunosuppressive effects on lymphocyte proliferation in vitro.**

*$CD4^+$ $CD25^-$ T-cells were purified from lymph nodes of BALB/c mice by magnetic bead separation. 3-day cultures were set up using 2.5 x $10^4$ T-cells stimulated by 5 x $10^4$ B-cells and 0.8µg/ml of anti-mouse CD3e antibody. $CD4^+$ T-cells were counted and percentage of maximal response across the groups calculated. MSCs exert a potent suppressive effect at 1:16, 1:8 and 1:4 ratios. (n=3, ***P<0.001 vs No MSCs).*

### 3.2.6 Mechanism of MSC immunosuppression

To determine the mechanism of MSC mediated suppression inhibitors of NO (L-NMMA), $PGE_2$ (Indomethacin), MMP 2&9 (SB-3CT) and IDO (1-Methyltryptophan) respectively were added individually to the proliferation assay.

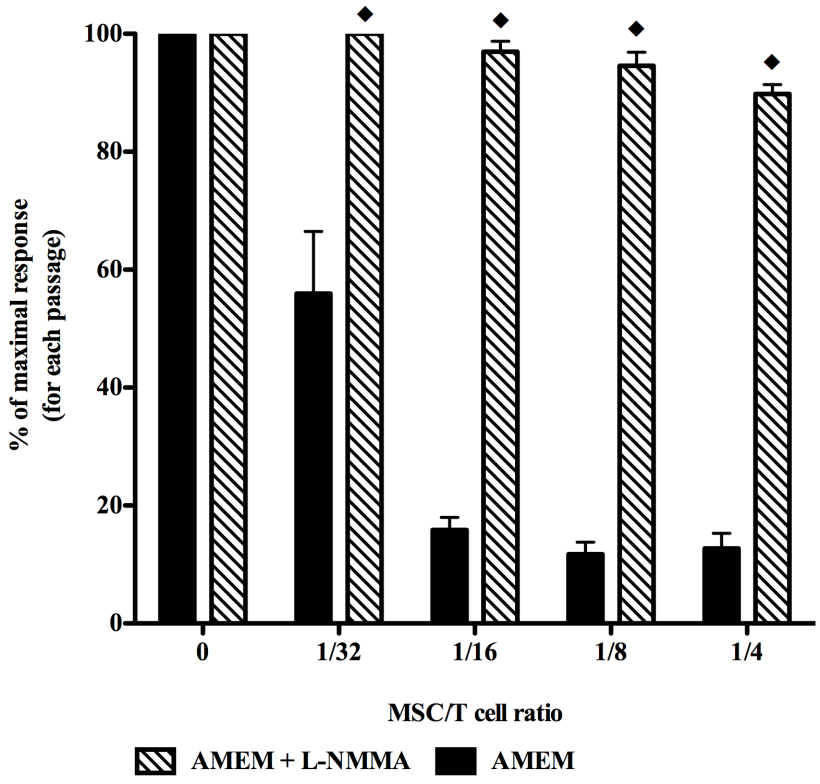


**Figure 3-6 PαS MSC immunosuppression is mediated by NO production.**

*The proliferation assay was repeated as described including the inhibitors described above. Addition of L-NMMA (1mM) potently inhibited the inhibitory effects of PαS MSCs on lymphocyte proliferation in vitro (n=3, ◆P<0.001 vs AMEM). The other inhibitors did not affect the immunosuppressive effect of the MSCs.*

### 3.2.7 Replicative senescence of MSCs

The effects of prolonged culture on PαS MSCs properties including tri-lineage differentiation and growth were examined.

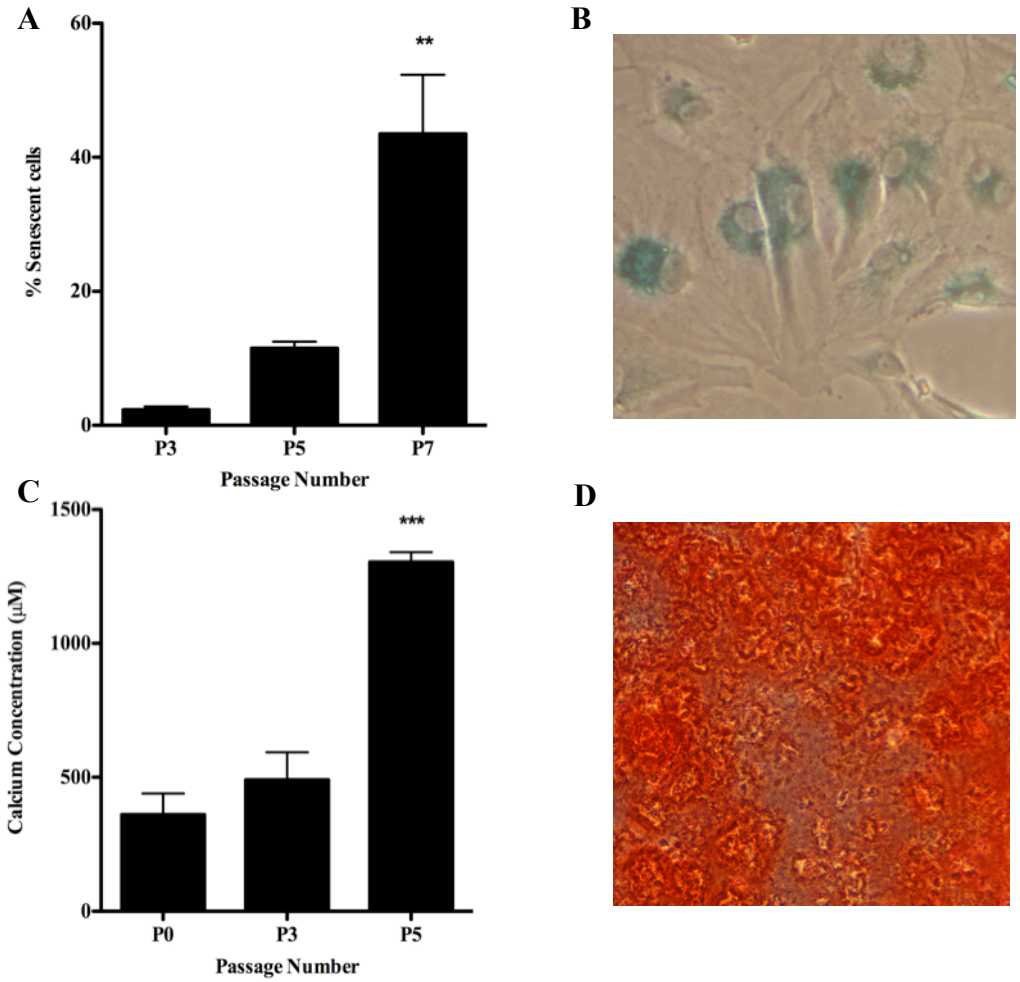


**Figure 3-7 Effects of prolonged culture on senescence and bone differentiation.**

*β-galactosidase staining was used to assess senescence. The proportion of senescent cells in standard PαS MSC culture increased over time (*Figure 3-7*A) [** p<0.01 vs. P3]. Following passage 7 almost half the cells in culture demonstrated positive β-galactosidase staining (*Figure 3-7*B). Interestingly bone formation increased with higher passage numbers [*** p<0.001 vs. P0] (*Figure 3-7*C & D).*

### 3.2.8 Fat differentiation after prolonged culture

To examine if prolonged culture of PαS MSCs altered fat differentiation I induced adipocyte differentiation in PαS MSCs at different passage numbers as described in the Methods section.

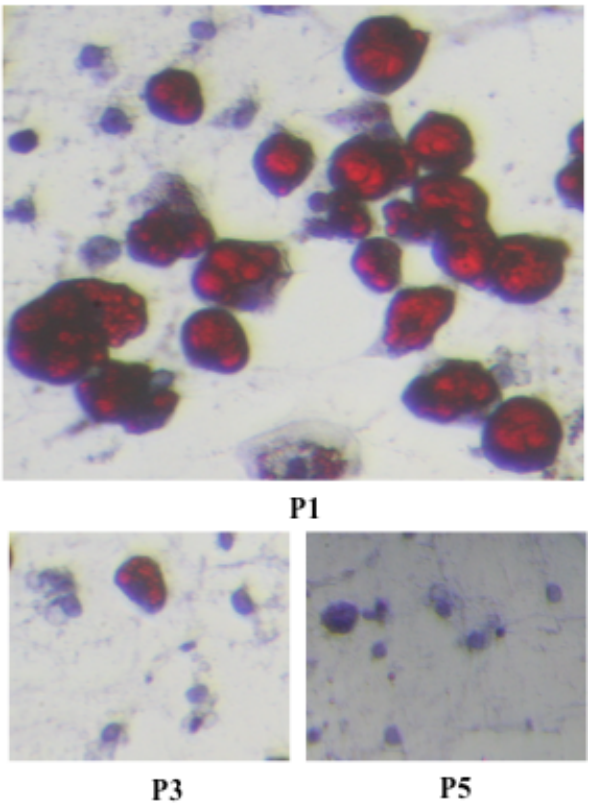


**Figure 3-8 Fat differentiation of PαS cells at different passage numbers.**

*PαS cells were cultured as previously descried. At passage 1, 3 and 5 once confluent media was changes to adipogenic induction media for 4 days followed by adipogenic maintenance media. Cells were stained for Oil red O (Figure 3-8). Unlike bone, fat differentiation is lost in during long-term culture of PαS MSCs.*

### 3.2.9 MSC immuosuppression after prolonged culture

I then examined the effects of prolonged culture on the immunosuppressive potential of MCSs in the $CD4^+$ T cell proliferation assay.

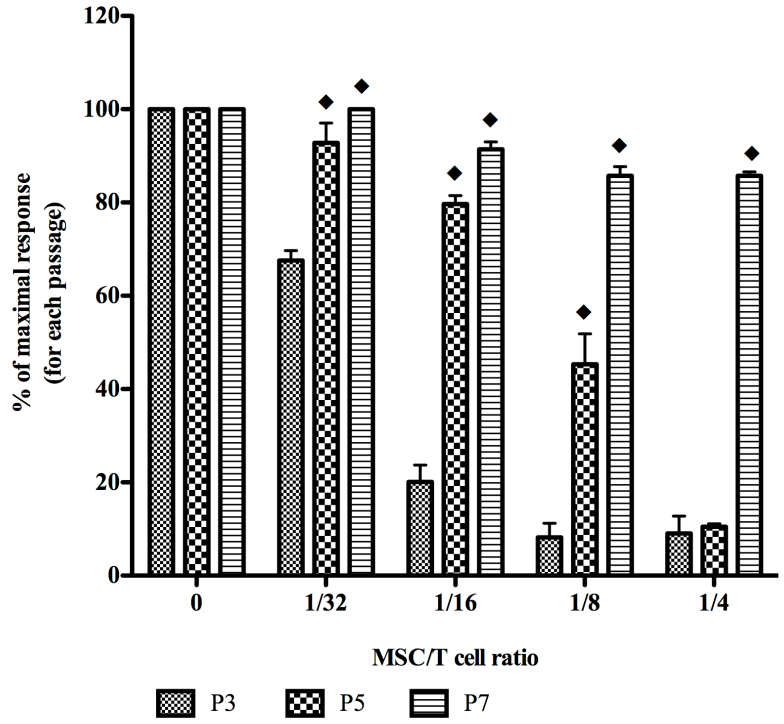


**Figure 3-9 Immunosuppressive effects of PαS MSCs at P3, P5 and P7 on $CD4^+$ T-cell proliferation.**

*PαS MSCs at P3, P5 and P7 were added to the CD4 T-cell proliferation assay as previously described. PαS at P5 and P7 were significantly less potent at inhibiting CD4 T-cell proliferation and MSC to lymphocyte ratios of 1/32, 1/16, 1/8 and 1/4 (n=3, ◆P<0.001 vs P3).*

## 3.3 Discussion

PαS cells were isolated accordingly to a published methodology (Morikawa et al., 2009a, Houlihan et al., 2012). The PαS fraction is greatly enriched for CFU-F generating almost 30 colonies per 2000 cells seeded. 1 in every 50 PαS cells is a CFU-F, almost 20,000 fold greater than that of whole BM. PαS cells differentiate robustly into fat, bone and cartilage and express typical MSC markers. This is the first demonstration that PαS MSCs exert a potent immunosuppressive effect on lymphocyte proliferation. This effect was mediated by NO production. Despite the potent nature of these cells, prolonged culture on plastic changes their phenotype profoundly. Over time cellular senescence increases (as evidenced by increased β-galactosidase staining) and fat differentiation potential diminishes. In contrast, bone differentiation increases as the cells age. Similar findings have been described before in hMSCs (Wagner et al., 2008).

PαS MSC isolation is a significant advance in the field. As previously stated traditional MSC isolations methods have been fraught with complications (Phinney et al., 1999). The prospective isolation of PαS MSCs avoids cellular contamination and the need for long-term culture. Additionally the identification specific murine MSCs markers (PDGFRα and Sca-1) allow in vivo visualization of MSCs within their niche (Morikawa et al., 2009a). These advances will enable investigators to interrogate MSC functions in vivo as well as define conditions to optimise their therapeutic potential. MSCs have potent immunosuppressive properties *in vitro* and *in vivo* (Uccelli et al., 2008). NO has been reported as a mechanism through which MSCs

suppress the immune system (Sato et al., 2007). In vivo, MSC infusion into a murine model of GVHD produced a significant survival benefit. MSCs isolated from NO knockout mice or use of the NO inhibitor L-NMMA blocked this effect entirely (Ren et al., 2008). Therefore PαS MSCs may provide a useful substrate for defining conditions that optimizing therapeutic potential of hMSCs.

PDGF-BB, TFG-β and bFGF signalling is activated during MSC differentiation to fat, bone and cartilage (Ng et al., 2008). I will examine the effects of these GFs on the growth kinetics, differentiation potential and immunosuppressive properties of freshly isolated PαS MSCs to test the hypothesis that in vitro culture conditions influence the fate and therapeutic potential of MSCs.

# 4 Growth factors direct the lineage fate of cultured MSCs

## 4.1 Introduction

### 4.1.1 Does an MSC hierarchy exist?

Lineage priming is a model of stem cell signalling and differentiation in which the proliferating cell expresses a subset of genes associated with the differentiation pathways to which they can commit (Delorme et al., 2009). In the HSC field, significant progress has been made in delineating developmental pathways of lymphoid and myeloid lineages that establish their fate (Laiosa et al., 2006). Lineage trees demonstrating HSC differentiation hierarchy and the key genetic regulation points, are now a familiar sight in the published literature (**Figure 4-1**). Studies identifying transcriptional programs involved in lineage priming are providing novel biological insight into the earliest stages of haematopoiesis (Ng et al., 2009) and are of significant relevance to the clinical field identifying therapeutic targets for specific haematological diseases. In contrast to HSCs, the molecular mechanisms that maintain MSCs in their undifferentiated state, or determine their differentiation pathways, are still poorly understood. Due to traditional limitations of the methods used to isolate MSCs, it has not been possible to obtain a sufficiently pure MSC population to address these questions.

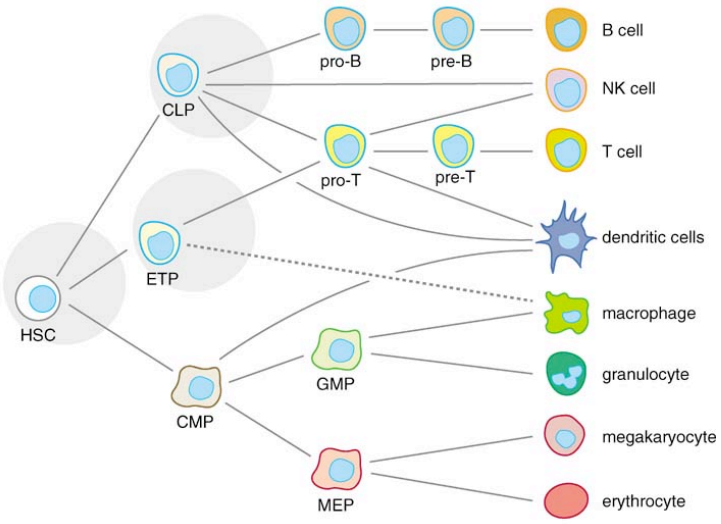


Figure 4-1 Lineage tree of adult haematopoiesis and lymphoid-myeloid branching points.

*HSCs are defined by their ability to generate all mature blood cell types and unlimited self renewal potency. This figure illustrates key steps in HSC differentiation to multipotent, oligopotent and unipotent progenitors that eventually give rise to terminally differentiated cells. Specific master regulator genes that determine each stage in the HSC differentiation and lineage fate have been identified. Although a similar schematic has been described for MSCs there are little data to support its existence. This figure was adapted from Laiosa et., 2006.*

### 4.1.2 Master regulators of fat, bone and cartilage have been identified

To investigate if MSC can be lineage primed by culture conditions it is first necessary to identify key genes or master regulators that pre-determine lineage specification. Master regulators of bone, fat and cartilage have been identified and will be discussed here. Sox9 mRNA is expressed at high levels predominantly in mesenchymal condensations throughout the embryo before and during the deposition of cartilage (Wright et al., 1995). $Sox9^{-/+}$ mice die shortly after birth, due to complications of skeletal malformation including respiratory distress supporting a critical role for Sox9

in regulating the rate of hypertrophic chondrocyte differentiation during development (Kist et al., 2002). Additionally, a Sox9 mutation was found to cause Campomelic dysplasia in humans, a rare genetic disorder characterised by significant skeletal abnormality (Wagner et al., 1994). Runx2 has been proposed as bone master regulator. Mice with a homozygous mutation in Runx2 lack of ossification of almost all bones and have significant skeletal abnormality (Kist et al., 2002, Komori et al., 1997). In humans it is linked to a rare condition called Cleidocranial dysplasia, which is characterized by severe skeletal dysplasia (Lee et al., 1997). Peroxisome proliferator-activated receptor gamma (PPARγ) is known to be a master regulator of fat differentiation (Tontonoz and Spiegelman, 2008). Forced expression of PPARγ is sufficient to induce adipocyte differentiation in fibroblasts. In fact no other factor promotes adipogenesis in fibroblasts in the absence of PPARγ (Tontonoz et al., 1994).

### 4.1.3 Aims

Hypothetically, defining conditions that lineage prime MSCs may be used to tailor cell therapy for specific indications. For example an osteogenic primed MSC would be an ideal choice for a patient with OI. Alternatively, a chondrogenic primed MSC would best treat a patient with cartilage damage or osteoarthritis. Defining precise culture conditions that lineage prime MSCs to their respective fates therefore is of significant interest. In addition to matrix stiffness it is likely that selected GFs might influence MSC fate. Ng *et al*. used a broad transcriptomics approach to identify PDGF-BB, FGF2, and TGF-β1 as key signalling pathways in human MSC proliferation and differentiation (Ng et al., 2008). PDGF signalling was active during adipogenesis and chondrogenesis, TGF-β signalling was active during

chondrogenesis, and FGF signalling was active during osteogenesis, adipogenesis and chondrogenesis. Inhibition of any of the three pathways resulted in an altered differentiation potential and increased population doubling times. Conversely, the addition of all three GFs was sufficient to maintain MSCs in serum-free media (Ng et al., 2008). The aim of this Chapter is therefore to assess lineage priming of PαS MSCs at a genetic level following culture in SM (αMEM +10%FCS) alone or supplemented with either bFGF, PDGF-BB or TGF-β.

## 4.2 Results

### 4.2.1 Gene expression during bone, cartilage and fat differentiation

A list of genes involved bone, fat and cartilage development and differentiation was compiled. Genes involved in the patterning and development of each tissue during growth of the embryo were listed (Section 1.2). Genes involved in lineage priming of MSCs to bone, cartilage and fat were listed (Delorme et al., 2009). Finally genes up regulated during MSC differentiation to each lineage were listed (Ng et al., 2008).

**Table 4-1** Genes involved in the development of cartilage, bone and fat.

| Condition | Master Regulators | Transcription factors | Signalling pathways |
|---|---|---|---|
| **Cartilage** | Sox5<br>Sox9 | HoxA, HoxD, Hoxd11, Hoxd13, Cebpb, Tfap2a, Nkx3.2, Gli3, Plzf, Sox6, Runx3 | Shh, Smo, Ptch1, Bmp2, Bmp4, Bmp7, Bmpr1a, Bmpr1b, Smad1, Smad5, Smad8, Mapk14, Mapk3, Mapk1, Fgf8, Fgf10, Wnt2, Wnt2c, Wnt3a, Ctnnb1, Col2a1, Col11a2, CDRAP, Col9a1, Acan, Ihh, Wnt4, Fgfr3, Pthr1, Comp, Col10a1, Agc1, Col2a1, Col11a1, Rankl, Mef2c, Hapln1, Col10a1 |
| **Bone** | Runx2<br>SP7 | Cbfb, Gata1, Gata2, Gata3, Cebpb, Ets1, Men1, Msx1, Msx 2, Dlx5, Dlx6, Jun, Egr2, SP3, Atf4, Osx, Znf145 | Bmp2, Bmp4, Bmp7, Wnt3a, Wnt10b, Lrp5, Smad1, Smad4, Smad5, Ctnnb1, Ihh, Bmp6, Igf1, Dkk1, Dkk2, Wisp1, Wisp2, Bmpr1a, Pthr1, Lifr, Thy1, Col1a2, Bgn, Dcn, Opn, Ogn, Comp, Alpl, Opg, Csf1, Il18, Kitl, Esr1, Col1a1, Ibsp, Tnfsf11, Bmp6 |
| **Fat** | Cebpa<br>Pparg | Hoxa5, Hoxa4, Hoxc8, Nr2f1, Hoxa10, Hoxc9, Twist1, Tbx15, Shox2, Gata3, Gli3, Cebpb, Cebpd, Srebf1, Cited1 | Bmp4, Fgf1, Fgf10, Fgf16, Fgf19, Gpc4, Sfrp2, Nodal, Nog, Dlk1, Wisp2, Smo, Pdgfrb, Cspg4, CD24, Col6a2, Sfrp2, Igf1, Adfp, Aoc3, Slco2a1, Lifr, Fabp4, Aqp7, Lpl, Plin1, Angptl4, Acdc, Rxra, Gpd1, Adipoq, Apoe, Apol6, Flrt3,Mrap |

### 4.2.2 Additional genes of interest

In addition to examining genes involved in cartilage, bone and fat development we also identified a panel of genes expressed in naive undifferentiated MSCs (Delorme et al., 2009). These might identify culture conditions that prevent MSC differentiation and maintain MSCs in a multipotent state. Cell cycle genes and embryonic stem cell markers are included to identify MSC potency. Finally, I have listed the genes that encode for FGF, PDGF and TGF receptor families.

**Table 4-2** Additional genes of interest to this study.

| Condition | Gene symbols |
|---|---|
| **Growth factor receptors** | Pdgfra, Pdgfrb, Fgfr1, Fgfr2, Fgfr3, Fgfr4, Fgfrl1, Tgfbr1, Tgfbr2, Tgfbr3 |
| **MCS markers** | Eras, Zfp42, Nr0b1, Gdf3, Dppa5a, Nanog, Pou5f1, Sox2, Gata2, Gata6, Fog2, Mef2a, LifIl6, Fgf2, Inha, Nrg1, Grem1, Ccl26, Wnt7b, Dlk1, Cd200, Bst1, Nt5e, Met, Eng, Dpp4, Tnfrsf12a |
| **Cell cycle** | Birc5, Ccnb1, Cdkn3, P16INK4a, P21, P14ARF |

### 4.2.3 Master regulators of bone, cartilage and fat.

Here we examine the expression of master regulator genes involved in fat, cartilage and bone differentiation. Gene expression was normalized to the mean value across all the groups to allow ease of comparison. The data are expressed as a fold change above or below the mean. For statistical comparison gene expression was normalised to control tissue (SM alone) and expressed as fold change.

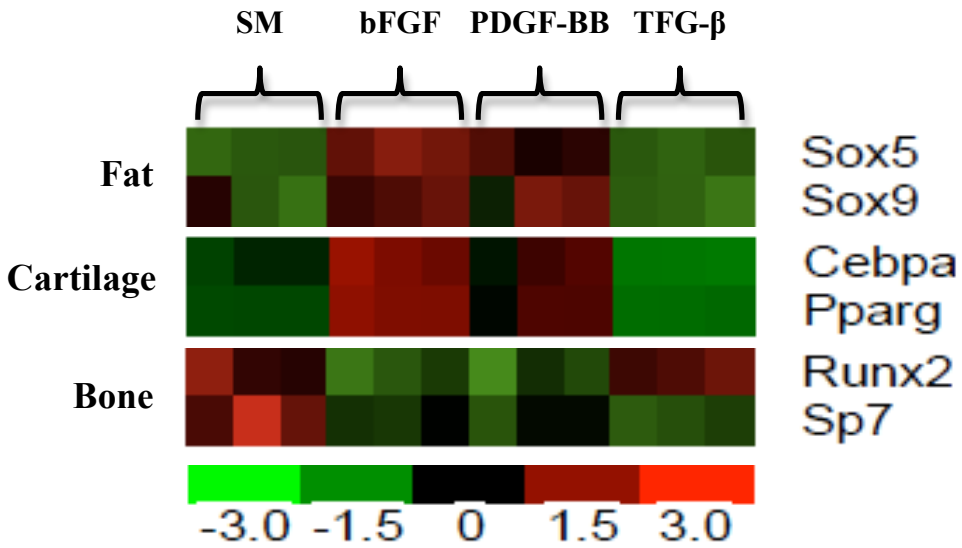


**Figure 4-2 Master regulators for fat, bone and cartilage differentiation are shown.**

*Expression of the master regulators of fat differentiation, Cebpa and PPARγ, was significantly increased in bFGF (2.55 and 4.53 fold) and PDGF-BB (1.7 and 2.97 fold) compared to SM ($P<0.001$ for all comparisons). In contrast, expression of the bone master regulator, Runx2, was significantly reduced in bFGF (-1.31 fold) and PDGF-BB (-1.3 fold) ($P<0.001$ for all comparisons). Finally, Sox5 and Sox9 (chondrogenic genes) expression were significantly increased in bFGF (4.56 and 1.42) and PDGF-BB (3.28 and 1.38 fold) compared to SM ($P<0.01$).*

### 4.2.4 Mesenchymal stem cell markers

In addition to examining genes involved in cartilage, bone and fat development I also identified gene expressed in naive undifferentiated MSCs (Delorme et al., 2009). A list of these genes including embryonic stem cells markers can be found in Table 4-2.

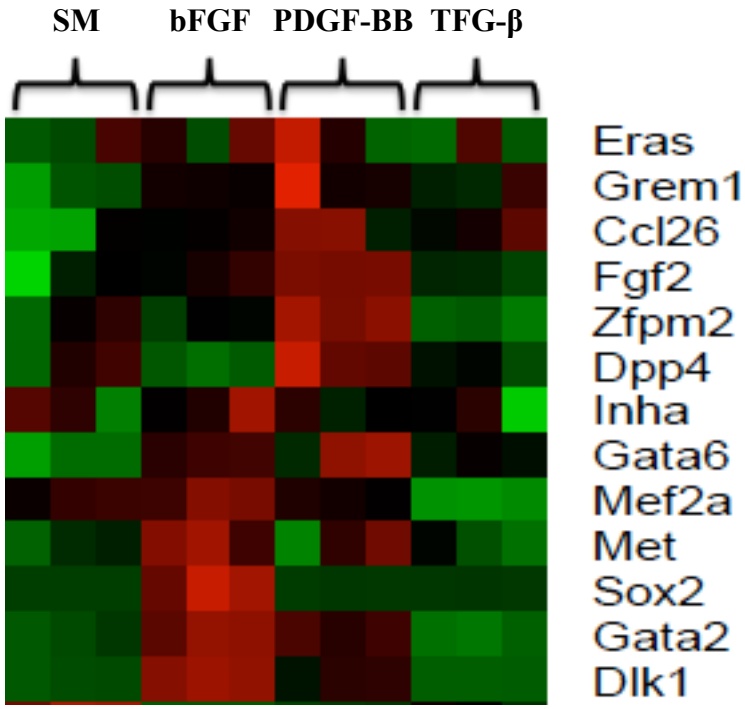


**Figure 4-3 Naive MSC markers and embryonic stem cell markers are shown.**

*The MSC markers examined include transcription factors, extracellular mediators and cell cycle regulators. The heat map demonstrated higher expression of these markers in the bFGF and PDGF-BB groups. Specifically expression of Sox2 (7.39 fold), GATA2 (1.56 fold), GATA6 (1.9 fold), and Dlk1 (11.07 fold) were increased in bFGF group compared to SM ($P<0.01$ for all comparisons).*

### 4.2.5 Surface receptors and cell cycle genes

bFGF signals through FGFR 1-4 and FGF receptor-like 1. PDGF-BB signals through receptors compromised of PDGFRα and PDGFRβ subunits. TGF-β signals through TGF-βR 1-3. Genes regulating cell cycle were also examined.

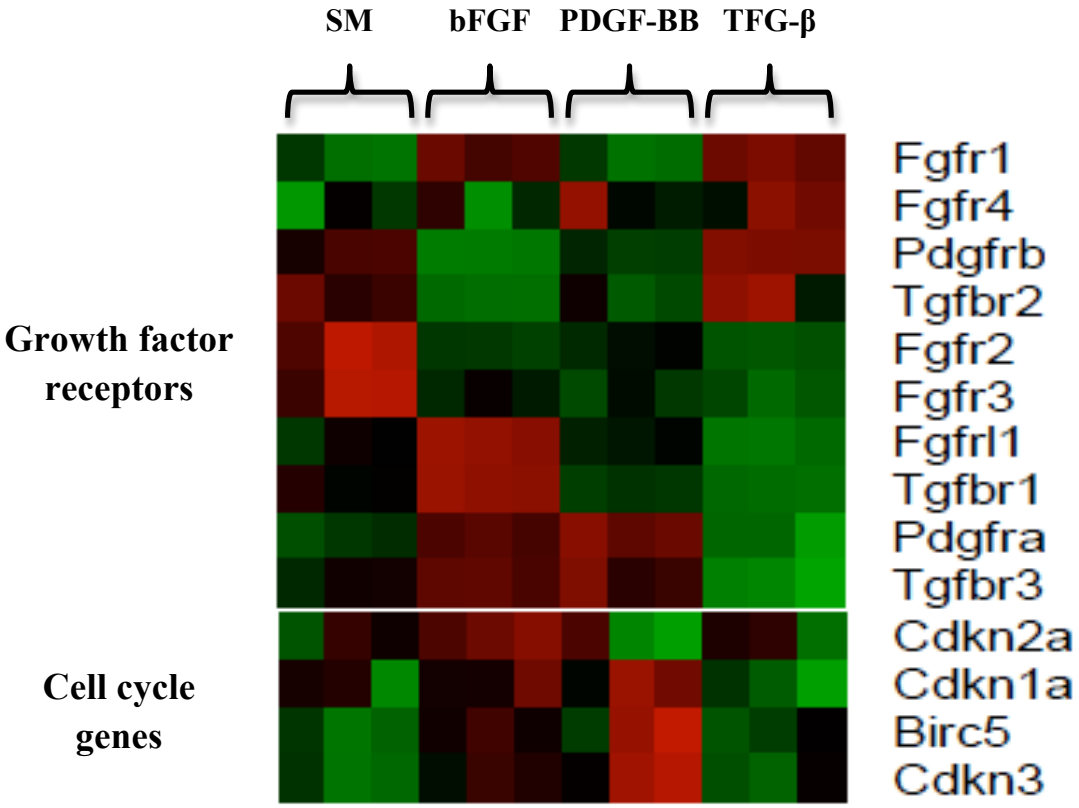


**Figure 4-4 Cell cycle and growth factor receptor gene expression in the different groups is shown.**

*This figure shows relative expression of growth factor cell cycle genes in each group. Expression of FGFR1 (1.42 fold), FGFrl1 (1.54 fold) and PDGFRα (1.62 fold) were increased in the bFGF group (P<0.01 vs SM). Similarly, PDGFRα (1.79 fold) expression was increased in PDGF-BB cells (P<0.01 vs SM). Interestingly expression of PDGFRβ was increased on TGF-β cells (P<0.05 vs SM). Expression of the cell cycle genes Birc5 (1.51 and 1.71 fold) and Cdkn3 (1.4 and 1.65 fold) was increased in bFGF and PDGF-BB respectively (P<0.01 vs SM).*

### 4.2.6 Transcription factors that regulate fat development

In order to look in detail at genes that might regulate tri-lineage differentiation I examined genes that encode transcription factors and signalling molecules involved in fat development. A list of transcription factors expressed during fat development is shown in Table 4-1.

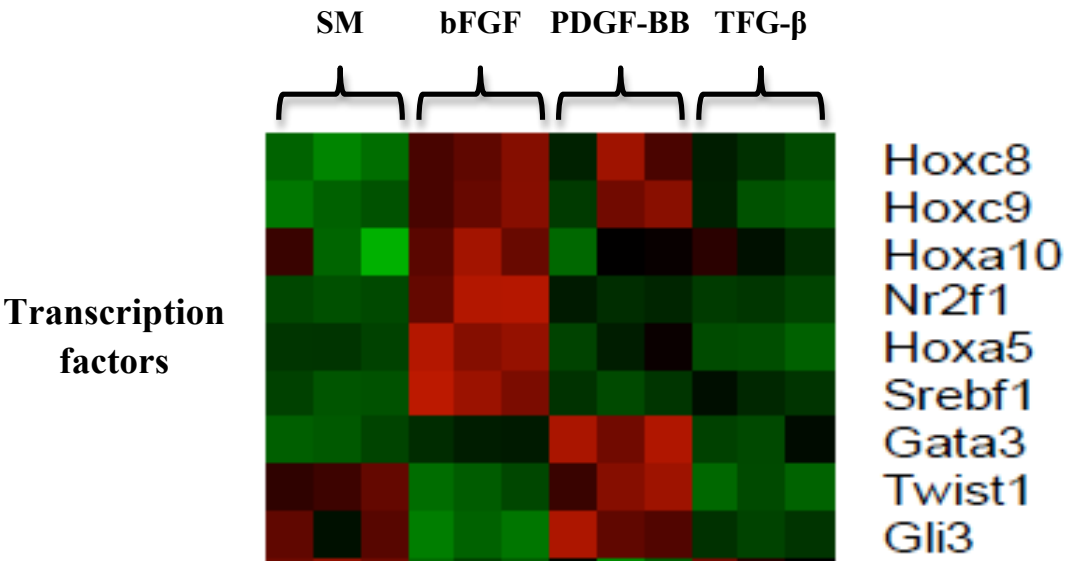


**Figure 4-5 Transcription factor expression for fat development are shown for all groups.**

*The heat map demonstrates higher gene expression in bFGF and PDGF-BB groups. The homeobox gene family plays an important role in mesenchymal lineage development. bFGF and PDGF-BB cells up regulate Hoxc8 (1.48 and 1.41 fold respectively; P<0.001 vs SM). Additionally bFGF cells have increased expression of Hoxc9 (1.37 fold) and Hoxa5 (1.92 fold) and Srebf1 compared to SM cells (2.47 fold) (P<0.001 vs SM for all comparisons).*

4.2.7 Adipogenic signalling molecules

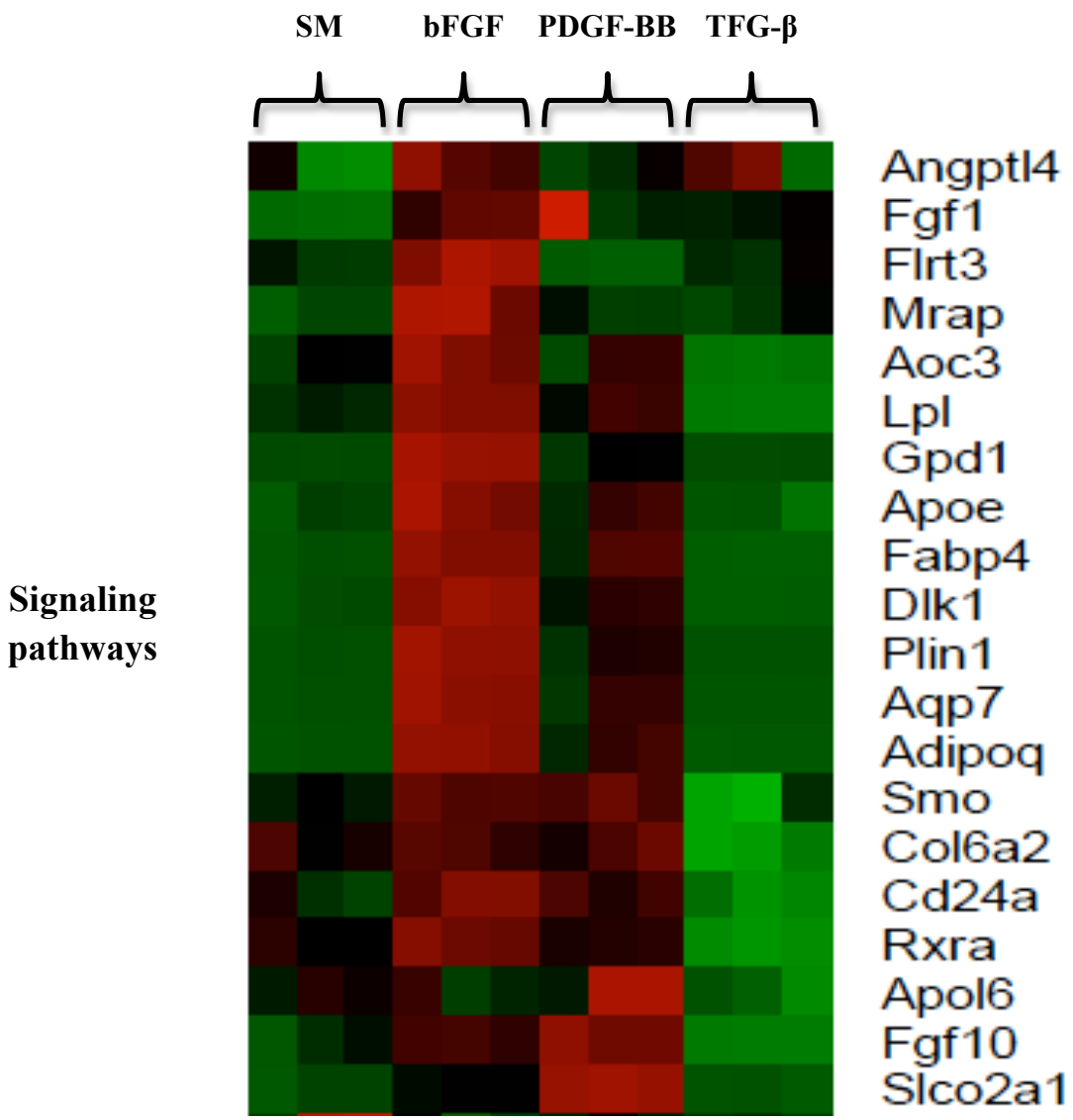


**Figure 4-6 Genes encoding for signalling molecules involved in fat development are shown.**

*The heat map demonstrates highest expression of gene transcripts in bFGF and PDGF-BB groups. These data combined with master regulator and transcription factor expression strongly suggest that addition of bFGF and PDGF-BB to culture media lineage prime MSCs to adipocytes.*

### 4.2.8 Bone transcription factors

Transcription factors implicated in bone development were then examined.

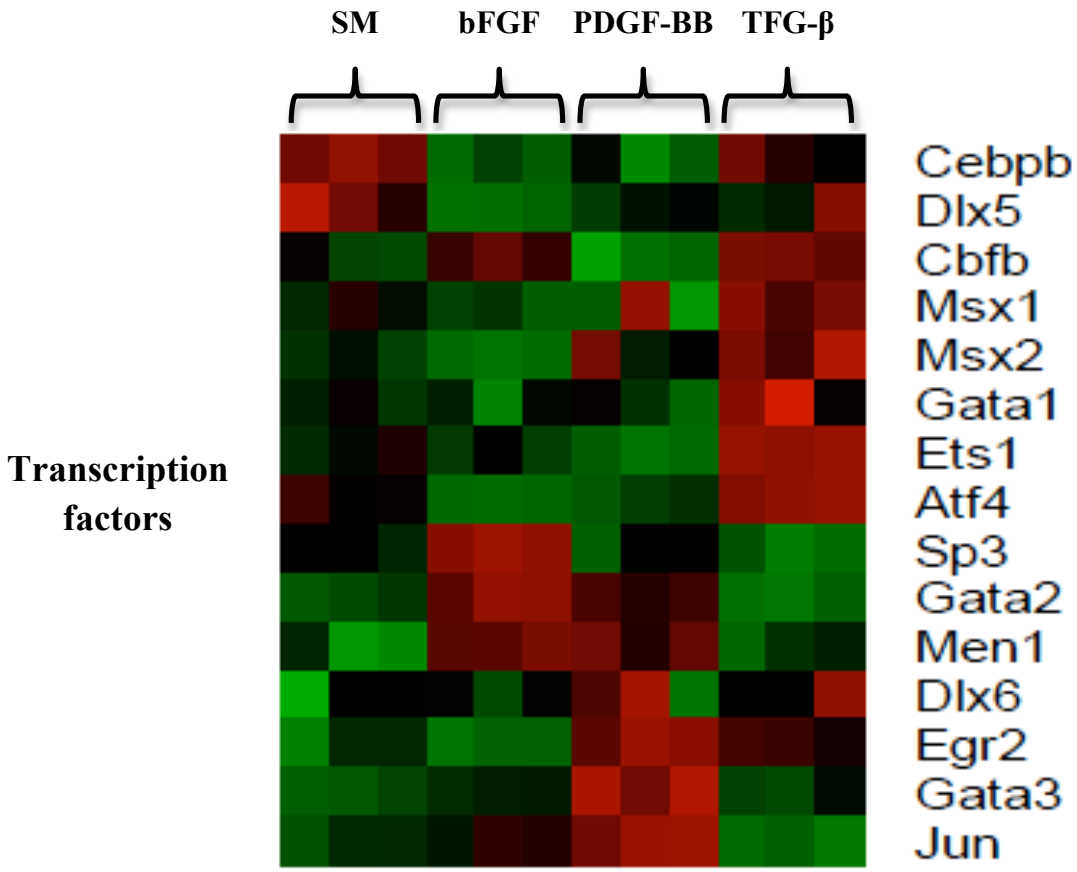


**Figure 4-7 Transcription factors involved in bone development.**

*Runx2 (master regulator for bone differentiation) was expressed at higher levels in SM cells compared to other groups (Figure 4-2). Additionally, Dlx5, Cebpb, Msx2 and Atf4 were expressed at higher levels in the SM group compared to bFGF and PDGF-BB (P<0.01 for all comparisons). Interestingly TGF-β cells up regulated several genes including Msx5 (1.45 fold), Gata1 (1.22 fold), Ets1 (1.37 fold), Atf4 (1.45 fold) above SM cells (P<0.001). bFGF and PDGF-BB also up regulated genes (Dlx6, Gata2, Men1, Sp3, Jun, Egr2) suggesting maintenance of multipotent phenotype.*

### 4.2.9 Bone signalling molecules

Down stream signalling during bone development was examined.

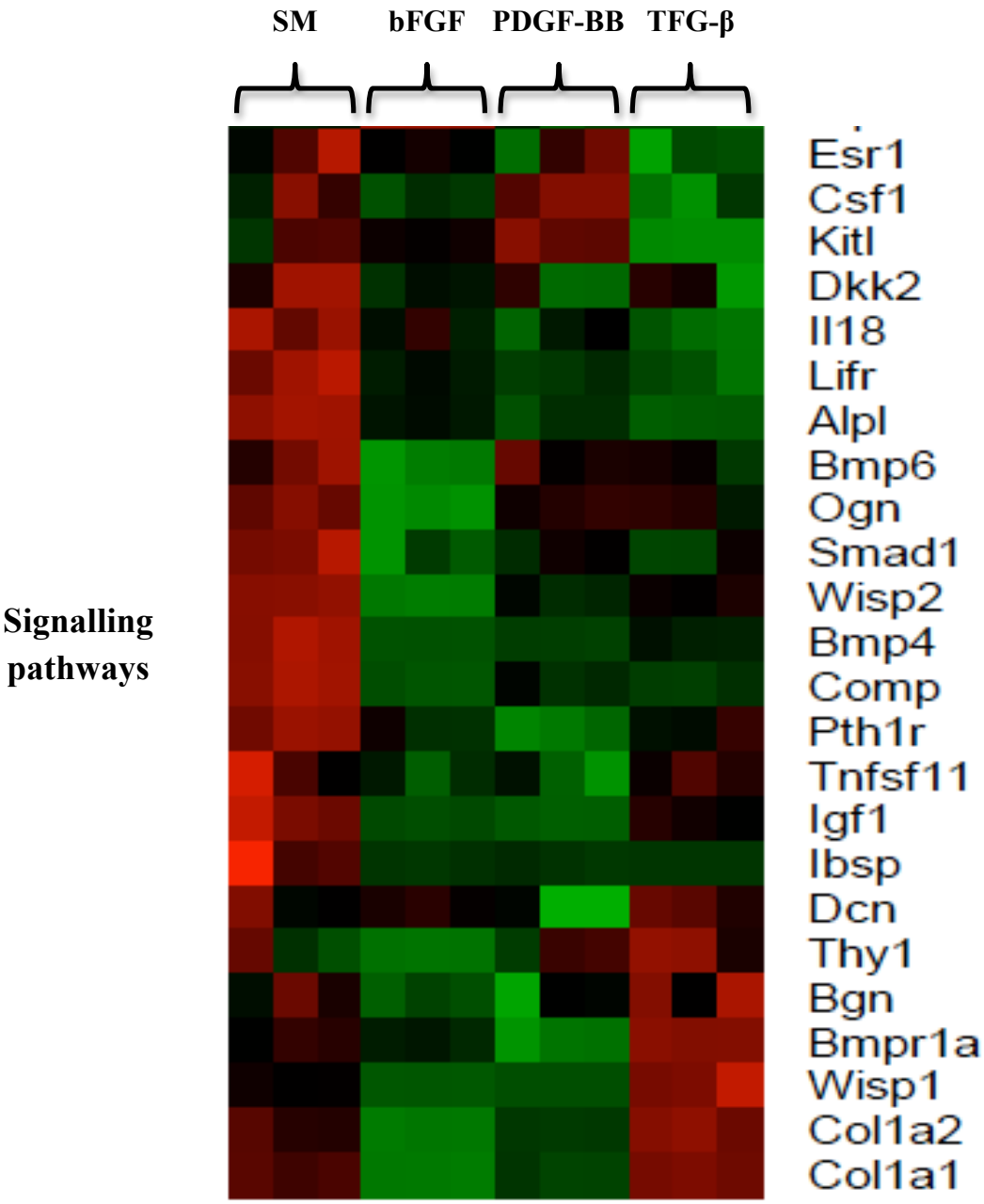


**Figure 4-8 Signalling molecules involved in bone development.**

*The heatmap demonstrates a clustering of high signal in the SM group. Quantitative assessment of gene expression is shown in Appendix 1.*

4.2.10 Chondrogenic transcription factors

The expression of chondrogenic transcription factors was compared across the groups. We previously identified increased expression of the master regulators Sox5 and Sox9 in bFGF and PDGF-BB groups.

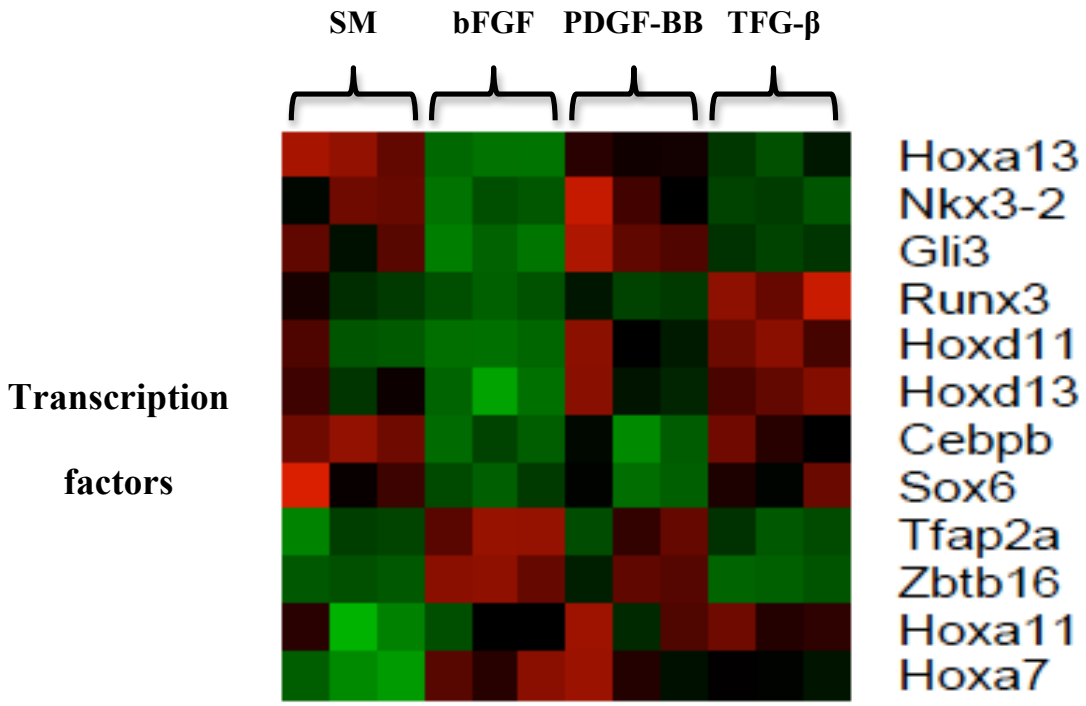


**Figure 4-9 Transcription factors involved in cartilage development.**

*There is no clear pattern of chondrogenic gene expression between the groups. Differentially expressed genes include reduced expression of Hoxa13, Nkx3-2, Gli3, Cebpb in bFGF ($P<0.01$ vs SM). Runx3 expression was increased in TGF-β compared to SM ($P<0.01$). Finally, Tfap2a, Zbtb16 and Hoxa7 expression was increased bFGF and PDGF-BB compared to SM. These data might suggest that SM and TGF-β are lineage primed towards cartilage.*

4.2.11 Cartilage signalling molecules

I then examined the relative gene expression of down stream molecules that determine chondrogenic development.

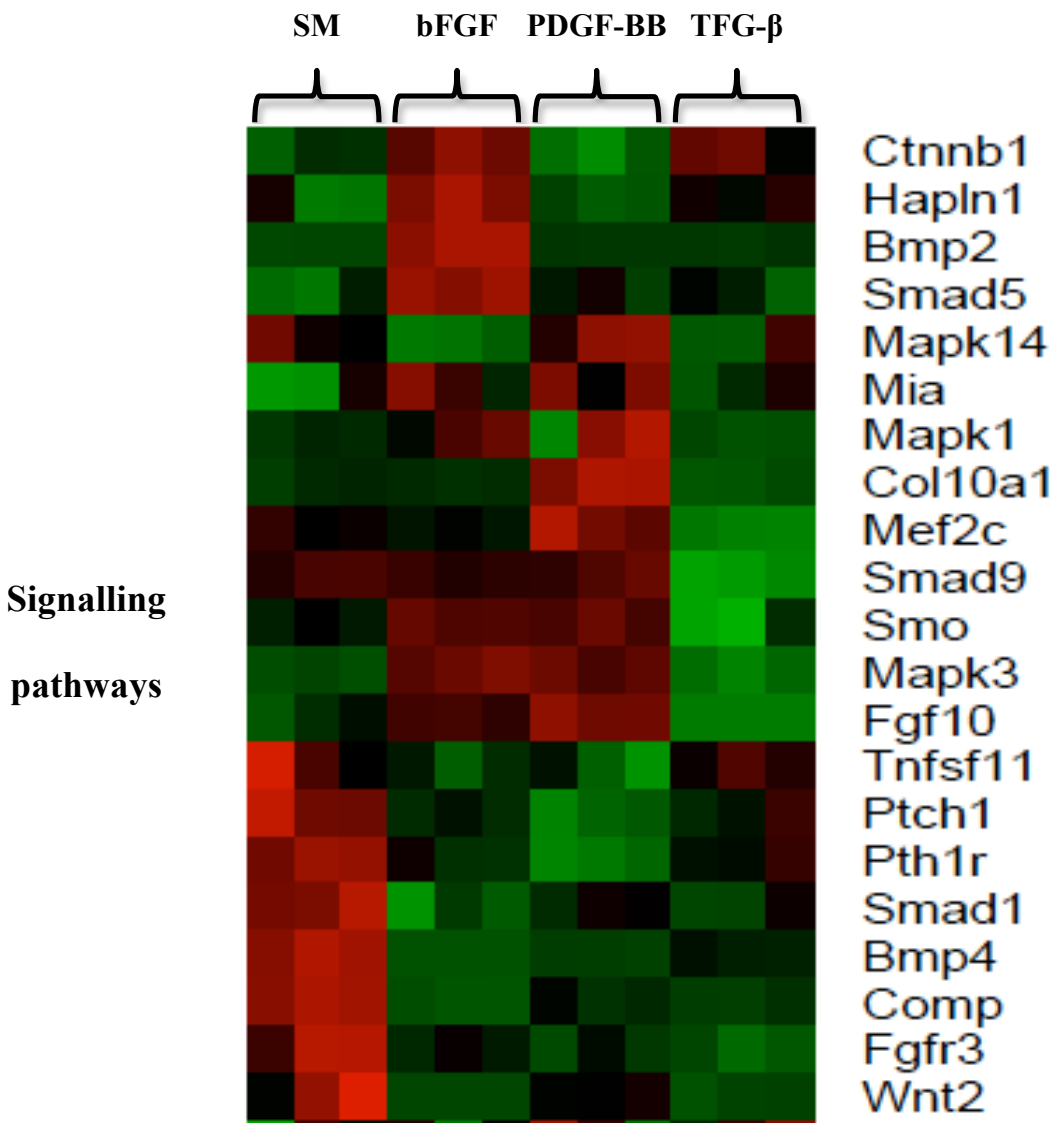


**Figure 4-10 Signalling molecules involved in cartilage development is shown.**

*MSCs cultured in SM, bFGF and PDGF-BB have increased expression of chondrogenic genes. These data suggest that TGF-β reduces chondrogenic potential of MSCs.*

## 4.3 Discussion

PαS MSCs cultured in SM alone are lineage primed towards bone. Addition of bFGF or PDGF-BB to SM significantly up regulated master regulators of fat (PPARγ) and cartilage (Sox9) compared to SM. These data strongly suggest that addition of GF to culture media can influence MSC fate. Additionally, cells cultured in bFGF maintain expression of naïve MSC markers (GATA2, GATA6, PDGFRα and Dlk1) and express higher levels of the pluripotency marker Sox2. bFGF and PDGF-BB groups have increased expression of cell cycle genes Birc5 and Cdkn3, suggesting augmented growth which is also a marker of MSC potency. Analysis of a broad selection of transcription factors and signalling proteins involved in tri-lineage differentiation broadly supported lineage priming of SM cells. The situation however appears less clear for cartilage. Although bFGF and PDGF-BB conditions up regulated Sox9 and Sox5, expression of other transcription factors and signalling molecules was highly variable between the groups. Further phenotypic study is required to confirm if supplementing media with GF can prime MSCs towards cartilage.

There are only limited data examining lineage priming in MSCs. One such study investigated mMSCs and hMSCs at a genetic and protein level for commitment to the following lineages: fat, bone, cartilage, vascular smooth muscle, cardiac and skeletal muscle, haematopoietic, hepatocytic and neuronal lineages (Delorme et al., 2009). Analogous to our approach they first identified 300 mRNA transcripts involved in lineage differentiation. They then compared genetic signatures of differentiated and undifferentiated cells to evaluate MSC lineage priming down selective routes. They

found that undifferentiated BM-MSCs were primed towards osteogenic, chondrocytic, adipocytic and vascular smooth muscle lineages. Primed cells readily differentiated down their pre-destined lineages. Additional evidence suggests that the stiffness of matrix upon which MSCs are cultured may lineage prime or restrict their fate (Engler et al., 2006). In brief, MSCs cultured on matrices of increasing elasticity or stiffness (1, 11, 34 kPa), preferentially express transcripts indicating neurogenic, myogenic and osteogenic differentiation respectively. Our data add to the existing literature and suggest further interrogation MSC differentiation is merited to help tease out mesenchymal hierarchy.

There are limitations of this work. Our results supports lineage priming of MSCs by supplementing culture media with GFs, these results need to be verified at a phenotypic level. Malignant transformation of murine MSCs after prolonged culture is well described and addition of GF to media may accelerate this process. While cells cultured in SM alone are primed towards osteogenic lineage and those cultured with bFGF or PDGF-BB are lineage primed to fat and cartilage, the situation is less clear for TGF-β. Nonetheless these data may have therapeutic implications with different culture media being selected depending on the therapeutic indication.

# 5 Growth factors influence the characteristics of cultured MSCs

## 5.1 Introduction

### 5.1.1 Commercially available contain GFs

I previously showed that supplementing culture media with different GFs (bFGF, PDGF-BB and TGF-β) activates genes involved in differentiation pathways for bone, cartilage and fat. There are currently several commercially available media for the expansion of hMSCs including Mesencult-XF (STEMCELL Technologies), StemPro MSC SFM Zeno-Free (Invitrogen), MSCGM-CD (Lonza) and PPRF-msc6 (Lonza). Many of these are xenobiotic-free, serum-free media, and are supplemented with GFs (Jung et al., 2010). These media are specifically designed to enhance MSC growth and fat differentiation, which are considered hallmarks of potency. Commonly used growth factors for expansion of MSCs in vitro include bFGF, PDGF-ββ and TGF-β (Chase et al., 2010, Jung et al., 2012b). Our previous results suggest that each of these GFs may lineage prime or restrict MSCs towards fat, bone or cartilage. It is currently not clear how GF lineage priming may affect the regenerative and immunosuppressive properties of MSCs.

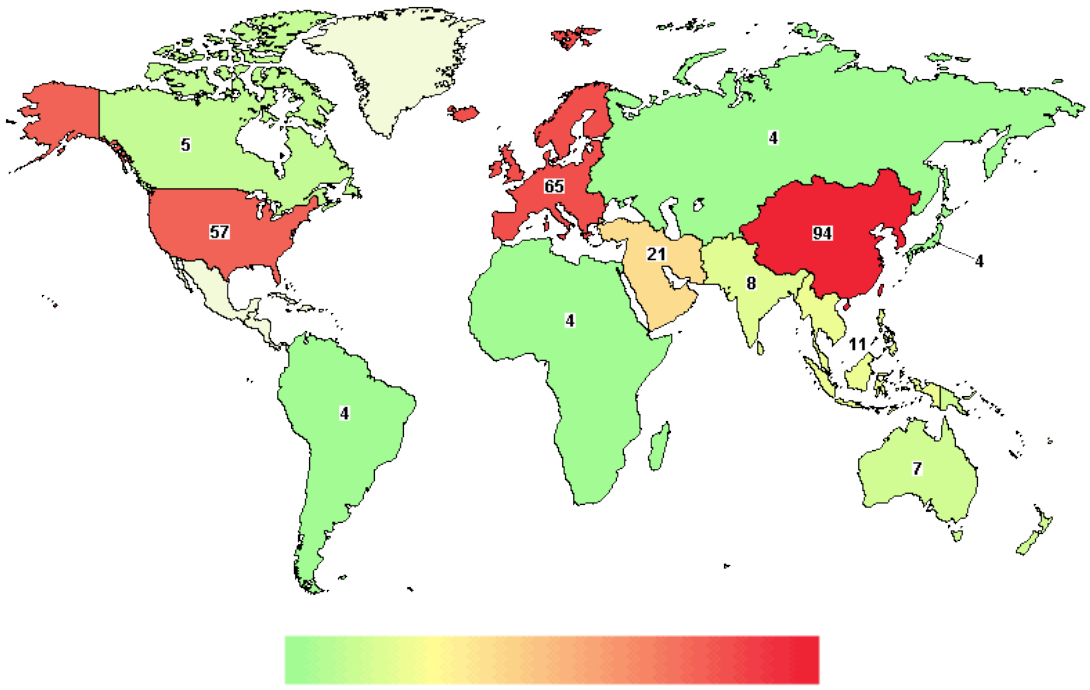


**Figure 5-1 Distribution of MSC clinical trials worldwide.**

*This figure illustrates the worldwide distribution of clinical trials using MSCs. There is significant interest the therapeutic potential of MSCs for a wide variety of diseases.*

### 5.1.2 MSCs are being used in clinical trials

The therapeutic potential of MSCs has generated significant excitement. There are currently 276 studies registered on 'ClinicalTrials.gov' investigating MSCs in a variety of different diseases. The worldwide distribution of these trials is shown in Figure 5-1. The speed at which MSCs have progressed from test tubes in laboratories to human therapies has been remarkable. There are several reasons for this. The most obvious of these is the significant clinical demand for novel therapies for difficult to treat conditions such as steroid refractory GVHD. mMSCs have been disappointing for pre-clinical testing. As highlighted earlier they are difficult to isolate and cultured

murine MSCs often undergo malignant transformation (Pittenger et al., 1999, Tolar et al., 2007). Several questions relevant to the use of MSCs therapeutically have therefore remained largely unanswered. These include 1. What is the best MSCs isolation method? 2. Do culture conditions including the addition of GFs to culture media influence their regenerative or immunosuppressive potential? 3. What is the optimal transfusion route and dosing schedule? The prospective isolation of a PαS MSCs provides an ideal substrate to address some of these questions.

### 5.1.3 Chapter Aims

The aims of this Chapter are manifold. Firstly, I wanted to compare the growth of PαS MSCs cultured in SM alone and supplemented with bFGF, PDGF-BB or TGF-β respectively. As robust proliferation and fat differentiation are indicative of a potent MSC population, I examine the phenotypic effects of GFs on fat differentiation. Thirdly, I examine the effects of GF priming on bone differentiation and immunosuppressive potential. Recent data in the literature suggest that mMSCs are prone to malignant transformation during prolonged culture. I therefore finish by examining the karyotype of cells cultured in each media type.

## 5.2 Results

### 5.2.1 Effects of GFs on colony forming potential

The CFU-F assay was performed as previously described. 2000 freshly isolated PαS cells were cultured in SM alone or supplemented with the following cytokines: bFGF, TGF-β or PDGF-ββ. Following 2 weeks of culture the colonies were stained with crystal violet.

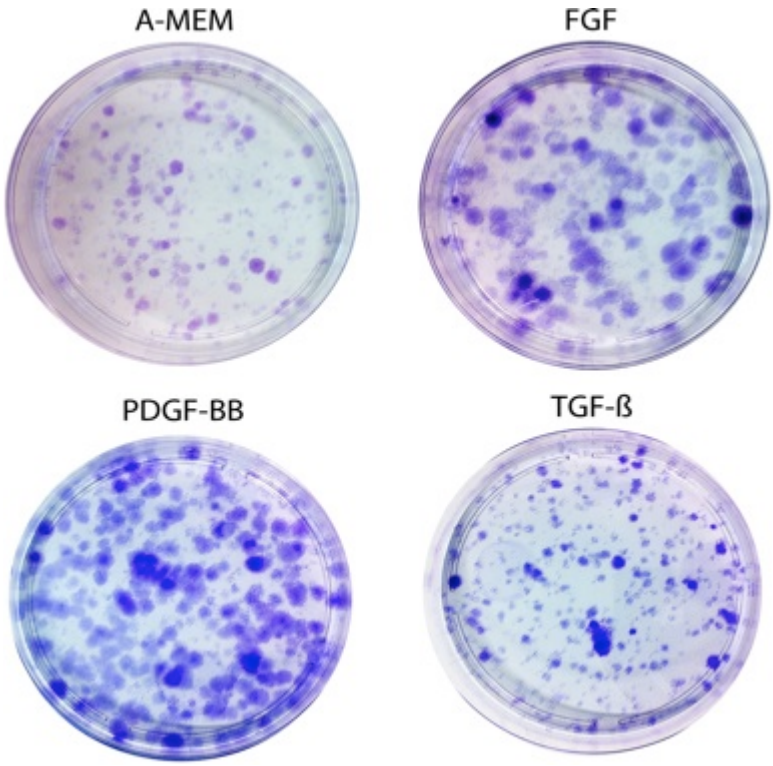


**Figure 5-2 CFU-F formation in the different media types.**

*Colony formation was increased following supplementation of the media with each growth factor (*Figure 5-2*). The effects were most pronounced following addition of bFGF or PDGF-BB as can be seen from this figure.*

### 5.2.2 Effects of cytokines on MSC growth curve

The proliferative effects of GFs on PαS growth were examined. 4,000 freshly isolated cells were cultured in SM alone or supplemented individually with the following cytokines: bFGF, TGF-β or PDGF-ββ.

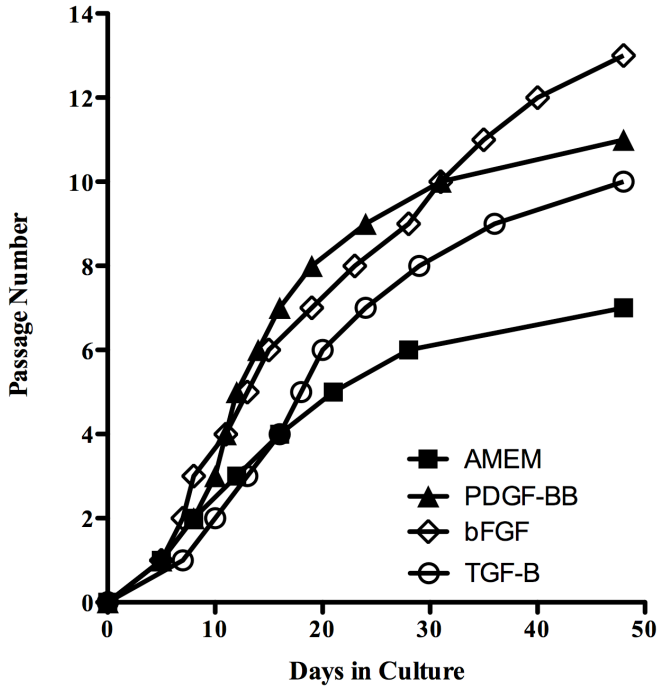


**Figure 5-3 Representative growth curves from each media type.**

*Growth curves for MSCs cultured in each media type are shown. Cells were split when confluent and re-seeded in a 1 to 2 ratio. Cells were counted after 30 days in culture. PαS cells cultured in the presence of GFs (bFGF > PDGF-ββ> TGF-β) grew more quickly than cells cultured in SM (*Figure 5-3*).*

### 5.2.3 Effects of cytokines on MSC growth

The morphology of PαS cells cultured in the different media types varied. In general smaller cells were observed in bFGF and TGF-β groups. Passage number was therefore not entirely reliable as an indicator of growth. Cell counts in each group were therefore performed at day 30.

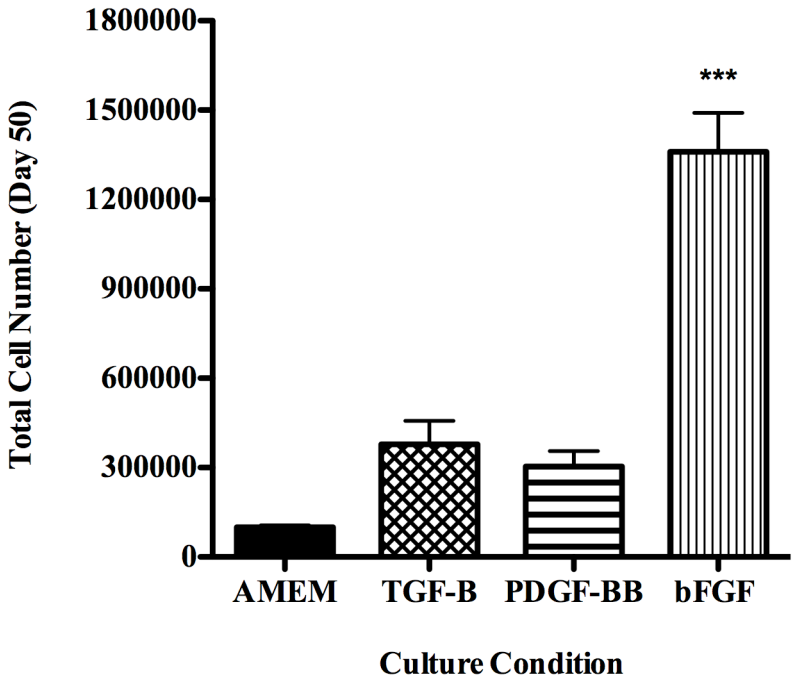


**Figure 5-4 Total cell numbers in each group following 30 days in culture.**

*30 days following initial seeding of PαS MSCs, all cells were harvested in each group and counted. There were significantly more cells in the bFGF group compared with SM (n=3, P<0.001 vs SM). TGF-β and PDGF-BB increased growth of PαS cells compared to SM, but failed to reach statistical significance (*Figure 5-4*).*

### 5.2.4 Effects of GFs on cellular senescence

To ascertain if the pro-proliferative effects of GFs was due to a reduction in cellular senescence, cells from each group were stained for β-galactosidase at day 30.

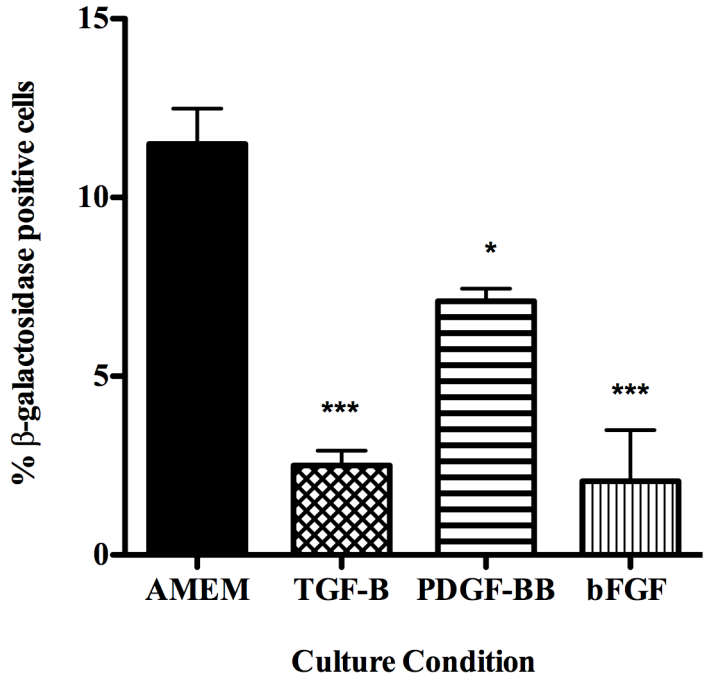


**Figure 5-5 Cellular senescence in each group after 30 days in culture.**

*The proportion of senescent cells (evidenced by positive β-galactosidase staining) following 30 days in culture is show for each group. The proportion of cells positive for β-galactosidase per field of view were counted and expressed as a proportion of the total cell number. These data are expressed as the mean number of cells from 10 fields of view in each condition. The addition of growth factors to culture media appears to inhibit senescence. The most potent effects were seen with bFGF and TGF-β (n=3, ***P<0.001 vs AMEM). Addition of PDGF-BB also inhibited cellular senescence (n=3, **P<0.01 vs AMEM).*

### 5.2.5 Effects of GFs on fat differentiation

The effects of GFs on PαS fat differentiation were investigated. In brief, 2000 freshly cells were seeded in a 48 well in each media type. When 90% confluent the cells were split or differentiated to fat. Cells in each condition were differentiated to fat up to passage 5. Fat differentiation was achieved by washing the cultured cells and placing them in fat induction media (Lonza) for 4 days. The cells were then cultured in fat maintenance media for a further 4 days. Cells were then fixed and stained for Oil Red O.

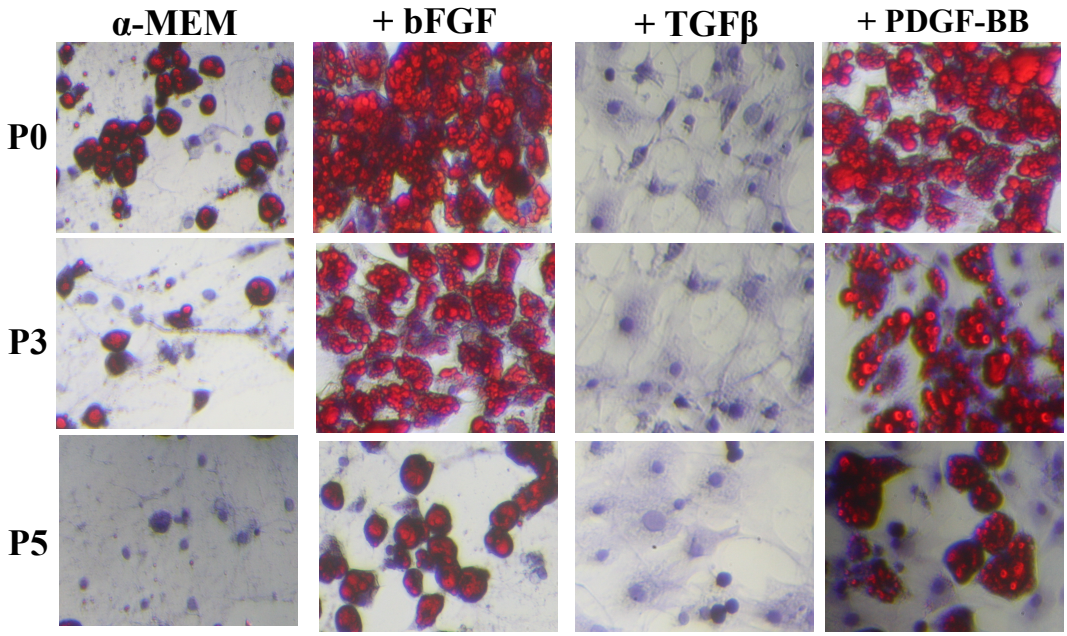


**Figure 5-6 Oil Red O staining of each group at different passage numbers.**

*Illustrative images of fat differentiation for each group at P0, P3 and P5 are shown (*Figure 5-6*). PαS cells lose their ability to differentiate into adipocytes after prolonged culture on plastic. The addition of bFGF and PDGF-ββ to the media greatly enhanced fat differentiation. These data support adipogenic lineage priming of bFGF and PDGF-BB from the microarray.*

### 5.2.6 Effects of cytokines on bone differentiation

We then assessed the effects of each culture media on PαS bone differentiation. In brief, 2000 freshly cells were seeded in a 48 well in each culture media. When 50% confluent the cells were split or underwent osteogenic differentiation. Following 2 weeks in differentiation media cells were fixed and stained with Alizarin Red to demonstrate calcium deposition.

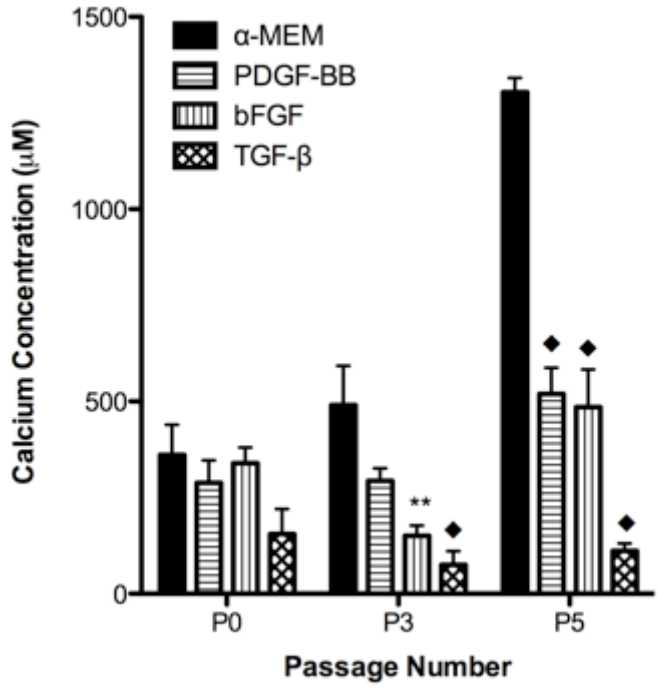


**Figure 5-7 Calcium quantification following bone differentiation in the different groups.**

*This figure shows calcium production for each group at P0, P3 and P5 following differentiation to bone. Alizarin Red staining was quantified and used to calculate calcium concentration in each well (*Figure 5-7*). All GFs reduced calcium deposition compared to SM at P5 (n=3, ◆P<0.001 vs AMEM).*

### 5.2.7 Effects of GFs on anti-proliferative effects of PαS MSCs

The $CD4^+$ T cell proliferation assay was carried out as before. Cells from each media type were added to the wells and their inhibitory effect measured.

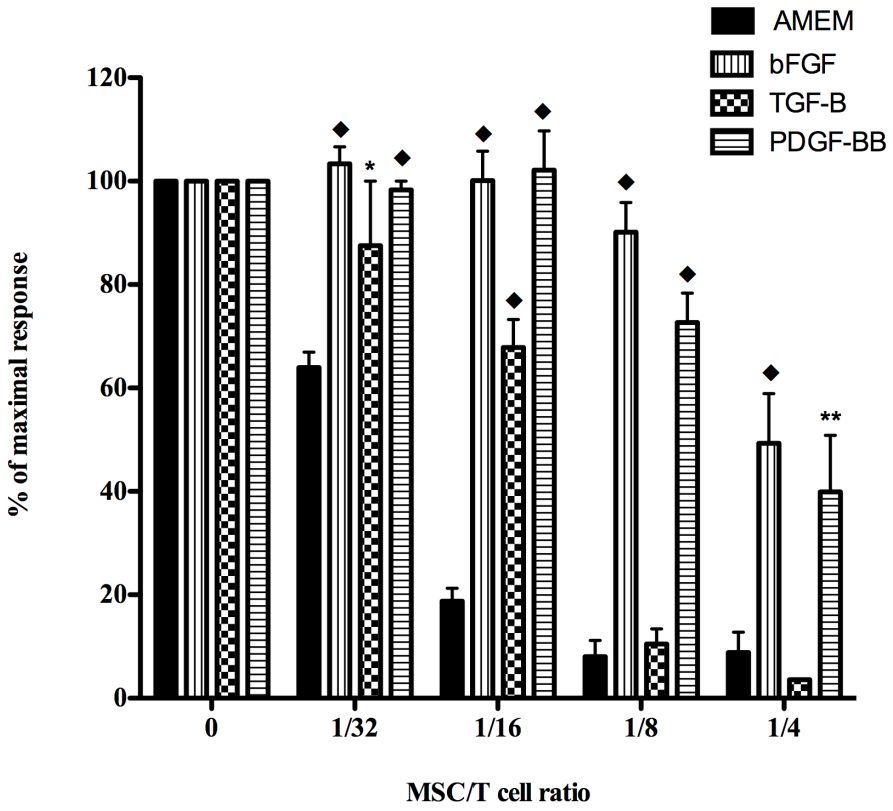


**Figure 5-8 Inhibitory effects of each cell type on $CD4^+$ T cells.**

*The immunosuppressive potency of each group following titration into a lymphocyte proliferation assay is illustrated in this figure. After 3 days in culture the $CD4^+$ cells were counted. Addition of GFs to MSC culture media had a significant impact on their anti-proliferative effects. There was no difference between cells cultured in TGF-β compared to AMEM at the higher concentrations (n=3) (*Figure 5-8*). In contrast bFGF and PDGF-BB had significant attenuation of immunosuppression at all tested doses (n=3, **P<0.01, ◆P<0.001 vs AMEM).*

### 5.2.8 Effects of GFs on nitric oxide production by PαS MSCs

We previously identified NO as a primary mechanism of MSC mediated immunosuppression. We therefore wanted to assess if the different anti-proliferative effects seen in the groups could be explained by differential production of NO.

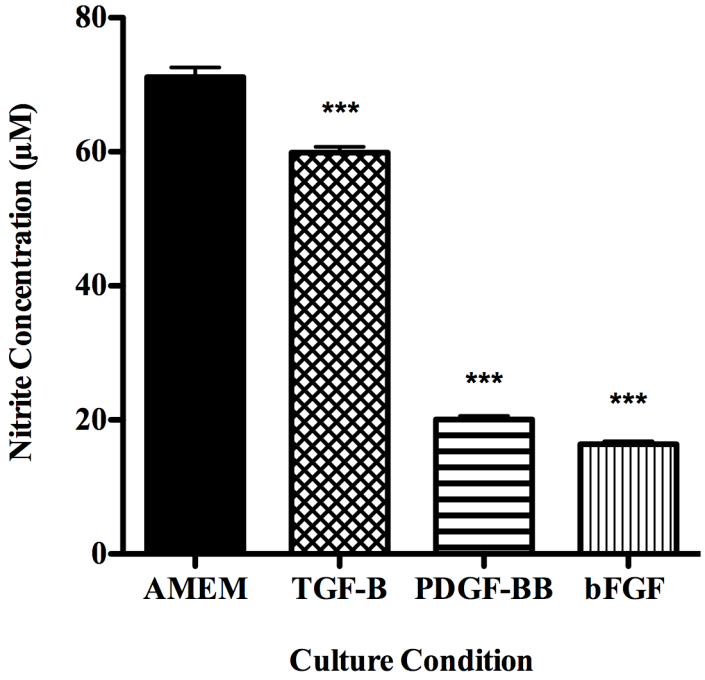


**Figure 5-9 NO production in the different groups.**

*The Greiss assay was used to measure NO production in the different groups. There was a significant reduction in NO production following addition of GFs to media (n=3, ***P<0.001 vs AMEM) (Figure 5-9). NO production appears to explain the different immunosuppressive effects among the groups observed in the $CD4^+$ T lymphocyte proliferation assay.*

### 5.2.9 Can addition of TGF-β maintain the anti-proliferative effects of MSCs?

We previously demonstrated that the anti-proliferative effects of PαS MSCs cultured in SM diminish over time. I examined if addition of TGF-β to culture media might maintain the anti-proliferative effects of MSCs. PαS MSCs were isolated and cultured in SM alone or supplemented with TGF-β. At passage 7 the cells were assayed in the $CD4^+$ lymphocyte proliferation assay.

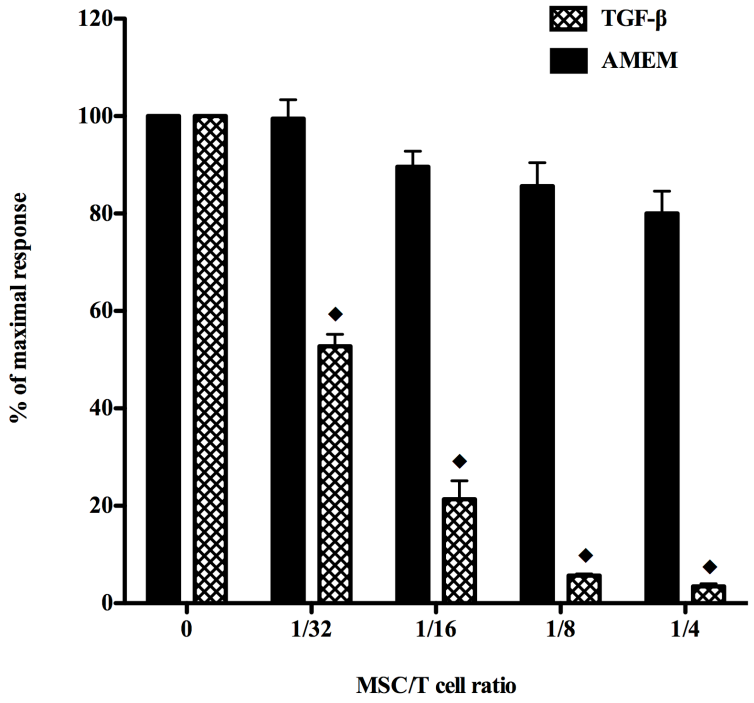


**Figure 5-10 PαS MSCs cultured in SM with TGF-β retain immunosuppressive potency.**

*This figure shows the immunosuppressive effects of P7 cells with and without TGF-β. These data confirm that MSCs cultured in SM loose their anti-proliferative effects following prolonged culture (*Figure 5-10*). Addition of TGF-β to culture media maintained immunosuppression even after 7 passages (n=3, ◆P<0.001 vs No MSCs).*

### 5.2.10 bFGF signalling and fat priming

In order to determine downstream signalling of bFGF, we added selective inhibitors to the growth media. Dasatinib is an inhibitor of Src while SU5402 inhibits Akt signalling. bFGF mediates it's effects via these divergent pathways. Cells were isolated and cultured in SM supplemented with bFGF with and without each of these inhibitors. Upon reaching confluence cells were swapped to fat differentiation media as described earlier. Staining for adipocytes was then carried out to determine the impact of each inhibitor on bFGF signalling.

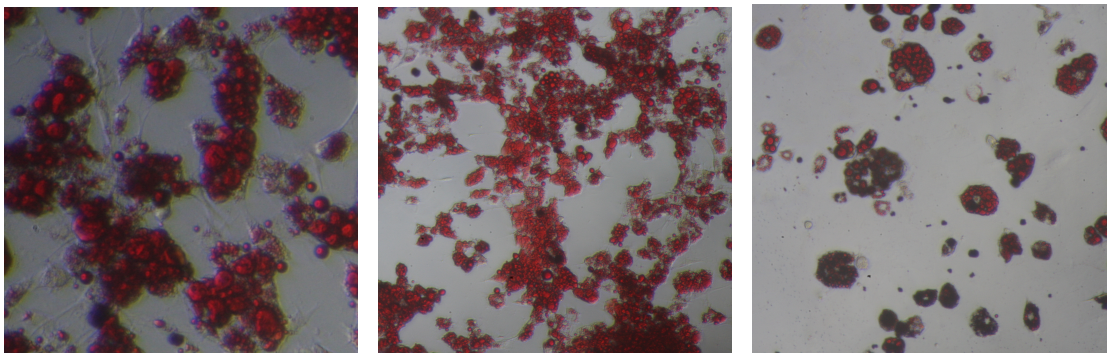

**Control** **Dasatinib** **SU5402**

**Figure 5-11 Images of bFGF cells after fat differentiation in the presence and absence of Dasatinib and SU5402.**

*The addition of the Src inhibitor Dasatinib did not affect fat differentiation. In contrast, SU5402 potently inhibited fat differentiation suggesting that the morphological changes induced by culturing PαS MSCs in media supplemented with bFGF occur in part via Akt signalling.*

5.2.11 Mechanism of action FGF

Using Image J the area of fat differentiation in each well was quantified. 4 pictures were taken from each quadrant of the well. The total area staining positive for Oil Red O was then calculated and a mean generated by averaging the 4 values. Experiments were repeated at P0, P1 and P2.

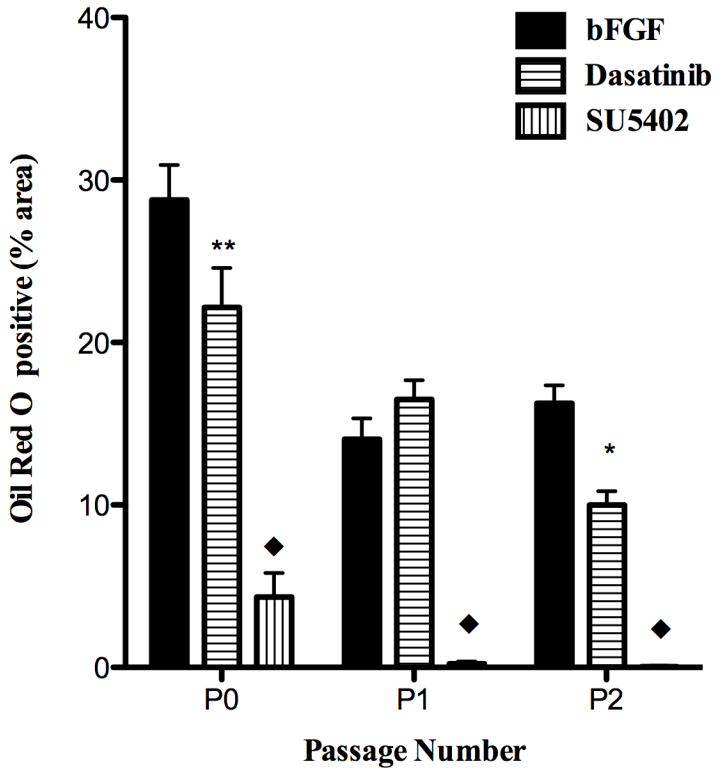


**Figure 5-12 bFGF priming of PαS MSCs down adipogenic lineage is mediated by Akt signalling.**

*Addition of SU5402, an inhibitor of Akt, markedly inhibited fat differentiation at all the passage numbers (n=3, ◆P<0.001 vs bFGF at each passage number). In contrast addition of Dasatinib had a minimal effect compared SU5402, suggesting that fat priming occurs through Akt signalling.*

### 5.2.12 Mechanism of fat priming of PDGF-BB

In order to determine which receptor is responsible for PDGF-BB fat priming, differentiation studies using MSCs expanded in SM supplemented with PDGF-BB or PDGF-AA were performed. PDGF-BB is a promiscuous ligand binding all receptor isoforms including PDGFαα, PDGFββ. In contrast PDGF-AA only binds the PDGFαα receptor.

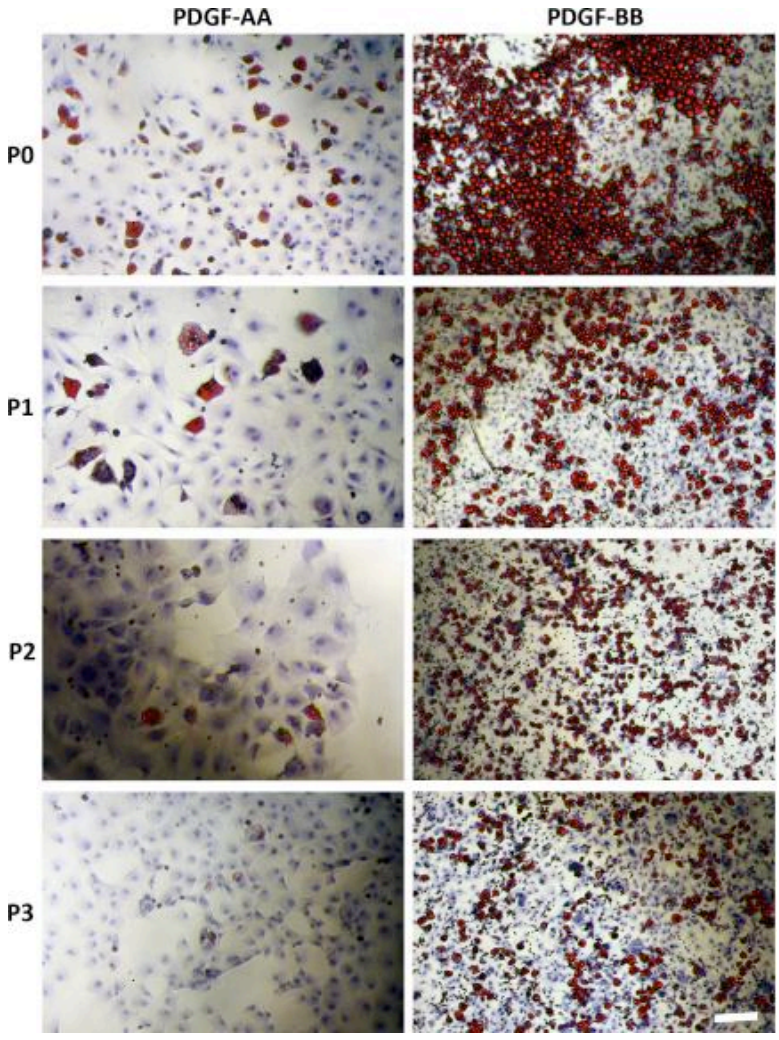


**Figure 5-13 PDGF-BB priming of PαS MSCs down adipogenic lineage is mediated by the PDGF-ββ receptor.**

*PαS MSCs cultured in media supplemented with PDGF-BB and not PDGF-AA demonstrate robust fat differentiation (*Figure 5-13*).*

### 5.2.13 Karyogram of PαS MSCs cultured in SM with PDGF-BB

A significant amount of literature suggests that mMSCs transform rapidly in culture and following infusion give rise to sarcoma's in rodent models. Our results suggests that such changes are present as early as passage 3. I therefore wanted to analyse the karyotype of our cultured cells to ensure that addition of bFGF, PDGF-BB and TGF-β had not selected for malignant clones.

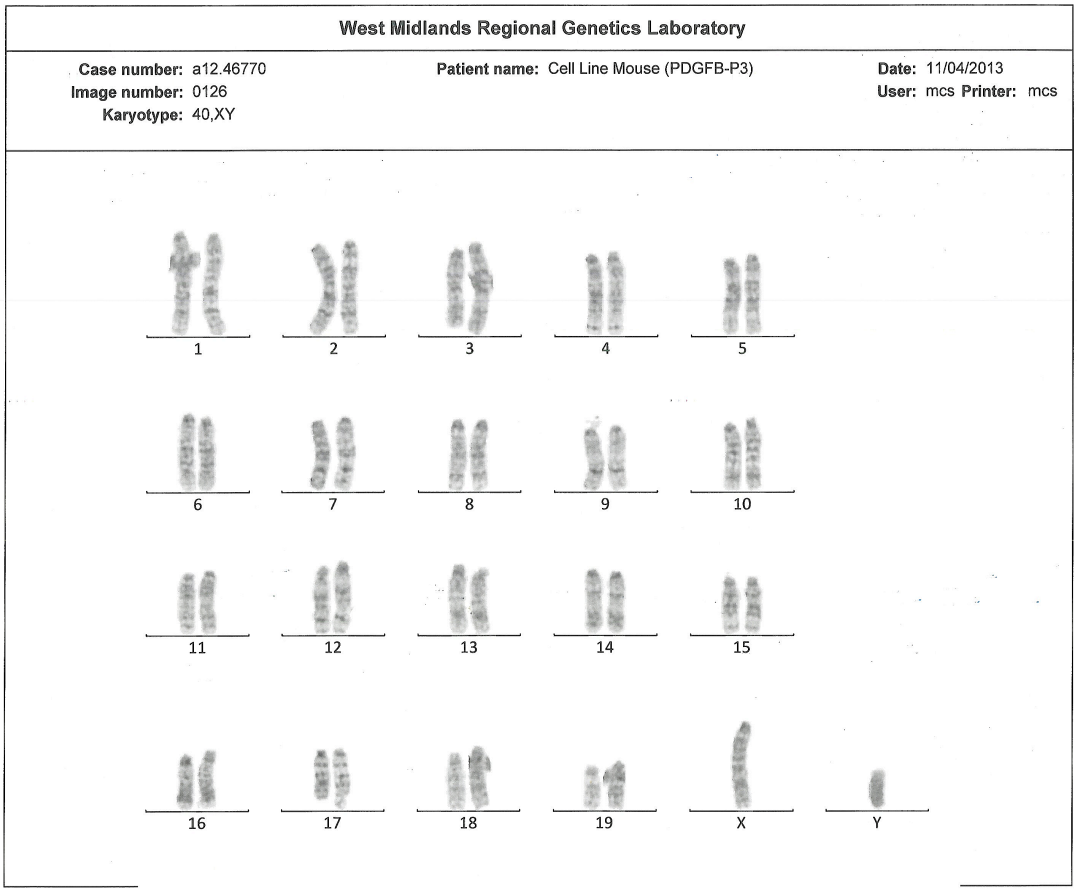


**Figure 5-14 Karyogram of P3 PαS MSCs cultured in SM with PDGF-BB.**

*The figure shows a normal mouse karyogram 40XY (*Figure 5-14*).*

5.2.14 Karyogram of PαS MSCs cultured in SM with bFGF

I also analysed the karyotype of our cultured cells to ensure that addition of bFGF to the culture media did not selected for malignant clones.

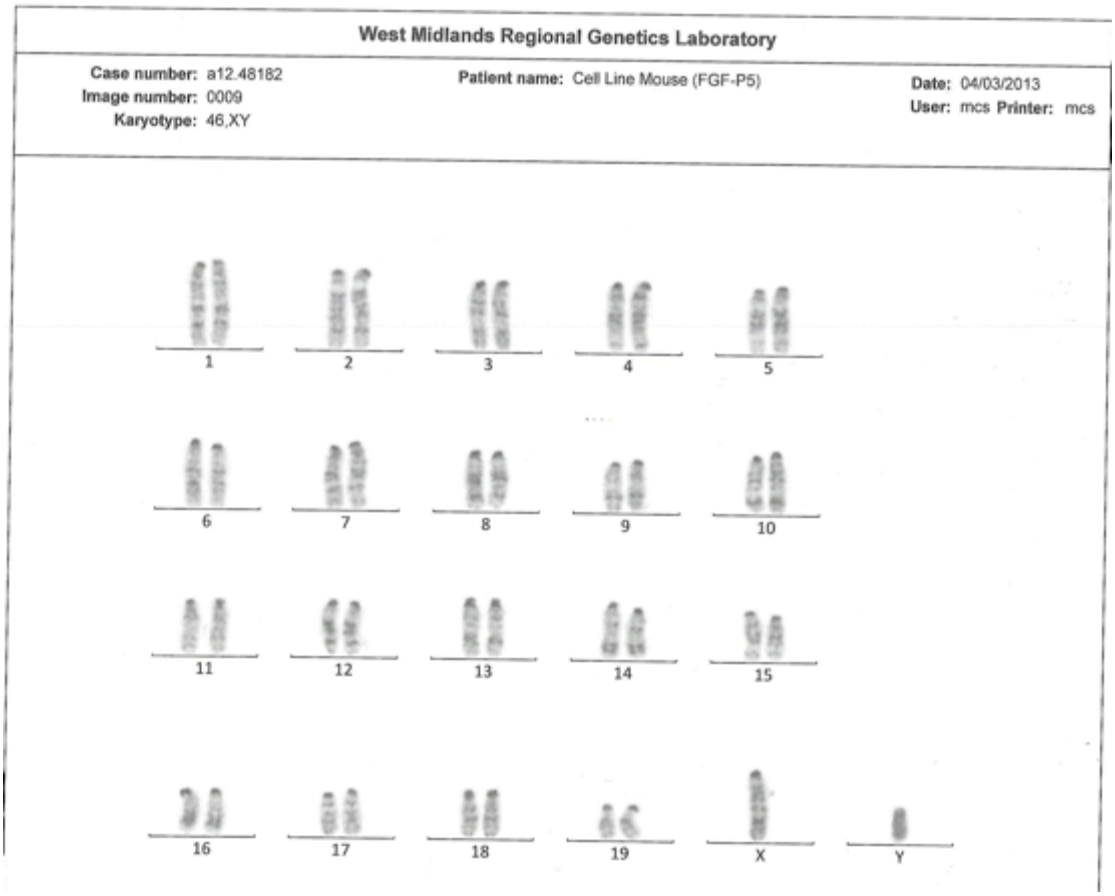


**Figure 5-15 Karyogram of P5 PS MSCs cultured in SM with bFGF.**

*The figure shows a normal mouse karyogram 40XY (*Figure 5-15*). There are no obvious deletions or insertions here.*

5.2.15 Karyogram of PαS MSCs cultured in media supplemented with TGF-β

I also analysed the karyotype of our cells cultured in SM supplemented with TGF-β to ensure this media type did not select malignant clones.

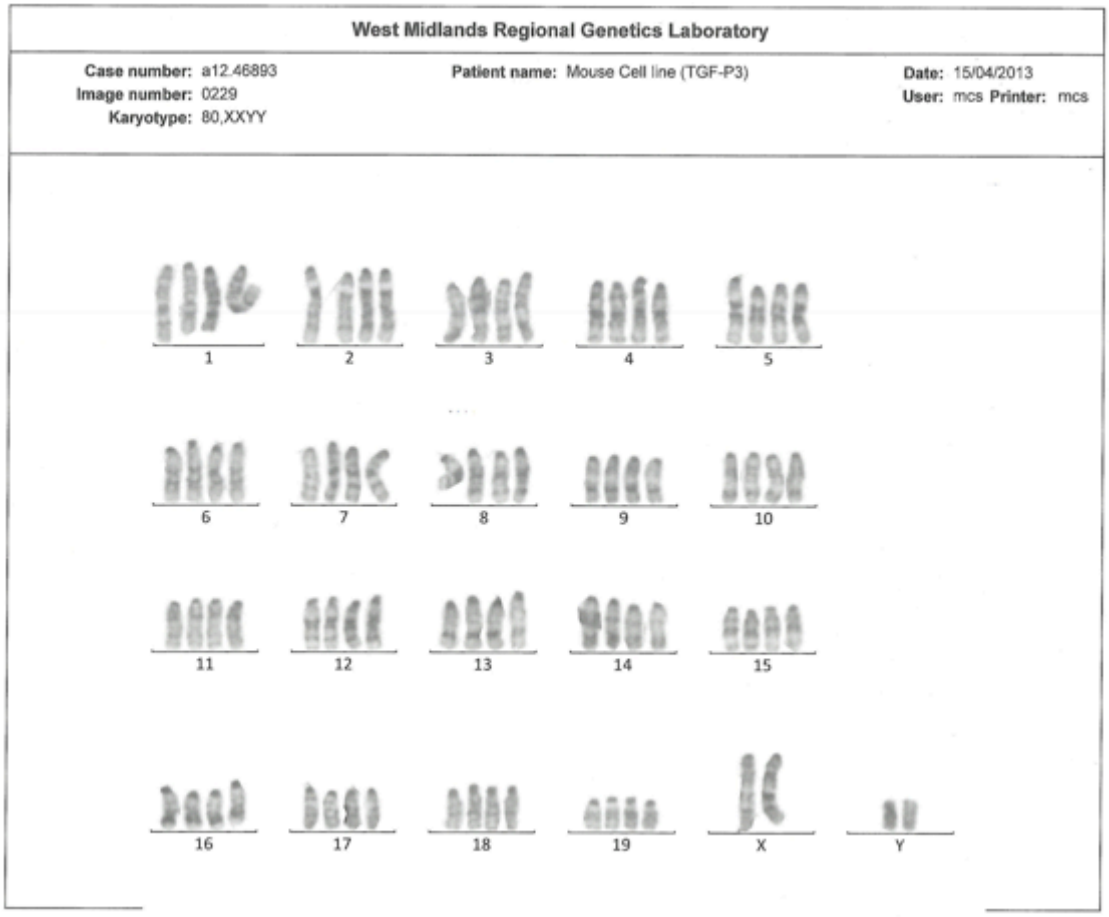


**Figure 5-16 Karyogram of P3 PαS MSCs cultured in SM with TGF-β**

Figure 5-16 *shows a diploid mouse karyogram 80XXYY . While this is not normal it has been associated with reduced tumourigenicity (Shoshani et al., 2012).*

### 5.2.16 Karyogram abnormalities

With the help of the Mary Strachan, Sara Dyer, Mike Griffiths and in the West Midlands Regional Genetics Laboratory, Birmingham Women's Hospital, multiple chromosomal spreads were analysed for error from each group and the results are tabulated below.

**Table 5-1** Summary of chromosomal abnormality identified in multiple chromosomal spreads in bFGF, PDGF-BB and TGF-β groups.

| Condition | Metaphase Spreads Counted | Abnormalities | Comments |
|---|---|---|---|
| P3 FGF | 21 | 3 | 39, XY, -4<br>40, XY, add(6q)<br>41, XY, +7 |
| P5 FGF | 23 | 3 | 40, XY, del(3q)<br>39, XY, -19<br>40, XY, ?add(8q) |
| P3 PDGF | 22 | 6 | 41, XY, +mar<br>37, XY, -13, -13, -19<br>78, XXYY, -13, -15<br>80, XXYY |
| P5 PDGF | 20 | 4 | 39, XY, -6<br>37, Y, -X, -10, -16<br>80, XXYY |
| P3 TGF-β | 20 | 4 | 39, XY, -19<br>38, XY, -13, -18<br>80, XXYY |

The frequency of abnormality detected varied between 15 – 30%. Abnormalities include chromosomal deletions, insertions and polyploidy.

## 5.3 Discussion

We demonstrate that the addition of GFs to MSC culture media alters cell morphology, growth kinetics and differentiation potential. These data support our observations from the microarray. The most significant increase in MSC growth was with bFGF followed by TGF-β and finally PDGF-BB. These observations correlated with lower levels of senescence (visualised by β–galactosidase staining) observed in cells cultured in SM with GFs. Interestingly, PαS MSCs cultured in bFGF and PDGF-BB supplemented media also robustly differentiate to fat suggesting that these GFs allow expansion of MSCs with retention of their plasticity. All GFs appear to attenuate bone differentiation compared with cells expanded in SM. There was significant variation in the immunosuppressive potential of the different groups with the order of potency as follows: SM > TGF-β > PDGF-BB > bFGF. These data provide additional evidence for lineage priming of MSCs and suggest that GFs can be used to augment or diminish specific MSC properties.

The use of mMSCs as a research tool has been significantly damaged by numerous reports demonstrating that traditionally isolated and expanded cells are transformed (Shoshani et al., 2012, Zhou et al., 2006). The prospective isolation of PαS MSCs avoids the need for prolonged culture during which transformation occurs. PαS MSCs cultured in media supplemented with bFGF, PDGF-BB and TGF-β have karyotype errors when examined between P3 – P5, at a frequency of between 15 – 30 %. Abnormalities included chromosomal deletions, insertions and polyploidy. Karyotypic abnormality been demonstrated in MSC cell lines that generate sarcomas

in vivo (Tolar et al., 2007, Shoshani et al., 2012) **(**Table 5-2**)**. The mechanism of mutagenesis most likely results from spontaneous unrepaired chromosomal lesion(s) that preceded the transposon insertion (Tolar et al., 2007)

**Table 5-2** Karyotype abnormalities in MSC cell lines

| Chromosome | S1 | S2 | MSC-7 | B6-T1 | B6-T2 | MSC-5 | B/c-11 |
|---|---|---|---|---|---|---|---|
| 1 | | | | | der(1)t(X;1) | | |
| 2 | −2 | −2 | | | | | |
| 3 | del(3)(F3) | del(3)(F3) | der(3)t(3;5) | der(3)t(3;5) | der(3)t(3;5) | −3 | |
| 4 | der(4)t(2F1;4C4) | | der(4)t(2;4) | der(4)t(2;4) | der(4)t(2;4) | der(4)t(4;7) | der(4)t(4;8) |
| 5 | der(5)dup(5) (DE2)del(5) (E2G2) | der(5)dup(5) (DE2)del(5) (E2G2) | | del(5) | del(5) | | |
| 6 | −6 | −6 | | | | | |
| 7 | −7, −7 | −7, −7 | −7,−7 | −7,−7 | −7, −7 | der(7)t(3:7) | |
| 8 | del(8)(E1) | −8, −8 | | | | | |
| 9 | −9, −9 | −9, −9 | | | | | |
| 11 | −11 | −11, i(11)(q10) | | | | | |
| 12 | −12 | −12 | | | | −12 | |
| 13 | | −13, −13 | | −13 | −13 | | −13, −13 |
| 14 | −14 | −14 | | | | | |
| 16 | −16 | −16 | | | | | |
| 17 | | | | | | | |
| 18 | | | | | | | |
| 19 | | | +19 | | | +19 | |

Twenty metaphase cells were screened in each cell line.
Abbreviations: del, deletion; der, derivative; dup, duplication; i, isochromosome.

Our cells demonstrated far fewer chromosomal abnormalities in comparison and since cellular transformation appears to result from an accumulation of chromosomal abnormality we hypothesise that our cells lines are more stable. In vivo transplantation experiments are on going to investigate their safety.

PαS cells will provide a robust substrate to interrogate physiological function and biology of MSCs. Additionally, they can be used to treat rodent models of disease and used to define conditions to optimise therapeutic potential, examine different routes and timing of infusions, and track the infused cells. In the next Chapter we will investigate in detail the potential of PαS MSCs for chondrogenesis.

# 6 Optimising cartilage production from mMSCs

## 6.1 Introduction

### 6.1.1 Cartilage

Cartilage is a flexible connective tissue found throughout the human body. It is composed of extracellular matrix (mostly Collagen II) admixed with ground substance (proteoglycan and aggrecan) and cartilage forming cells called chondrocytes (Hunziker, 2002). There are several different types of cartilage in the human body including: elastic cartilage, hyaline cartilage and fibrocartilage. Articular cartilage covers the ends of long bones and lies within the synovium. It provides an essential cushion that protects bone from ware and tear of every day life. It is a relatively avascular tissue with exchange of nutrients and waste occurring mostly by diffusion. Osteoarthritis (OA) describes a spectrum of pathological changes with the synovial cavity of long weight bearing bones and leads to pain, stiffness loss of function (Dieppe and Lohmander, 2005). It is the commonest cause of arthritis in the world and a significant health care burden (Peat et al., 2001). The pathological hallmark of OA is loss of cartilage that leads to boney injury and reactive changes within the joint. There is increasing focus on alternative therapies to joint replacement for the therapy of OA (Smelter and Hochberg, 2013).

### 6.1.2 MSC-derived cartilage to generate transplant grafts

The successful transplantation of a bioengineered trachea in 2008 by UK and Spanish teams, has generated significant excitement within the field of regenerative medicine (Macchiarini et al., 2008). Since this pioneering work was performed, it is estimated that 14 other patients including paediatric cases have received bioengineered tracheal transplants for indications ranging from carcinoma to stenosis (Vogel, 2013). These procedures have not been without complication and one report estimated that at least 2 patients have died in the early post-operative period from torrential bleeding which may have been caused by the implant eroding adjacent blood vessels. In the reported case series, recurrent collapse of the graft requiring stenting is a common problem (Elliott et al., 2012, Macchiarini et al., 2008). Pioneering techniques including the use of bioartificial scaffolds have been used to overcome some of these issues (Jungebluth et al., 2011). These problems may stem from poor quality cartilage, weakening of the tracheal scaffold during the bioengineering process and lack of a viable blood supply to maintain the healthy graft. Critics of field claim that there is not enough pre-clinical evidence and too many unanswered questions to justify continuing with a human transplant program (Delaere, 2013). Large animal studies are few and lack long-term follow to provide answers to pressing question (Birchall et al., 2012). Nonetheless the field has attracted significant investment and clinical trials will soon be underway.

### 6.1.3 Chapter Aims

In this Chapter, I will examine if culturing PαS MSCs in SM supplemented with GFs generates superior quality cartilage as evidenced by bigger pellet size and higher

content of collagen type II and glycosaminoglycan. This work was performed in collaboration with Shang Zhang and Anthony Hollander (Bristol University). Cartilage differentiation was confirmed by Safranin O staining and with additional immunohistochemical stains for collagen type I and II. Using lineage primed MSCs we then screen a number of growth factors including TGF-β3, BMP-2, BMP-6 alone or in combination to identify optimal conditions for cartilage production from PαS MSCs. Finally using the information we attempt to make tissue-engineered cartilage that might be suitable of therapeutic use.

## 6.2 Results

### 6.2.1 Chondrogenic assays using lineage primed PαS MSCs

To characterize the chondrogenic capacity of lineage primed PαS MSCs we first used the pellet culture system. In brief, pellets of PαS cells cultured in SM or supplemented with bFGF, PDGF-BB or TGF-β were produced by centrifugation and then transferred into chondrogenesis medium containing TGF-β3 for 3 weeks culture.

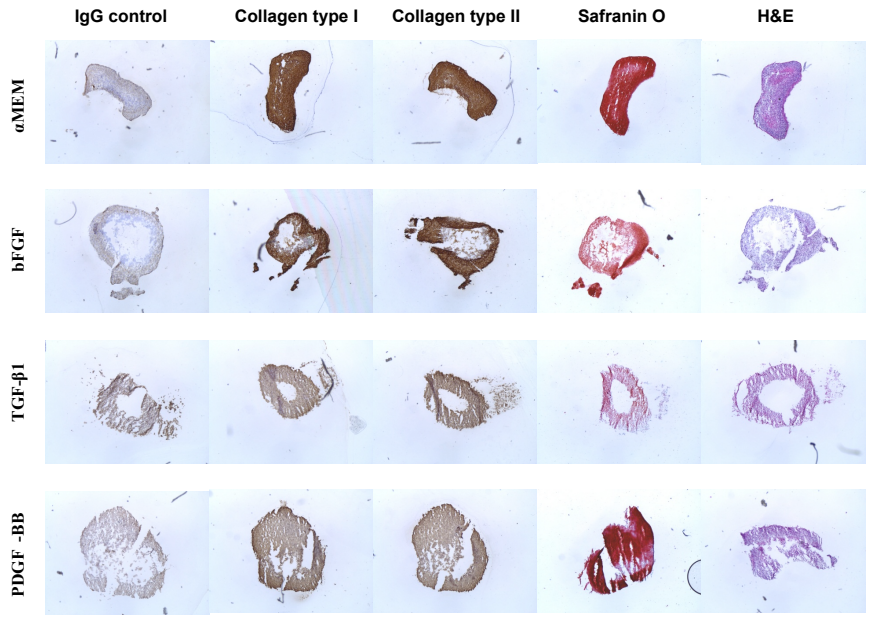


**Figure 6-1 Immunohistochemical staining of ECM in the different groups.**

*Sections of cartilage pellets from each group were stained for ECM as shown (*Figure 6-1*). PαS MSCs cultured in SM alone or supplemented with bFGF make superior quality cartilage to the PDGF-BB and TGF-β groups as evidenced by more intense staining for collagen type II and GAGs (Safranin O). Additionally cells expanded in SM supplemented with TGF-β frequently failed to form solid a pellet supporting this hypothesis.*

### 6.2.2 Pellet size and GAG content following chondrogenic differentiation

In order to quantify the quality of the cartilage in each pellet more objectively, ECM content (Collagen type I an II) was measured by ELISA. DMB was used to measure the GAG content of each pellet as described in the Methods section. We started by screening pellets from each group (SM, bFGF, PDGF-BB and TGF-β) to decide which conditions to further investigate in more complex assays.

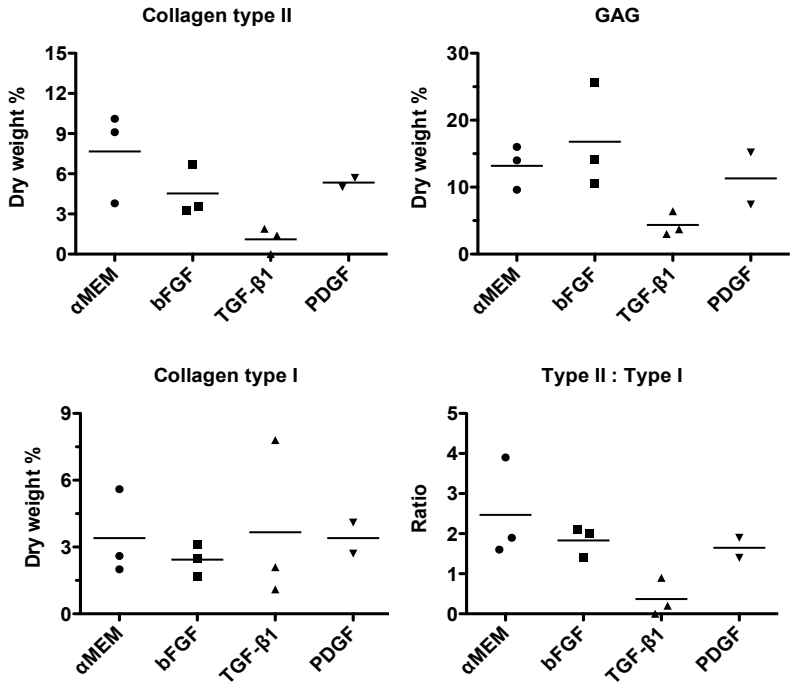


**Figure 6-2 Chondrogenesis related production of ECM in the pellets.**

*This figure shows collagen and GAG content (expressed as a percentage of dry weight) as measured by ELISA in each group. Good quality cartilage has a high Collagen type II and GAG content and low Collagen type I content. αMEM and bFGF groups produced the best collagen quality cartilage (*Figure 6-2*). TGF-β produced the poorest quality cartilage. We selected SM, bFGF and TGF-β for further study as bFGF media give the optimal in vitro expansion while TGF-β signalling is important in chondrogenesis. SM was the control.*

### 6.2.3 Quality of cartilage produced by the different groups

The pellet size and GAG content was compared between the groups. The dry weight of each pellet was measured after freeze drying. DMB was used to measure the GAG content of each pellet as described in the Methods section.

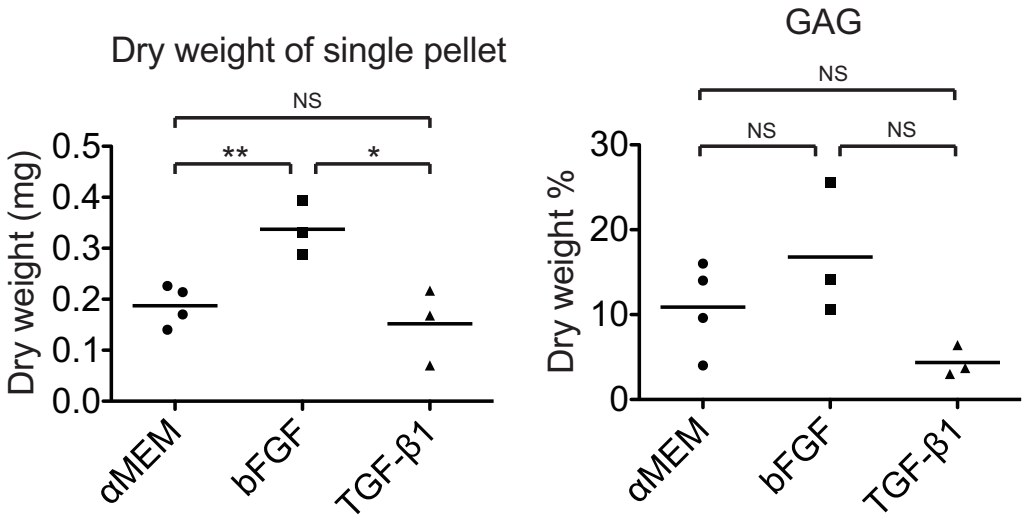


**Figure 6-3 The dry weight and GAG content of cartilage pellets produced from each culture condition.**

*$5 \times 10^5$ cells cultured in each media type were used to produce the cellular pellet prior to differentiation. SM supplemented with bFGF produced a significantly larger cartilage pellet compared to the other groups (Figure 6-3) (n=3, **P<0.01 vs. αMEM; *P<0.05 vs TGF-β) The GAG content did not differ between the groups, however there was a suggestion that cells expanded in SM supplemented with bFGF produced the most. Bars show the mean value for each group.*

### 6.2.4 Collagen I and II content following chondrogenic differentiation

Collagen type I and II content was then measured in all groups. High Collagen II content and a high Collagen type II : type I ratio indicate good quality cartilage.

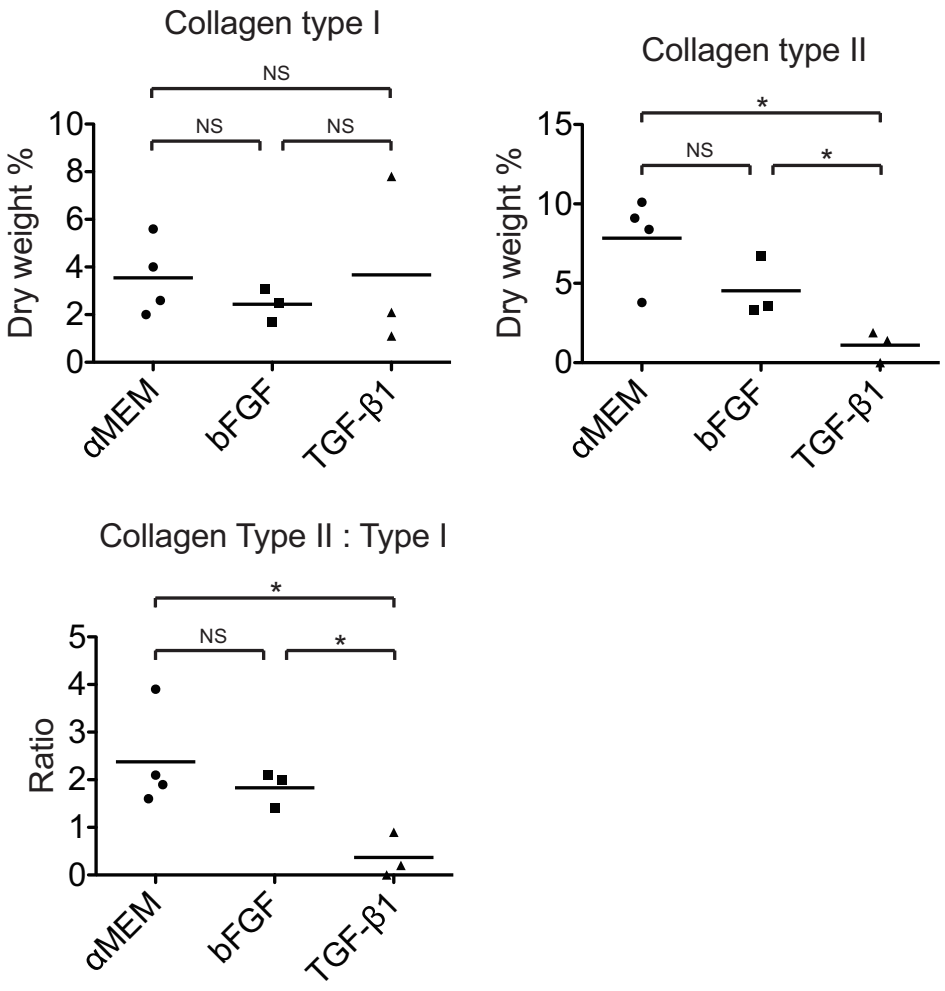


**Figure 6-4 Collagen type I and II content of each group.**

*αMEM and bFGF groups had a higher Collagen type II content and Collagen type II : Type I ratio compared to TGF-β (n=3, *P<0.05 vs TGF-β) Bars show the mean value for each group.*

### 6.2.5 Optimising chondrogenic differentiation bFGF MSCs

It was clear that PαS MSCs expanded in media supplemented with bFGF produced the best quality cartilage. We therefore selected this cell type for all further study. To improve chondrogenesis further we investigated addition of GFs including TGF-β3, BMP-2, BMP-6 alone or in combination to the chondrogenic media. Comparative Q-PCR analysis of chondrogenic differentiation-related genes was carried in the monolayer culture system.

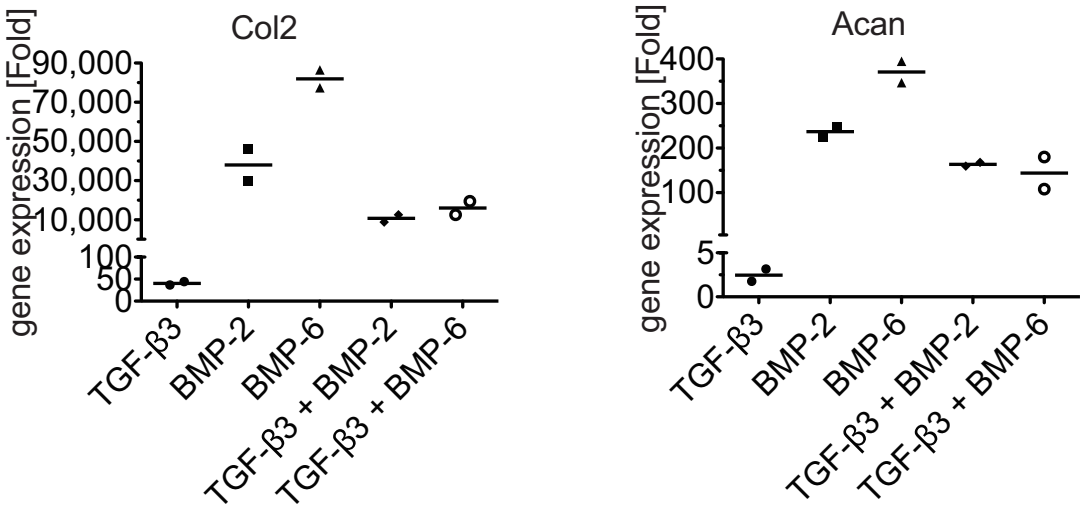


**Figure 6-5 Chondrogenic gene expression is shown for bFGF PαS MSCs differentiated in the different media types.**

*Cells cultured in bFGF media were differentiated to cartilage using various media types. High expression of Col2 and Acan expression in the pellet suggests high quality cartilage. These data suggest that supplementing chondrogenic media with either BMP-2 and BMP-6 produces the highest quality cartilage using bFGF PαS MSCs (*Figure 6-5*). Bars show the mean value for each group.*

### 6.2.6 Optimising chondrogenic differentiation of bFGF MSCs

The same experiment was performed and once again the quality of cartilage was assayed by examining gene expression of Collagen X and Aggrecan expression by Q-PCR. Low expression of ColX and high expression of Acan represents good quality cartilage. The previous data suggest that BMP-2 or BMP-6 added to chondrogenic differentiation media produces best quality cartilage.

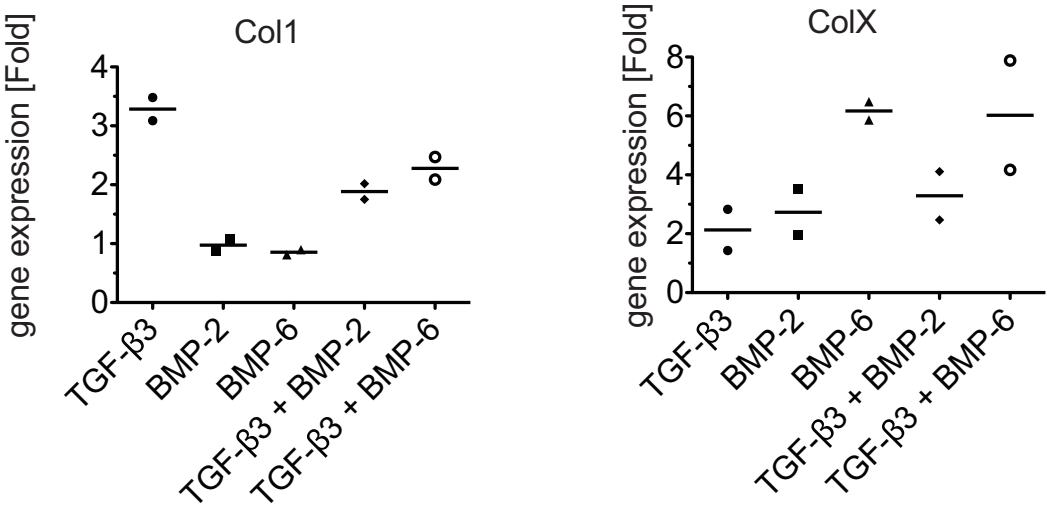


**Figure 6-6 Col1 and ColX expression in bFGF PαS MSCs differentiated in the media types.**

*Good quality cartilage also expresses low levels of Collagen type I and type X. The results here show that BMP-2 in particular produces the lowest levels of Col1 and ColX gene expression (*Figure 6-6*). Therefore the logical choice for further study is to add BMP-2 to differentiation media. Bars show the mean value for each group.*

### 6.2.7 Tissue engineering with PαS MSCs expanded in SM with bFGF

PαS MSCs expanded SM supplemented in bFGF were used to make tissue-engineered cartilage on biodegradable PGA scaffolds. The chondrogenic media contained TGF-β3 alone or was supplemented with BMP-2 (as a result of previous data). Pictures of the tissue engineered cartilage pellets are shown.

A.

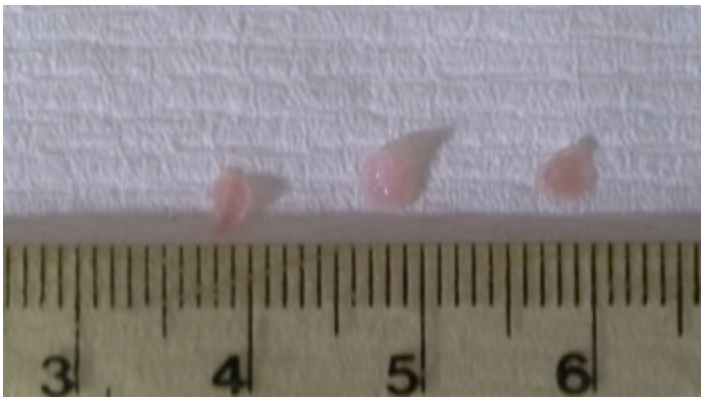


B.

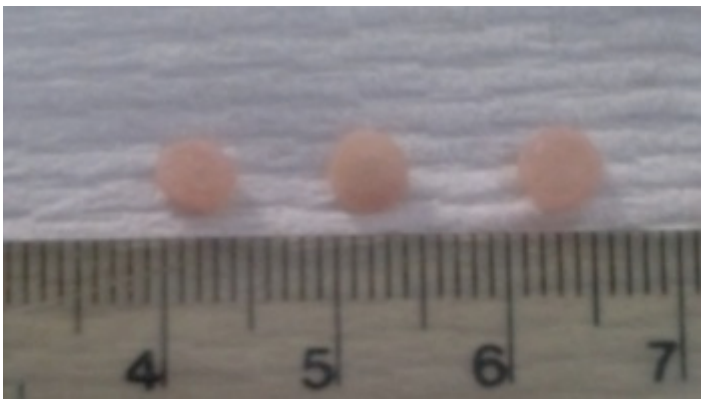


**Figure 6-7 Tissue engineered cartilage pellets differentiated in the presence or absence of BMP2.**

Chondrogenic differentiation medium containing the combination of TGF- β3 and BMP2 (Fig 6-7B) derived bigger cartilage then TGF- β3 alone (Fig 6-7A).

### 6.2.8 ECM measurement in tissue engineered cartilage formed in media with and without BMP-2

Collagen type II, type I and GAGs were measured as previously described. Cartilage with high Collagen type II and GAG content is considered high quality.

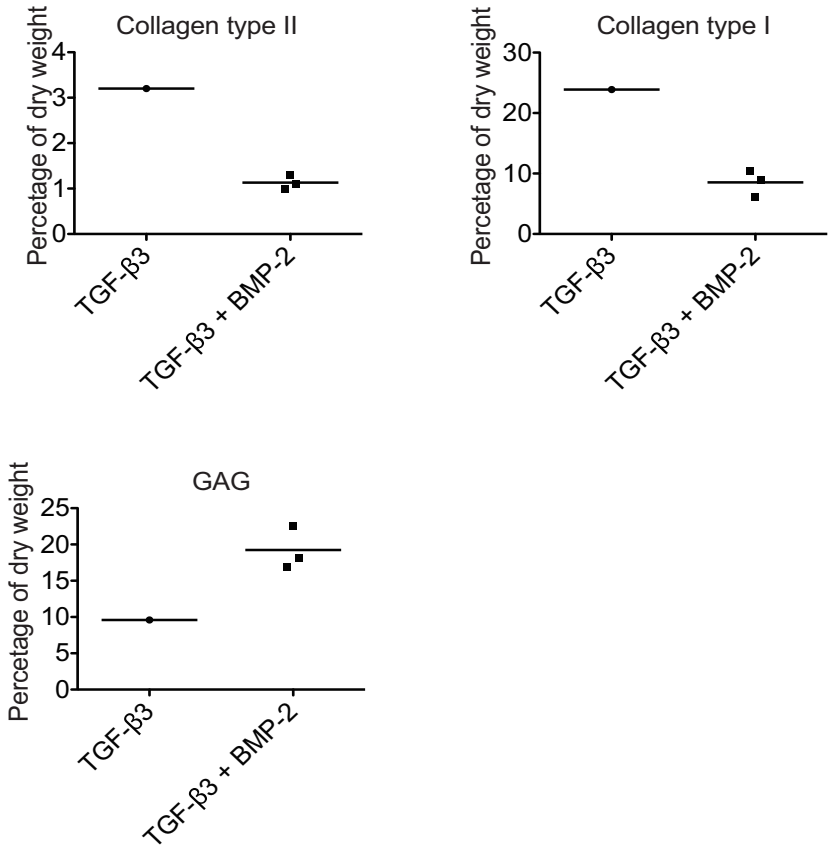


**Figure 6-8 Comparison of ECM components in tissue engineered cartilage in the presence and absence of BMP-2.**

*The combination of TGF- β3 and BMP2 increased GAG production (*Figure 6-8*). For group TGF- β3, three tissue engineered cartilage samples were pooled to derive one measurement. For group TGF- β3 + BMP-2, each symbol in the graph stands for one tissue engineered cartilage sample.*

## 6.3 Discussion

The chondrogenic differentiation of murine PαS cells was tested on three different systems including: 1. Monolayer culture for chondrogenesis related gene analysis 2. Pellet culture system for ECM production and 3. Tissue engineering culture (cells on biodegradable scaffold). We hypothesised, based on gene array data, that addition of bFGF, PDGF-BB, or TGF-β might lineage prime or restrict towards or away from cartilage. Immunohistochemistry demonstrated robust Safranin O staining using αMEM alone or that supplemented with bFGF suggesting that these groups are primed for cartilage formation. Measurement of the pellet size and chondrogenic markers (GAGs and Collagen type II) confirmed these findings. PαS MSCs grow far more quickly in SM with bFGF compared to PDGF-BB and only the former were carried forward for further study. A direct comparison between αMEM, bFGF and TGF-β cells demonstrated that the TGF-β MSCs produced inferior cartilage as evidenced by low levels of Collage type II and GAGs. Although αMEM and bFGF cells generated cartilage of equivalent quality, MSCs cultured with bFGF grow far more quickly and generate much larger pellets. Therefore, all further studies were carried out with PαS MSCs that were cultured in media supplemented with bFGF.

Standard chondrogenic differentiation media is supplemented with TGF-β3 (Kafienah et al., 2007). BMP-2 and BMP-6 are important regulators of MSC chondrogenic differentiation (Sekiya et al., 2005). We therefore examined the impact of adding BMP-2 and BMP-6 to TGFβ3 in chondrogenic media. We noted that the addition of either BMP-2 or BMP-6 to the differentiation media (containing TFGβ3) enhanced gene expression for cartilage markers Col2 and Acan suggesting better quality

cartilage. Finally, we generated cartilage by tissue engineering on biodegradable scaffold using standard chondrogenic differentiation media or that supplemented with BMP-2. Addition of BMP-2 lead to increases in the size of cartilage generated. Additionally, the larger scaffolds contained increased amount of GAGs.

There are many challenges to successfully using MSCs for cartilage repair or regenerative therapy. For a start the MSCs should be readily available, expandable and capable of robust differentiation to cartilage. PαS MSCs expanded in standard culture media supplemented with 10ng/ml bFGF generate 20-fold more cells than SM. These cells produce a greater quantity of high quality cartilage pellets compared to control. Therefore PαS provide a robust substrate for regenerative therapy. Additionally, differentiated cells should maintain features of mature chondrocytes that are resistant to hypertrophy and terminal differentiation. We define optimal conditions by adding BMP-2 to chondrogenic media to produce high quality chondrocytes as evidenced by low expression of Col I and Col X (indicating hypertrophy) and higher expression of Col2 and Acan. High quality cartilage such as this may avoid common complications of mineralisation and vascularisation (Pelttari et al., 2008). Finally, to treat patients with OA it is likely that cartilage must be engineered as 3-D implants. I demonstrate using novel tissue engineering techniques that PαS MSCs cultured in SM supplemented with bFGF, then differentiated in standard chondrogenic media supplemented with BPM-2, generated substantial 3-D cartilage pellets. These data have significant translational relevance for human regenerative therapy.

# 7 Discussion

## 7.1 Summary of principle findings

I have for the first time reproducibly isolated murine MSCs based on expression of PDGFRα and Sca-1 outside Japan where the technique was originally described (Houlihan et al., 2012). PαS MSCs are highly proliferative and robustly differentiate into bone, cartilage and fat. In addition PαS MSCs suppress the proliferation of stimulated $CD4^+$ lymphocytes via NO production in vitro. During culture MSCs enlarge, their doubling time diminishes and expression of β-galactosidase increases indicating progressive cellular senescence. The addition of the GFs bFGF, PDGF-BB and TGF-β to culture media alters gene expression in PαS MSCs. Cells cultured in SM are lineage primed towards an osteogenic lineage. In contrast, cells cultured in media supplemented with PDGF-BB and bFGF have higher expression of genes that regulate adipogenic and chondrogenesis.

The addition of GFs to MSC culture media produces significant phenotypic changes in cultured PαS cells. In summary cell morphology, growth kinetics, differentiation immunosuppressive potential were altered. In particular cells cultured in bFGF have an elongated slender appearance and are much smaller that cells cultured in SM. Cells cultured with TGF-β appear fibroblastic and are also smaller then cells cultured in SM. The most significant increase in MSC growth also occurred following the addition of bFGF. These data correlated with lower levels of senescence (visualised

by β–galactosidase staining) observed in this group. Interestingly, PαS MSCs cultured in bFGF and PDGF-BB supplemented media also robustly differentiate to fat suggesting that these growth factors allow expansion of MSCs with retention of their plasticity. All growth factors appear to attenuate bone differentiation compared with cell expanded in SM, suggesting that PαS are naturally primed towards a bone phenotype. There was significant variation in the immunosuppressive potential of the different groups with the order of potency as follows: SM > TGF-β > PDGF-BB > bFGF. This correlated with differential production of NO across the groups. Finally, karyotypic abnormality was identified in cells cultured in growth factor supplemented media the frequency of these changes low and not reflective of transformed cells.

We hypothesised, based on gene array data, that addition of bFGF, PDGF-BB, or TGF-β might lineage prime or restrict towards or away from cartilage. We therefore assessed cartilage differentiation in the different groups. Immunohistochemistry demonstrated robust Safranin O staining using SM or that supplemented with bFGF suggesting that these groups are primed for cartilage formation. Measurement of the pellet size and chondrogenic markers, GAGs and Collagen type II, confirmed these findings. All further studies were carried out with PαS MSCs that were cultured in media supplemented with bFGF as these culture conditions yield the greatest number of cells and good quality cartilage. In collaboration with Shang Zhang and Prof Anthony Hollander in Bristol we then optimised chondrogenic differentiation conditions for bFGF PαS MSCs and assayed the effectiveness of this modification using tissue engineering on biodegradable scaffold. I demonstrate that PαS MSCs

expanded in SM supplemented with bFGF form robust cartilage pellets when differentiated in chondrogenic media supplemented with BMP-2.

## 7.2 Current literature and what this adds

### 7.2.1 Pure population of MSCs.

The Tissue Stem Cell Committee of the International Society for Cellular Therapy has defined the hMSCs as plastic adherent cells that express CD73, CD90 and CD105, without expression of CD45, CD34, CD14 or CD11b, CD79 or CD19 and HLA-DR surface markers. MSCs must also be capable of differentiating into osteoblasts, adipocytes and chondrocytes *in vitro* (Dominici et al., 2006). This definition has however been heavily criticised (Bianco et al., 2013). MSCs defined in this way do not fulfil the basic requirements of a stem cell (Bianco et al., 2008). Additionally, due to lack of specificity of the surface markers, much of the MSC literature is not representative of true MSCs, but rather a heterogeneous population of stromal cells (Haniffa et al., 2009). Despite this the therapeutic potential of MSCs are now routinely being investigated in clinical trials. The reasons for this include startling reports of efficacy in difficult to treat diseases including GVHD and OI ((Horwitz et al., 2001, Le Blanc et al., 2004) and significant limitations in the mMSC field including cellular contamination and malignant change (Phinney et al., 1999, Zhou et al., 2006). I demonstrate that a pure population of MSCs can be isolated prospectively from murine BM. These cells appear to be stable in culture demonstrating only minor karyotypic change at P5. I identify culture conditions that enhance or diminish basic

MSCs properties including tri-lineage differentiation and immunosuppression and show that bFGF cells would most likely be advantageous for cartilage regeneration. This model is of direct relevance to human MSC therapy and provides a framework in which to model human therapy.

### 7.2.2 Effects of growth factors

The addition of GFs to enhance or retain certain MSC properties is not novel. Murine MSCs isolated by plastic adherence contain contaminating cells (Pittenger et al., 1999). Immunodepletion of haemopoiteic cells has been successfully used to purify the isolates MSCs. FGF2 has been previously used to overcome poor growth following immunodepletion and to maintain MSC multi-potency during culture. More recently it has been demonstrated that rare mesenchymal progenitors residing in the MSC niches in vivo express FGFR1/2 (Coutu et al., 2011), suggesting FGF signalling may be an important self-maintenance factor for mMSCs. There are limited data on the impact of GF supplementation on lineage priming or therapeutic potential of MSCs. FGF2 expanded MSCs have been successfully used to induce healing in a rodent bone fracture model (Baddoo et al., 2003). Other studies suggest that MSC culture in media supplemented with bFGF and TGF-α can improve differentiation to bone and cartilage respectively (Yamachika et al., 2012, Zhao and Hantash, 2011). Despite our limited understanding of the impact of GFs on mMSCs, there has been widespread use of growth factors for hMSCs expansion (Jung et al., 2012a). My results demonstrate the addition of GFs to culture media lineage primes MSCs. Gene expression and phenotypic data demonstrate that PαS cultured in SM are primed towards osteogenic lineage. bFGF and PDGF-BB enhance fat and cartilage gene

expression and differentiation. Interestingly, the addition of TFG-β to culture media impaired tri-lineage differentiation but maintained the immunosuppressive effects of MSCs during *in vitro* expansion. In contrast bFGF and PDGF-BB significantly attenuated the immunosuppressive effects of PαS MSCs in vitro. These data have significant implications for the expansion of human MSCs intended for therapeutic use in humans. For bone disease, cells cultured without GFs may provide the most effective therapy. In contrast for cartilage repair cells cultured in media supplemented with bFGF would seem a good choice. Finally for autoimmune and inflammatory disease supplementing culture media with TGF-β over comes cellular senescence and maintains potent immunosuppression.

### 7.2.3 MSC derived cartilage for the treatment of osteoarthritis

There are currently 16 trials investigating the efficacy of MSCs for the treatment of OA. The majority of these are using BM derived MSCs (n=14) with the remaining trials using adipose tissue derived cells. Isolated case reports have suggested benefits of MSC infusion of the treatment of both OA and cartilage injury (Kuroda et al., 2007, Wakitani et al., 2007). One of the largest studies carried out to date compared the therapeutic benefit of chondrocyte infusion (n=36) to MSC infusion in 72 matched patients (Nejadnik et al., 2010). Patients were evaluated at regular intervals for 2 years following the treatment. Therapeutic response was assessed with the "International Cartilage Repair Society Cartilage Injury Evaluation Package'. Improvements were broadly similar in both groups however Physical Role Functioning was higher in the MSC treated group. In addition to providing symptomatic improvement MSCs appear to heal cartilage defects as evidenced by

MRI imaging and biopsy (Davatchi et al., 2011, Centeno et al., 2008). Nonetheless some studies are less encouraging reporting only modest benefit, suggesting the there is significant work left to optimise MSC therapy (Davatchi et al., 2011). There is little consensus on the ideal isolation method, culture conditions or differentiation media to optimise cartilage differentiation for therapeutic use. I demonstrated for the first time that using tissue engineering, cartilage scaffolds can be made using mMSCs cultures expanded in media supplemented with bFGF and differentiated in media supplemented with BMP-2.

## 7.3 Future directions

### 7.3.1 Toxic and Immune mediated liver disease

#### *7.3.1.1 Autoimmune hepatitis*

Autoimmune hepatitis is a chronic hepatitis characterized by circulating auto-antibodies frequently directed to self antigen (ANA, ASMA, ASLA, ALP and ALKM) and a high serum globulin concentration. Liver injury is initiated by naïve $CD4^+$ T cells that recognize self-antigen (Krawitt, 2006). Following their activation, naïve CD4+ T cells differentiate into distinct T helper cell lineages, including pro-inflammatory Th1 cells, anti-inflammatory Th2 cells, T regs and Th17 cells (Oo et al., 2010). Autoimmune hepatitis has been associated with a dominant Th1 response and a reduction in functioning T regs, and as such is thought to occur predominantly due to a defect in the regulation of the immune response (Longhi et al., 2006).

Subsequent activation and recruitment of CD8 T cells, γδ T cells, cytotoxic T cells and NKT cells to the liver cause waves inflammation and progressive fibrosis. For most patients a prolonged period of treatment with immunosuppressive medications (steroids and Azathioprine) brings about a lasting remission, unfortunately approximately 10 percent of patients have clinical and laboratory deterioration despite compliance with conventional treatment (Manns et al., 2010). Despite augmentation of the immunosuppression or the introduction of newer agents these patient frequently decompensate or develop liver failure and liver transplantation is the only therapeutic option for such individuals and this is associated with significant morbidity and mortality. We currently see 10-20 patients per year in our unit that have refractory autoimmune hepatitis.

*7.3.1.2 Alcoholic Hepatitis*

Nearly one third of the patients presenting with alcoholic liver disease will have evidence of alcohol-induced hepatic inflammation (Hislop et al., 1983). Alcoholic hepatitis is the most dramatic presentation of alcoholic liver disease, and may be potentially reversible. Scoring systems have been developed to assess the severity and prognosis of this condition, and those scoring 9 or more on the Glasgow Alcoholic Hepatitis Score (GAHS) have a 28-day mortality of 60% (Forrest et al., 2005). Controversy exists about the efficacy of current treatments, corticosteroids and pentoxyphylline (Parker et al., 2013). Even if their efficacy is proven there will still be a large unmet need as, from prior trials indicate a 15% mortality at 28 days in treated patients (Mathurin et al., 2002).

In alcoholic hepatitis, immune mediated injury occurs secondary to increased translocation of lipopolysaccharide from the bowel into the portal venous system, which together with elevated reactive oxygen species levels directly activate Kupffer cells leading to up regulation of nuclear factor kappa-b (Wiest and Garcia-Tsao, 2005, Adachi et al., 1994). This results in the production of several inflammatory cytokines including TNF-alpha, IL-8 and monocyte chemotactic protein 1 resulting in the recruitment and activation of inflammatory cells (neutrophils/macrophages) to the liver propagating cellular injury (Zhao et al., 2008, Williams and Barry, 1987). Moreover, lipid-peroxidation products combine with alcohol breakdown products (acetaldehyde) to produce neoantigens which can also stimulate a T cell driven autoimmune response (Meagher et al., 1999). Thus amelioration of macrophage, neutrophil and T cell function in alcoholic hepatitis has potential to reduce the severity of liver damage. Activated MSCs (stimulation with TNF-alpha, LPS) produce TNF-alpha stimulated gene/protein 6 and PGE2, which switch activated pro-inflammatory macrophages to a regulatory phenotype (Prockop and Oh, 2012). MSCs have also been shown to suppress T cell proliferation and function as well as neutrophil function (Raffaghello et al., 2008).

Moreover, sepsis is a major cause of death in patients with alcoholic hepatitis, and studies have indicated anti-septic properties of MSC in a variety of different animal models. Mechanisms underpinning this are incompletely understood but likely relate to an augmentation of bacterial killing and phagocytosis (Mei et al., 2010).

### 7.3.2 Murine models of liver disease

#### *7.3.2.1 OVA-bil model of autoimmune liver injury*

I have recently established a transgenic murine model of AIH (Ova-bil model) in Birmingham. Ova-bil mice specifically express ovalbumin on the biliary epithelium of their liver. Adoptive transfer of OVA-specific $CD4^+$ and $CD8^+$ T cells into Ova-bil mice results in their migration to the biliary tree where they proliferate and induce necro-inflammatory damage (Buxbaum et al., 2006). I have completed preliminary studies to show that peak liver inflammation occurs 10 days following adoptive transfer and is characterized by a mean peak ALT of 500 and a 10 fold increase in mononuclear cell infiltration to the injured livers (Figure 7-1). Liver damage is reflected by high serum levels of TNF-α and IFN-γ and raised serum transaminases due to spill over of biliary inflammation into the parenchyma. Liver histology typically shows a mononuclear infiltrate in the biliary tract with mild/moderate interface hepatitis. I have infused MSC cultured in SM and SM supplemented with TGF-β into OVA-Bil mice to assess impact on liver injury. I have examined various outputs including peak ALT at day 10 and quantitive and qualitative analysis of biliary infiltration by flow cytometry and histology. The early data are encouraging however further work is required to show definitive differences.

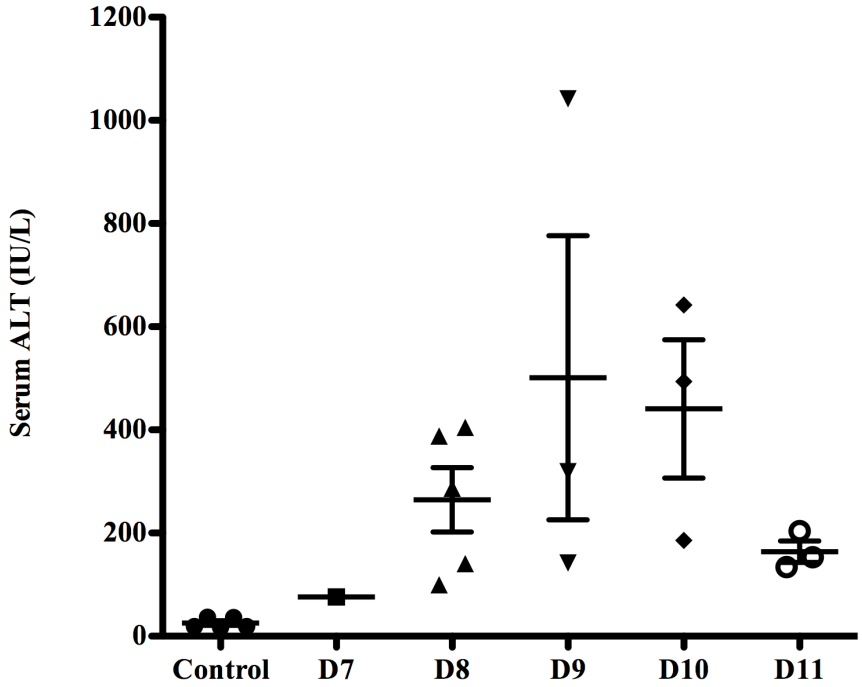


**Figure 7-1 ALT concentration in OVA-bil mice at different time points following infusion of OT1 and OT2 cells.**

*This figure shows the mean ALT level in OVA-Bil mice at different stages following re-constitution with OT1 and OT2 splenocytes. The peak injury occurs at day 9.*

*7.3.2.2 Nrf2$^{-/-}$ model of alcohol hepatitis*

Rodent models of alcoholic hepatitis have been problematic. The nuclear factor-erythroid 2-related factor 2 knockout (Nrf2$^{-/-}$) mouse develops a florid pattern of acute liver injury after alcohol administration with a high mortality (Buxbaum et al., 2006). Nrf2 protects cells from oxidative and xenobiotic stress, such that Nrf2$^{-/-}$ mice exposed to alcohol rapidly deplete their glutathione stores and demonstrate abnormalities of mitochondrial function. Mice subsequently develop a profound Kupffer cell mediated inflammatory response as reflected by high levels of TNF-α.

Mice develop hepatic steatosis, progressive hepatocellular injury, hypoglycaemia and death (Figure 7-2).

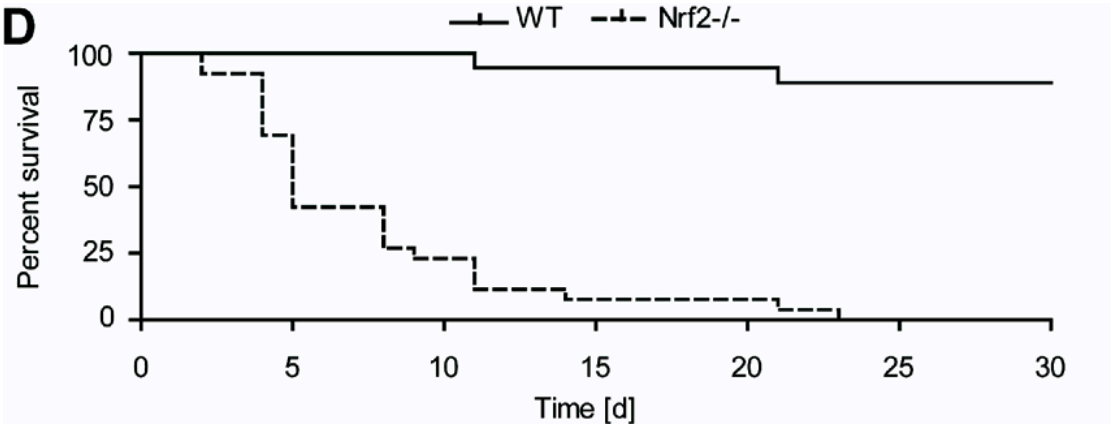


**Figure 7-2 Survival curve of NRF2$^{-/-}$ mice fed on an alcohol diet.**

*This figure shows survival curves for NRF2-/- mice and control mice fed the Lieber-DeCarli diet. Mice lacking the anti-oxidant NRF2 develop steatoheptatis with inflammation that closely resembles human alcoholic hepatitis. The mice die from liver failure as is often the case with the human condition.*

I recently acquired these mice from Sabrina Werner's laboratory in the University of Vienna and am currently expanding the mouse colony. I have the Lieber-DeCarli diet in house and will establish this model. I will infuse MSCs (1 million IP on day 3 and 7) and examine the impact on the natural course of murine alcoholic hepatitis. Specifically I will measure the proportion that develop hypoglycaemia (surrogate for death), peak ALT prior to culling (approximately 4000IU/ml and immunohistochemistry to examine infiltrating/proliferating neutrophils and lymphocytes will be measured.

## 7.4 Limitations

There are limitations to this work. The prospective isolation of PαS MSC is a significant development for the field. For the first time scientists interrogate the basic biology a pure MSC population. Additionally, the use of PαS MSC in rodent models of disease will provide critical translational information that may make hMSC therapy more effective and safer. The isolation of these cells is however far more challenging compare to traditional methods. In addition to several delicate isolation steps, experience and access to high-speed cell sorter is required. This may limit access of some laboratories to these cells. Although our data suggest that PαS MSC are not transformed by in vitro expansion, confirmation of these findings will only be provided following in vivo injection into immunodeficient recipients with long-term follow-up.

We show exciting results supporting lineage priming of MSCs when cultured in GF supplemented media. Additional experiments using combinations of GFs would be of interest. Additionally, withdrawal of the GF following a period of expansion might be studied. For example it is possible MSCs expanded in bFGF supplemented media regain their osteogenic and immunosuppressive potential following removal of the GF. One exciting finding is that cells cultured in SM alone and supplemented with TGF-β have potent in vitro immunosuppressive potential. This has not however been confirmed *in vivo*. Finally, cell homing to target organ is likely to be of critical for effective cellular therapy. Further studies are required to interrogate this property for each cell group. Additional projects might focus on augmenting cell homing as has been described in the Introduction.

## 7.5 Conclusions

Testing experimental drugs in rodent models of disease is a critical and necessary step for drug development. Information regarding dosage, route of infusion, potential toxicity ensure as far as possible drug safety and efficacy when tested in early clinical trials. Due to limitations in the isolation and expansion in mMSCs, cell therapy has progressed uncomfortably quickly in humans, potentially putting patients at risk. The prospective isolation of PαS MSCs overcomes many of avoid many complications of traditional murine isolation. They are multipotent and immunosuppressive in vitro and will provide invaluable pre-clinical data pertaining to MSC cellular therapy.

# REFERENCES


ADACHI, Y., BRADFORD, B. U., GAO, W., BOJES, H. K. & THURMAN, R. G. 1994. Inactivation of Kupffer cells prevents early alcohol-induced liver injury. *Hepatology,* 20**,** 453-60.

AGGARWAL, S. & PITTENGER, M. F. 2005. Human mesenchymal stem cells modulate allogeneic immune cell responses. *Blood,* 105**,** 1815-22.

ALDRIDGE, V., GARG, A., DAVIES, N., BARTLETT, D. C., YOUSTER, J., BEARD, H., KAVANAGH, D. P., KALIA, N., FRAMPTON, J., LALOR, P. F. & NEWSOME, P. N. 2012. Human mesenchymal stem cells are recruited to injured liver in a beta1-integrin and CD44 dependent manner. *Hepatology,* 56**,** 1063-73.

AMARIGLIO, N., HIRSHBERG, A., SCHEITHAUER, B. W., COHEN, Y., LOEWENTHAL, R., TRAKHTENBROT, L., PAZ, N., KOREN-MICHOWITZ, M., WALDMAN, D., LEIDER-TREJO, L., TOREN, A., CONSTANTINI, S. & RECHAVI, G. 2009. Donor-derived brain tumor following neural stem cell transplantation in an ataxia telangiectasia patient. *PLoS medicine,* 6**,** e1000029.

ANNABI, B., LEE, Y. T., TURCOTTE, S., NAUD, E., DESROSIERS, R. R., CHAMPAGNE, M., ELIOPOULOS, N., GALIPEAU, J. & BELIVEAU, R. 2003. Hypoxia promotes murine bone-marrow-derived stromal cell migration and tube formation. *Stem Cells,* 21**,** 337-47.

ARANGO, N. A., SZOTEK, P. P., MANGANARO, T. F., OLIVA, E., DONAHOE, P. K. & TEIXEIRA, J. 2005. Conditional deletion of beta-catenin in the mesenchyme of the developing mouse uterus results in a switch to adipogenesis in the myometrium. *Dev Biol,* 288**,** 276-83.

ASLAN, H., ZILBERMAN, Y., KANDEL, L., LIEBERGALL, M., OSKOUIAN, R. J., GAZIT, D. & GAZIT, Z. 2006. Osteogenic differentiation of noncultured immunoisolated bone marrow-derived CD105+ cells. *Stem Cells,* 24**,** 1728-37.

AUGELLO, A., TASSO, R., NEGRINI, S. M., AMATEIS, A., INDIVERI, F., CANCEDDA, R. & PENNESI, G. 2005. Bone marrow mesenchymal progenitor cells inhibit lymphocyte proliferation by activation of the programmed death 1 pathway. *European journal of immunology,* 35**,** 1482-90.

AUGELLO, A., TASSO, R., NEGRINI, S. M., CANCEDDA, R. & PENNESI, G. 2007. Cell therapy using allogeneic bone marrow mesenchymal stem cells prevents tissue damage in collagen-induced arthritis. *Arthritis Rheum,* 56**,** 1175-86.

AULETTA, J. J., DEANS, R. J. & BARTHOLOMEW, A. M. 2012. Emerging roles for multipotent, bone marrow-derived stromal cells in host defense. *Blood,* 119**,** 1801-9.

BADDOO, M., HILL, K., WILKINSON, R., GAUPP, D., HUGHES, C., KOPEN, G. C. & PHINNEY, D. G. 2003. Characterization of mesenchymal stem cells isolated from murine bone marrow by negative selection. *J Cell Biochem,* 89**,** 1235-49.

BARNA, M., PANDOLFI, P. P. & NISWANDER, L. 2005. Gli3 and Plzf cooperate in proximal limb patterning at early stages of limb development. *Nature,* 436**,** 277-81.

BARRY, M. & BLEACKLEY, R. C. 2002. Cytotoxic T lymphocytes: all roads lead to death. *Nat Rev Immunol,* 2**,** 401-9.

BARTHOLOMEW, A., STURGEON, C., SIATSKAS, M., FERRER, K., MCINTOSH, K., PATIL, S., HARDY, W., DEVINE, S., UCKER, D., DEANS, R., MOSELEY, A. & HOFFMAN, R. 2002. Mesenchymal stem cells suppress lymphocyte proliferation in vitro and prolong skin graft survival in vivo. *Exp Hematol,* 30**,** 42-8.

BARTOSH, T. J., YLOSTALO, J. H., MOHAMMADIPOOR, A., BAZHANOV, N., COBLE, K., CLAYPOOL, K., LEE, R. H., CHOI, H. & PROCKOP, D. J. 2010. Aggregation of human mesenchymal stromal cells (MSCs) into 3D spheroids enhances their antiinflammatory properties. *Proc Natl Acad Sci U S A,* 107**,** 13724-9.

BATTULA, V. L., BAREISS, P. M., TREML, S., CONRAD, S., ALBERT, I., HOJAK, S., ABELE, H., SCHEWE, B., JUST, L., SKUTELLA, T. & BUHRING, H. J. 2007. Human placenta and bone marrow derived MSC cultured in serum-free, b-FGF-containing medium express cell surface frizzled-9 and SSEA-4 and give rise to multilineage differentiation. *Differentiation; research in biological diversity,* 75**,** 279-91.

BATTULA, V. L., TREML, S., BAREISS, P. M., GIESEKE, F., ROELOFS, H., DE ZWART, P., MULLER, I., SCHEWE, B., SKUTELLA, T., FIBBE, W. E., KANZ, L. & BUHRING, H. J. 2009. Isolation of functionally distinct mesenchymal stem cell subsets using antibodies against CD56, CD271, and mesenchymal stem cell antigen-1. *Haematologica,* 94**,** 173-84.

BEN-DAVID, U. & BENVENISTY, N. 2011. The tumorigenicity of human embryonic and induced pluripotent stem cells. *Nature reviews. Cancer,* 11**,** 268-77.

BEN-DAVID, U., MAYSHAR, Y. & BENVENISTY, N. 2011. Large-scale analysis reveals acquisition of lineage-specific chromosomal aberrations in human adult stem cells. *Cell Stem Cell,* 9**,** 97-102.

BENVENUTO, F., FERRARI, S., GERDONI, E., GUALANDI, F., FRASSONI, F., PISTOIA, V., MANCARDI, G. & UCCELLI, A. 2007. Human mesenchymal stem cells promote survival of T cells in a quiescent state. *Stem Cells,* 25**,** 1753-60.

BEYTH, S., BOROVSKY, Z., MEVORACH, D., LIEBERGALL, M., GAZIT, Z., ASLAN, H., GALUN, E. & RACHMILEWITZ, J. 2005. Human mesenchymal stem cells alter antigen-presenting cell maturation and induce T-cell unresponsiveness. *Blood,* 105**,** 2214-9.

BIANCO, P., CAO, X., FRENETTE, P. S., MAO, J. J., ROBEY, P. G., SIMMONS, P. J. & WANG, C. Y. 2013. The meaning, the sense and the significance: translating the science of mesenchymal stem cells into medicine. *Nature medicine,* 19**,** 35-42.

BIANCO, P., ROBEY, P. G. & SIMMONS, P. J. 2008. Mesenchymal stem cells: revisiting history, concepts, and assays. *Cell Stem Cell,* 2**,** 313-9.

BIRCHALL, M. A., AYLING, S. M., HARLEY, R., MURISON, P. J., BURT, R., MITCHARD, L., JONES, A., MACCHIARINI, P., STOKES, C. R. & BAILEY, M. 2012. Laryngeal transplantation in minipigs: early immunological outcomes. *Clinical and experimental immunology,* 167**,** 556-64.

BOIRET, N., RAPATEL, C., VEYRAT-MASSON, R., GUILLOUARD, L., GUERIN, J. J., PIGEON, P., DESCAMPS, S., BOISGARD, S. & BERGER, M. G. 2005. Characterization of nonexpanded mesenchymal progenitor cells from normal adult human bone marrow. *Exp Hematol,* 33**,** 219-25.

BRAULT, V., MOORE, R., KUTSCH, S., ISHIBASHI, M., ROWITCH, D. H., MCMAHON, A. P., SOMMER, L., BOUSSADIA, O. & KEMLER, R. 2001. Inactivation of the beta-catenin gene by Wnt1-Cre-mediated deletion results in dramatic brain malformation and failure of craniofacial development. *Development,* 128**,** 1253-64.

BROWNLIE, R. J. & ZAMOYSKA, R. 2013. T cell receptor signalling networks: branched, diversified and bounded. *Nat Rev Immunol,* 13**,** 257-69.

BUXBAUM, J., QIAN, P., KHUU, C., SHNEIDER, B. L., DAIKH, D. I., GERSHWIN, M. E., ALLEN, P. M. & PETERS, M. G. 2006. Novel model of antigen-specific induction of bile duct injury. *Gastroenterology,* 131**,** 1899-906.

CALVI, L. M., ADAMS, G. B., WEIBRECHT, K. W., WEBER, J. M., OLSON, D. P., KNIGHT, M. C., MARTIN, R. P., SCHIPANI, E., DIVIETI, P., BRINGHURST, F. R., MILNER, L. A., KRONENBERG, H. M. & SCADDEN, D. T. 2003. Osteoblastic cells regulate the haematopoietic stem cell niche. *Nature,* 425**,** 841-6.

CAPLAN, A. I. 1991. Mesenchymal stem cells. *J Orthop Res,* 9**,** 641-50.

CAPLAN, A. I. 1994. The mesengenic process. *Clin Plast Surg,* 21**,** 429-35.

CENTENO, C. J., BUSSE, D., KISIDAY, J., KEOHAN, C., FREEMAN, M. & KARLI, D. 2008. Increased knee cartilage volume in degenerative joint disease using percutaneously implanted, autologous mesenchymal stem cells. *Pain physician,* 11**,** 343-53.

CHAPLIN, D. D. 2006. 1. Overview of the human immune response. *The Journal of allergy and clinical immunology,* 117**,** S430-5.

CHASE, L. G., LAKSHMIPATHY, U., SOLCHAGA, L. A., RAO, M. S. & VEMURI, M. C. 2010. A novel serum-free medium for the expansion of human mesenchymal stem cells. *Stem Cell Res Ther,* 1**,** 8.

CORCIONE, A., BENVENUTO, F., FERRETTI, E., GIUNTI, D., CAPPIELLO, V., CAZZANTI, F., RISSO, M., GUALANDI, F., MANCARDI, G. L., PISTOIA, V. & UCCELLI, A. 2006. Human mesenchymal stem cells modulate B-cell functions. *Blood,* 107**,** 367-72.

COUTU, D. L., FRANCOIS, M. & GALIPEAU, J. 2011. Inhibition of cellular senescence by developmentally regulated FGF receptors in mesenchymal stem cells. *Blood,* 117**,** 6801-12.

CRISAN, M., YAP, S., CASTEILLA, L., CHEN, C. W., CORSELLI, M., PARK, T. S., ANDRIOLO, G., SUN, B., ZHENG, B., ZHANG, L., NOROTTE, C., TENG, P. N., TRAAS, J., SCHUGAR, R., DEASY, B. M., BADYLAK, S., BUHRING, H. J., GIACOBINO, J. P., LAZZARI, L., HUARD, J. & PEAULT, B. 2008. A perivascular origin for mesenchymal stem cells in multiple human organs. *Cell Stem Cell,* 3**,** 301-13.

CYSTER, J. G. & SCHWAB, S. R. 2012. Sphingosine-1-phosphate and lymphocyte egress from lymphoid organs. *Annual review of immunology,* 30**,** 69-94.

DA SILVA MEIRELLES, L., CAPLAN, A. I. & NARDI, N. B. 2008. In search of the in vivo identity of mesenchymal stem cells. *Stem Cells,* 26**,** 2287-99.

DAS, R., JAHR, H., VAN OSCH, G. J. & FARRELL, E. 2010. The role of hypoxia in bone marrow-derived mesenchymal stem cells: considerations for regenerative medicine approaches. *Tissue engineering. Part B, Reviews,* 16**,** 159-68.

DAVATCHI, F., ABDOLLAHI, B. S., MOHYEDDIN, M., SHAHRAM, F. & NIKBIN, B. 2011. Mesenchymal stem cell therapy for knee osteoarthritis. Preliminary report of four patients. *International journal of rheumatic diseases,* 14**,** 211-5.

DELAERE, P. R. 2013. Stem-cell-based, tissue-engineered tracheal replacement in a child. *Lancet,* 381**,** 113.

DELAROSA, O. & LOMBARDO, E. 2010. Modulation of adult mesenchymal stem cells activity by toll-like receptors: implications on therapeutic potential. *Mediators of inflammation,* 2010**,** 865601.

DELORME, B., RINGE, J., PONTIKOGLOU, C., GAILLARD, J., LANGONNE, A., SENSEBE, L., NOEL, D., JORGENSEN, C., HAUPL, T. & CHARBORD, P. 2009. Specific lineage-priming of bone marrow mesenchymal stem cells provides the molecular framework for their plasticity. *Stem Cells,* 27**,** 1142-51.

DERYNCK, R. & ZHANG, Y. E. 2003. Smad-dependent and Smad-independent pathways in TGF-beta family signalling. *Nature,* 425**,** 577-84.

DI NICOLA, M., CARLO-STELLA, C., MAGNI, M., MILANESI, M., LONGONI, P. D., MATTEUCCI, P., GRISANTI, S. & GIANNI, A. M. 2002. Human bone marrow stromal cells suppress T-lymphocyte proliferation induced by cellular or nonspecific mitogenic stimuli. *Blood,* 99**,** 3838-43.

DIEPPE, P. A. & LOHMANDER, L. S. 2005. Pathogenesis and management of pain in osteoarthritis. *Lancet,* 365**,** 965-73.

DIGIROLAMO, C. M., STOKES, D., COLTER, D., PHINNEY, D. G., CLASS, R. & PROCKOP, D. J. 1999. Propagation and senescence of human marrow stromal cells

in culture: a simple colony-forming assay identifies samples with the greatest potential to propagate and differentiate. *Br J Haematol,* 107**,** 275-81.

DING, L., SAUNDERS, T. L., ENIKOLOPOV, G. & MORRISON, S. J. 2012. Endothelial and perivascular cells maintain haematopoietic stem cells. *Nature,* 481**,** 457-62.

DING, Y., XU, D., FENG, G., BUSHELL, A., MUSCHEL, R. J. & WOOD, K. J. 2009. Mesenchymal stem cells prevent the rejection of fully allogenic islet grafts by the immunosuppressive activity of matrix metalloproteinase-2 and -9. *Diabetes,* 58**,** 1797-806.

DJOUAD, F., CHARBONNIER, L. M., BOUFFI, C., LOUIS-PLENCE, P., BONY, C., APPARAILLY, F., CANTOS, C., JORGENSEN, C. & NOEL, D. 2007. Mesenchymal stem cells inhibit the differentiation of dendritic cells through an interleukin-6-dependent mechanism. *Stem Cells,* 25**,** 2025-32.

DOMINICI, M., LE BLANC, K., MUELLER, I., SLAPER-CORTENBACH, I., MARINI, F., KRAUSE, D., DEANS, R., KEATING, A., PROCKOP, D. & HORWITZ, E. 2006. Minimal criteria for defining multipotent mesenchymal stromal cells. The International Society for Cellular Therapy position statement. *Cytotherapy,* 8**,** 315-7.

DROST, A. C., WENG, S., FEIL, G., SCHAFER, J., BAUMANN, S., KANZ, L., SIEVERT, K. D., STENZL, A. & MOHLE, R. 2009. In vitro myogenic differentiation of human bone marrow-derived mesenchymal stem cells as a potential treatment for urethral sphincter muscle repair. *Annals of the New York Academy of Sciences,* 1176**,** 135-43.

ELLIOTT, M. J., DE COPPI, P., SPEGGIORIN, S., ROEBUCK, D., BUTLER, C. R., SAMUEL, E., CROWLEY, C., MCLAREN, C., FIERENS, A., VONDRYS, D., COCHRANE, L., JEPHSON, C., JANES, S., BEAUMONT, N. J., COGAN, T., BADER, A., SEIFALIAN, A. M., HSUAN, J. J., LOWDELL, M. W. & BIRCHALL,

M. A. 2012. Stem-cell-based, tissue engineered tracheal replacement in a child: a 2-year follow-up study. *Lancet,* 380**,** 994-1000.

ENGLER, A. J., SEN, S., SWEENEY, H. L. & DISCHER, D. E. 2006. Matrix elasticity directs stem cell lineage specification. *Cell,* 126**,** 677-89.

ERICES, A., CONGET, P. & MINGUELL, J. J. 2000. Mesenchymal progenitor cells in human umbilical cord blood. *British journal of haematology,* 109**,** 235-42.

ESLAMINEJAD, M. B., NIKMAHZAR, A., TAGHIYAR, L., NADRI, S. & MASSUMI, M. 2006. Murine mesenchymal stem cells isolated by low density primary culture system. *Dev Growth Differ,* 48**,** 361-70.

FALLA, N., VLASSELAER, V., BIERKENS, J., BORREMANS, B., SCHOETERS, G. & VAN GORP, U. 1993. Characterization of a 5-fluorouracil-enriched osteoprogenitor population of the murine bone marrow. *Blood,* 82**,** 3580-91.

FLETCHER, A. L., LUKACS-KORNEK, V., REYNOSO, E. D., PINNER, S. E., BELLEMARE-PELLETIER, A., CURRY, M. S., COLLIER, A. R., BOYD, R. L. & TURLEY, S. J. 2010. Lymph node fibroblastic reticular cells directly present peripheral tissue antigen under steady-state and inflammatory conditions. *The Journal of experimental medicine,* 207**,** 689-97.

FORBES, S. J., RUSSO, F. P., REY, V., BURRA, P., RUGGE, M., WRIGHT, N. A. & ALISON, M. R. 2004. A significant proportion of myofibroblasts are of bone marrow origin in human liver fibrosis. *Gastroenterology,* 126**,** 955-63.

FORREST, E. H., EVANS, C. D., STEWART, S., PHILLIPS, M., OO, Y. H., MCAVOY, N. C., FISHER, N. C., SINGHAL, S., BRIND, A., HAYDON, G., O'GRADY, J., DAY, C. P., HAYES, P. C., MURRAY, L. S. & MORRIS, A. J. 2005. Analysis of factors predictive of mortality in alcoholic hepatitis and derivation and validation of the Glasgow alcoholic hepatitis score. *Gut,* 54**,** 1174-9.

FRIEDENSTEIN, A. J., CHAILAKHJAN, R. K. & LALYKINA, K. S. 1970. The development of fibroblast colonies in monolayer cultures of guinea-pig bone marrow and spleen cells. *Cell Tissue Kinet,* 3**,** 393-403.

FRIEDENSTEIN, A. J., CHAILAKHYAN, R. K., LATSINIK, N. V., PANASYUK, A. F. & KEILISS-BOROK, I. V. 1974. Stromal cells responsible for transferring the microenvironment of the hemopoietic tissues. Cloning in vitro and retransplantation in vivo. *Transplantation,* 17**,** 331-40.

GALVIN, K. A. & JONES, D. G. 2002. Adult human neural stem cells for cell-replacement therapies in the central nervous system. *The Medical journal of Australia,* 177**,** 316-8.

GANG, E. J., BOSNAKOVSKI, D., FIGUEIREDO, C. A., VISSER, J. W. & PERLINGEIRO, R. C. 2007. SSEA-4 identifies mesenchymal stem cells from bone marrow. *Blood,* 109**,** 1743-51.

GESTA, S., TSENG, Y. H. & KAHN, C. R. 2007. Developmental origin of fat: tracking obesity to its source. *Cell,* 131**,** 242-56.

GLORIEUX, F. H., BISHOP, N. J., PLOTKIN, H., CHABOT, G., LANOUE, G. & TRAVERS, R. 1998. Cyclic administration of pamidronate in children with severe osteogenesis imperfecta. *The New England journal of medicine,* 339**,** 947-52.

GOKER, H., HAZNEDAROGLU, I. C. & CHAO, N. J. 2001. Acute graft-vs-host disease: pathobiology and management. *Exp Hematol,* 29**,** 259-77.

GOLDRING, M. B., TSUCHIMOCHI, K. & IJIRI, K. 2006. The control of chondrogenesis. *J Cell Biochem,* 97**,** 33-44.

GRONTHOS, S., ZANNETTINO, A. C., HAY, S. J., SHI, S., GRAVES, S. E., KORTESIDIS, A. & SIMMONS, P. J. 2003. Molecular and cellular characterisation of highly purified stromal stem cells derived from human bone marrow. *Journal of cell science,* 116**,** 1827-35.

GUILLOT, P. V., ABASS, O., BASSETT, J. H., SHEFELBINE, S. J., BOU-GHARIOS, G., CHAN, J., KURATA, H., WILLIAMS, G. R., POLAK, J. & FISK, N. M. 2008. Intrauterine transplantation of human fetal mesenchymal stem cells from first-trimester blood repairs bone and reduces fractures in osteogenesis imperfecta mice. *Blood,* 111**,** 1717-25.

HANIFFA, M. A., COLLIN, M. P., BUCKLEY, C. D. & DAZZI, F. 2009. Mesenchymal stem cells: the fibroblasts' new clothes? *Haematologica,* 94**,** 258-63.

HASHIMOTO, N., JIN, H., LIU, T., CHENSUE, S. W. & PHAN, S. H. 2004. Bone marrow-derived progenitor cells in pulmonary fibrosis. *J Clin Invest,* 113**,** 243-52.

HISLOP, W. S., BOUCHIER, I. A., ALLAN, J. G., BRUNT, P. W., EASTWOOD, M., FINLAYSON, N. D., JAMES, O., RUSSELL, R. I. & WATKINSON, G. 1983. Alcoholic liver disease in Scotland and northeastern England: presenting features in 510 patients. *The Quarterly journal of medicine,* 52**,** 232-43.

HORWITZ, E. M., PROCKOP, D. J., GORDON, P. L., KOO, W. W., FITZPATRICK, L. A., NEEL, M. D., MCCARVILLE, M. E., ORCHARD, P. J., PYERITZ, R. E. & BRENNER, M. K. 2001. Clinical responses to bone marrow transplantation in children with severe osteogenesis imperfecta. *Blood,* 97**,** 1227-31.

HOULIHAN, D. D., MABUCHI, Y., MORIKAWA, S., NIIBE, K., ARAKI, D., SUZUKI, S., OKANO, H. & MATSUZAKI, Y. 2012. Isolation of mouse mesenchymal stem cells on the basis of expression of Sca-1 and PDGFR-alpha. *Nat Protoc,* 7**,** 2103-11.

HOULIHAN, D. D. & NEWSOME, P. N. 2008. Critical review of clinical trials of bone marrow stem cells in liver disease. *Gastroenterology,* 135**,** 438-50.

HU, E., ZHU, Y., FREDRICKSON, T., BARNES, M., KELSELL, D., BEELEY, L. & BROOKS, D. 1998. Tissue restricted expression of two human Frzbs in preadipocytes and pancreas. *Biochem Biophys Res Commun,* 247**,** 287-93.

HU, X., YU, S. P., FRASER, J. L., LU, Z., OGLE, M. E., WANG, J. A. & WEI, L. 2008. Transplantation of hypoxia-preconditioned mesenchymal stem cells improves infarcted heart function via enhanced survival of implanted cells and angiogenesis. *The Journal of thoracic and cardiovascular surgery,* 135**,** 799-808.

HUEBSCH, N., ARANY, P. R., MAO, A. S., SHVARTSMAN, D., ALI, O. A., BENCHERIF, S. A., RIVERA-FELICIANO, J. & MOONEY, D. J. 2010. Harnessing traction-mediated manipulation of the cell/matrix interface to control stem-cell fate. *Nature materials,* 9**,** 518-26.

HUMPHRIES, J. D., BYRON, A. & HUMPHRIES, M. J. 2006. Integrin ligands at a glance. *Journal of cell science,* 119**,** 3901-3.

HUNG, S. P., HO, J. H., SHIH, Y. R., LO, T. & LEE, O. K. 2012. Hypoxia promotes proliferation and osteogenic differentiation potentials of human mesenchymal stem cells. *Journal of orthopaedic research : official publication of the Orthopaedic Research Society,* 30**,** 260-6.

HUNZIKER, E. B. 2002. Articular cartilage repair: basic science and clinical progress. A review of the current status and prospects. *Osteoarthritis and cartilage / OARS, Osteoarthritis Research Society,* 10**,** 432-63.

IBRAHIMI, A., BERTRAND, B., BARDON, S., AMRI, E. Z., GRIMALDI, P., AILHAUD, G. & DANI, C. 1993. Cloning of alpha 2 chain of type VI collagen and expression during mouse development. *Biochem J,* 289 ( Pt 1)**,** 141-7.

INOUE, S., POPP, F. C., KOEHL, G. E., PISO, P., SCHLITT, H. J., GEISSLER, E. K. & DAHLKE, M. H. 2006. Immunomodulatory effects of mesenchymal stem cells in a rat organ transplant model. *Transplantation,* 81**,** 1589-95.

ISHII, M., KOIKE, C., IGARASHI, A., YAMANAKA, K., PAN, H., HIGASHI, Y., KAWAGUCHI, H., SUGIYAMA, M., KAMATA, N., IWATA, T., MATSUBARA, T., NAKAMURA, K., KURIHARA, H., TSUJI, K. & KATO, Y. 2005. Molecular

markers distinguish bone marrow mesenchymal stem cells from fibroblasts. *Biochem Biophys Res Commun,* 332**,** 297-303.

ISHII, M., MERRILL, A. E., CHAN, Y. S., GITELMAN, I., RICE, D. P., SUCOV, H. M. & MAXSON, R. E., JR. 2003. Msx2 and Twist cooperatively control the development of the neural crest-derived skeletogenic mesenchyme of the murine skull vault. *Development,* 130**,** 6131-42.

JIANG, X. X., ZHANG, Y., LIU, B., ZHANG, S. X., WU, Y., YU, X. D. & MAO, N. 2005. Human mesenchymal stem cells inhibit differentiation and function of monocyte-derived dendritic cells. *Blood,* 105**,** 4120-6.

JIANG, Y., JAHAGIRDAR, B. N., REINHARDT, R. L., SCHWARTZ, R. E., KEENE, C. D., ORTIZ-GONZALEZ, X. R., REYES, M., LENVIK, T., LUND, T., BLACKSTAD, M., DU, J., ALDRICH, S., LISBERG, A., LOW, W. C., LARGAESPADA, D. A. & VERFAILLIE, C. M. 2002. Pluripotency of mesenchymal stem cells derived from adult marrow. *Nature,* 418**,** 41-9.

JOHNSON, L. A., CLASPER, S., HOLT, A. P., LALOR, P. F., BABAN, D. & JACKSON, D. G. 2006. An inflammation-induced mechanism for leukocyte transmigration across lymphatic vessel endothelium. *The Journal of experimental medicine,* 203**,** 2763-77.

JONES, E. & MCGONAGLE, D. 2008. Human bone marrow mesenchymal stem cells in vivo. *Rheumatology (Oxford),* 47**,** 126-31.

JUNG, S., PANCHALINGAM, K. M., ROSENBERG, L. & BEHIE, L. A. 2012a. Ex vivo expansion of human mesenchymal stem cells in defined serum-free media. *Stem cells international,* 2012**,** 123030.

JUNG, S., SEN, A., ROSENBERG, L. & BEHIE, L. A. 2010. Identification of growth and attachment factors for the serum-free isolation and expansion of human mesenchymal stromal cells. *Cytotherapy,* 12**,** 637-57.

JUNG, S., SEN, A., ROSENBERG, L. & BEHIE, L. A. 2012b. Human mesenchymal stem cell culture: rapid and efficient isolation and expansion in a defined serum-free medium. *J Tissue Eng Regen Med,* 6**,** 391-403.

JUNG, Y., BAUER, G. & NOLTA, J. A. 2012c. Concise review: Induced pluripotent stem cell-derived mesenchymal stem cells: progress toward safe clinical products. *Stem Cells,* 30**,** 42-7.

JUNGEBLUTH, P., ALICI, E., BAIGUERA, S., LE BLANC, K., BLOMBERG, P., BOZOKY, B., CROWLEY, C., EINARSSON, O., GRINNEMO, K. H., GUDBJARTSSON, T., LE GUYADER, S., HENRIKSSON, G., HERMANSON, O., JUTO, J. E., LEIDNER, B., LILJA, T., LISKA, J., LUEDDE, T., LUNDIN, V., MOLL, G., NILSSON, B., RODERBURG, C., STROMBLAD, S., SUTLU, T., TEIXEIRA, A. I., WATZ, E., SEIFALIAN, A. & MACCHIARINI, P. 2011. Tracheobronchial transplantation with a stem-cell-seeded bioartificial nanocomposite: a proof-of-concept study. *Lancet,* 378**,** 1997-2004.

KAFIENAH, W., MISTRY, S., DICKINSON, S. C., SIMS, T. J., LEARMONTH, I. & HOLLANDER, A. P. 2007. Three-dimensional cartilage tissue engineering using adult stem cells from osteoarthritis patients. *Arthritis and rheumatism,* 56**,** 177-87.

KARNOUB, A. E., DASH, A. B., VO, A. P., SULLIVAN, A., BROOKS, M. W., BELL, G. W., RICHARDSON, A. L., POLYAK, K., TUBO, R. & WEINBERG, R. A. 2007. Mesenchymal stem cells within tumour stroma promote breast cancer metastasis. *Nature,* 449**,** 557-63.

KATAKAI, T., HARA, T., LEE, J. H., GONDA, H., SUGAI, M. & SHIMIZU, A. 2004. A novel reticular stromal structure in lymph node cortex: an immuno-platform for interactions among dendritic cells, T cells and B cells. *International immunology,* 16**,** 1133-42.

KEATING, A. 2012. Mesenchymal stromal cells: new directions. *Cell Stem Cell,* 10**,** 709-16.

KENNELL, J. A. & MACDOUGALD, O. A. 2005. Wnt signaling inhibits adipogenesis through beta-catenin-dependent and -independent mechanisms. *J Biol Chem,* 280**,** 24004-10.

KIM, J., KANG, J. W., PARK, J. H., CHOI, Y., CHOI, K. S., PARK, K. D., BAEK, D. H., SEONG, S. K., MIN, H. K. & KIM, H. S. 2009. Biological characterization of long-term cultured human mesenchymal stem cells. *Arch Pharm Res,* 32**,** 117-26.

KIM, K. Y., KOVACS, M., KAWAMOTO, S., SELLERS, J. R. & ADELSTEIN, R. S. 2005. Disease-associated mutations and alternative splicing alter the enzymatic and motile activity of nonmuscle myosins II-B and II-C. *The Journal of biological chemistry,* 280**,** 22769-75.

KIST, R., SCHREWE, H., BALLING, R. & SCHERER, G. 2002. Conditional inactivation of Sox9: a mouse model for campomelic dysplasia. *Genesis,* 32**,** 121-3.

KMITA, M., TARCHINI, B., ZAKANY, J., LOGAN, M., TABIN, C. J. & DUBOULE, D. 2005. Early developmental arrest of mammalian limbs lacking HoxA/HoxD gene function. *Nature,* 435**,** 1113-6.

KOIDE, Y., MORIKAWA, S., MABUCHI, Y., MUGURUMA, Y., HIRATSU, E., HASEGAWA, K., KOBAYASHI, M., ANDO, K., KINJO, K., OKANO, H. & MATSUZAKI, Y. 2007. Two distinct stem cell lineages in murine bone marrow. *Stem Cells,* 25**,** 1213-21.

KOMORI, T. 2006. Regulation of osteoblast differentiation by transcription factors. *J Cell Biochem,* 99**,** 1233-9.

KOMORI, T., YAGI, H., NOMURA, S., YAMAGUCHI, A., SASAKI, K., DEGUCHI, K., SHIMIZU, Y., BRONSON, R. T., GAO, Y. H., INADA, M., SATO, M., OKAMOTO, R., KITAMURA, Y., YOSHIKI, S. & KISHIMOTO, T. 1997. Targeted disruption of Cbfa1 results in a complete lack of bone formation owing to maturational arrest of osteoblasts. *Cell,* 89**,** 755-64.

KRAMPERA, M., COSMI, L., ANGELI, R., PASINI, A., LIOTTA, F., ANDREINI, A., SANTARLASCI, V., MAZZINGHI, B., PIZZOLO, G., VINANTE, F., ROMAGNANI, P., MAGGI, E., ROMAGNANI, S. & ANNUNZIATO, F. 2006. Role for interferon-gamma in the immunomodulatory activity of human bone marrow mesenchymal stem cells. *Stem Cells,* 24**,** 386-98.

KRAWITT, E. L. 2006. Autoimmune hepatitis. *The New England journal of medicine,* 354**,** 54-66.

KUCI, S., KUCI, Z., KREYENBERG, H., DEAK, E., PUTSCH, K., HUENECKE, S., AMARA, C., KOLLER, S., RETTINGER, E., GREZ, M., KOEHL, U., LATIFI-PUPOVCI, H., HENSCHLER, R., TONN, T., VON LAER, D., KLINGEBIEL, T. & BADER, P. 2010. CD271 antigen defines a subset of multipotent stromal cells with immunosuppressive and lymphohematopoietic engraftment-promoting properties. *Haematologica,* 95**,** 651-9.

KURODA, R., ISHIDA, K., MATSUMOTO, T., AKISUE, T., FUJIOKA, H., MIZUNO, K., OHGUSHI, H., WAKITANI, S. & KUROSAKA, M. 2007. Treatment of a full-thickness articular cartilage defect in the femoral condyle of an athlete with autologous bone-marrow stromal cells. *Osteoarthritis and cartilage / OARS, Osteoarthritis Research Society,* 15**,** 226-31.

LAIOSA, C. V., STADTFELD, M. & GRAF, T. 2006. Determinants of lymphoid-myeloid lineage diversification. *Annual review of immunology,* 24**,** 705-38.

LE BLANC, K. & MOUGIAKAKOS, D. 2012. Multipotent mesenchymal stromal cells and the innate immune system. *Nature reviews. Immunology,* 12**,** 383-96.

LE BLANC, K., RASMUSSON, I., SUNDBERG, B., GOTHERSTROM, C., HASSAN, M., UZUNEL, M. & RINGDEN, O. 2004. Treatment of severe acute graft-versus-host disease with third party haploidentical mesenchymal stem cells. *Lancet,* 363**,** 1439-41.

LEE, B., THIRUNAVUKKARASU, K., ZHOU, L., PASTORE, L., BALDINI, A., HECHT, J., GEOFFROY, V., DUCY, P. & KARSENTY, G. 1997. Missense mutations abolishing DNA binding of the osteoblast-specific transcription factor OSF2/CBFA1 in cleidocranial dysplasia. *Nature genetics,* 16**,** 307-10.

LEE, J. W., EPARDAUD, M., SUN, J., BECKER, J. E., CHENG, A. C., YONEKURA, A. R., HEATH, J. K. & TURLEY, S. J. 2007. Peripheral antigen display by lymph node stroma promotes T cell tolerance to intestinal self. *Nature immunology,* 8**,** 181-90.

LEE, R. H., SEO, M. J., REGER, R. L., SPEES, J. L., PULIN, A. A., OLSON, S. D. & PROCKOP, D. J. 2006. Multipotent stromal cells from human marrow home to and promote repair of pancreatic islets and renal glomeruli in diabetic NOD/scid mice. *Proc Natl Acad Sci U S A,* 103**,** 17438-43.

LEE, S. J., VOGELSANG, G. & FLOWERS, M. E. 2003. Chronic graft-versus-host disease. *Biol Blood Marrow Transplant,* 9**,** 215-33.

LEFEBVRE, V., BEHRINGER, R. R. & DE CROMBRUGGHE, B. 2001. L-Sox5, Sox6 and Sox9 control essential steps of the chondrocyte differentiation pathway. *Osteoarthritis Cartilage,* 9 Suppl A**,** S69-75.

LEFEBVRE, V., LI, P. & DE CROMBRUGGHE, B. 1998. A new long form of Sox5 (L-Sox5), Sox6 and Sox9 are coexpressed in chondrogenesis and cooperatively activate the type II collagen gene. *EMBO J,* 17**,** 5718-33.

LI, C., KONG, Y., WANG, H., WANG, S., YU, H., LIU, X., YANG, L., JIANG, X. & LI, L. 2009. Homing of bone marrow mesenchymal stem cells mediated by sphingosine 1-phosphate contributes to liver fibrosis. *J Hepatol,* 50**,** 1174-83.

LI, J., DEANE, J. A., CAMPANALE, N. V., BERTRAM, J. F. & RICARDO, S. D. 2007. The contribution of bone marrow-derived cells to the development of renal interstitial fibrosis. *Stem Cells,* 25**,** 697-706.

LI, Y., CHEN, J., CHEN, X. G., WANG, L., GAUTAM, S. C., XU, Y. X., KATAKOWSKI, M., ZHANG, L. J., LU, M., JANAKIRAMAN, N. & CHOPP, M. 2002. Human marrow stromal cell therapy for stroke in rat: neurotrophins and functional recovery. *Neurology,* 59**,** 514-23.

LINK, A., VOGT, T. K., FAVRE, S., BRITSCHGI, M. R., ACHA-ORBEA, H., HINZ, B., CYSTER, J. G. & LUTHER, S. A. 2007. Fibroblastic reticular cells in lymph nodes regulate the homeostasis of naive T cells. *Nature immunology,* 8**,** 1255-65.

LIOTTA, F., ANGELI, R., COSMI, L., FILI, L., MANUELLI, C., FROSALI, F., MAZZINGHI, B., MAGGI, L., PASINI, A., LISI, V., SANTARLASCI, V., CONSOLONI, L., ANGELOTTI, M. L., ROMAGNANI, P., PARRONCHI, P., KRAMPERA, M., MAGGI, E., ROMAGNANI, S. & ANNUNZIATO, F. 2008. Toll-like receptors 3 and 4 are expressed by human bone marrow-derived mesenchymal stem cells and can inhibit their T-cell modulatory activity by impairing Notch signaling. *Stem Cells,* 26**,** 279-89.

LIU, H., XUE, W., GE, G., LUO, X., LI, Y., XIANG, H., DING, X., TIAN, P. & TIAN, X. 2010. Hypoxic preconditioning advances CXCR4 and CXCR7 expression by activating HIF-1alpha in MSCs. *Biochemical and biophysical research communications,* 401**,** 509-15.

LOGAN, C. Y. & NUSSE, R. 2004. The Wnt signaling pathway in development and disease. *Annu Rev Cell Dev Biol,* 20**,** 781-810.

LONGHI, M. S., HUSSAIN, M. J., MITRY, R. R., ARORA, S. K., MIELI-VERGANI, G., VERGANI, D. & MA, Y. 2006. Functional study of CD4+CD25+ regulatory T cells in health and autoimmune hepatitis. *Journal of immunology,* 176**,** 4484-91.

LUKACS-KORNEK, V., MALHOTRA, D., FLETCHER, A. L., ACTON, S. E., ELPEK, K. G., TAYALIA, P., COLLIER, A. R. & TURLEY, S. J. 2011. Regulated

release of nitric oxide by nonhematopoietic stroma controls expansion of the activated T cell pool in lymph nodes. *Nature immunology,* 12**,** 1096-104.

LYSY, P. A., SMETS, F., SIBILLE, C., NAJIMI, M. & SOKAL, E. M. 2007. Human skin fibroblasts: From mesodermal to hepatocyte-like differentiation. *Hepatology,* 46**,** 1574-85.

MABUCHI, Y., HOULIHAN, D. D., AKAZAWA, C., OKANO, H. & MATSUZAKI, Y. 2013. Prospective isolation of murine and human bone marrow mesenchymal stem cells based on surface markers. *Stem cells international,* 2013**,** 507301.

MACCHIARINI, P., JUNGEBLUTH, P., GO, T., ASNAGHI, M. A., REES, L. E., COGAN, T. A., DODSON, A., MARTORELL, J., BELLINI, S., PARNIGOTTO, P. P., DICKINSON, S. C., HOLLANDER, A. P., MANTERO, S., CONCONI, M. T. & BIRCHALL, M. A. 2008. Clinical transplantation of a tissue-engineered airway. *Lancet,* 372**,** 2023-30.

MALHOTRA, D., FLETCHER, A. L. & TURLEY, S. J. 2013. Stromal and hematopoietic cells in secondary lymphoid organs: partners in immunity. *Immunological reviews,* 251**,** 160-76.

MANNS, M. P., CZAJA, A. J., GORHAM, J. D., KRAWITT, E. L., MIELI-VERGANI, G., VERGANI, D. & VIERLING, J. M. 2010. Diagnosis and management of autoimmune hepatitis. *Hepatology,* 51**,** 2193-213.

MARTIN, P. J., UBERTI, J. P., SOIFFER, R. J., KLINGEMANN, H., WALLER, E. K., DALY, A. S., HERRMANN, R. P. & KEBRIAEI, P. 2010. Prochymal Improves Response Rates In Patients With Steroid-Refractory Acute Graft Versus Host Disease (SR-GVHD) Involving The Liver And Gut: Results Of A Randomized, Placebo-Controlled, Multicenter Phase III Trial In GVHD. *Biol Blood Marrow Transplant,* 16**,** S169-S170.

MATHURIN, P., MENDENHALL, C. L., CARITHERS, R. L., JR., RAMOND, M. J., MADDREY, W. C., GARSTIDE, P., RUEFF, B., NAVEAU, S., CHAPUT, J. C. & POYNARD, T. 2002. Corticosteroids improve short-term survival in patients with severe alcoholic hepatitis (AH): individual data analysis of the last three randomized placebo controlled double blind trials of corticosteroids in severe AH. *Journal of hepatology,* 36**,** 480-7.

MAURI, C. & BOSMA, A. 2012. Immune regulatory function of B cells. *Annu Rev Immunol,* 30**,** 221-41.

MAYSHAR, Y., BEN-DAVID, U., LAVON, N., BIANCOTTI, J. C., YAKIR, B., CLARK, A. T., PLATH, K., LOWRY, W. E. & BENVENISTY, N. 2010. Identification and classification of chromosomal aberrations in human induced pluripotent stem cells. *Cell Stem Cell,* 7**,** 521-31.

MEAGHER, E. A., BARRY, O. P., BURKE, A., LUCEY, M. R., LAWSON, J. A., ROKACH, J. & FITZGERALD, G. A. 1999. Alcohol-induced generation of lipid peroxidation products in humans. *The Journal of clinical investigation,* 104**,** 805-13.

MEI, S. H., HAITSMA, J. J., DOS SANTOS, C. C., DENG, Y., LAI, P. F., SLUTSKY, A. S., LILES, W. C. & STEWART, D. J. 2010. Mesenchymal stem cells reduce inflammation while enhancing bacterial clearance and improving survival in sepsis. *American journal of respiratory and critical care medicine,* 182**,** 1047-57.

MEIRELLES LDA, S. & NARDI, N. B. 2003. Murine marrow-derived mesenchymal stem cell: isolation, in vitro expansion, and characterization. *Br J Haematol,* 123**,** 702-11.

MENDEZ-FERRER, S., MICHURINA, T. V., FERRARO, F., MAZLOOM, A. R., MACARTHUR, B. D., LIRA, S. A., SCADDEN, D. T., MA'AYAN, A., ENIKOLOPOV, G. N. & FRENETTE, P. S. 2010. Mesenchymal and haematopoietic stem cells form a unique bone marrow niche. *Nature,* 466**,** 829-34.

MIURA, M., MIURA, Y., PADILLA-NASH, H. M., MOLINOLO, A. A., FU, B., PATEL, V., SEO, B. M., SONOYAMA, W., ZHENG, J. J., BAKER, C. C., CHEN, W., RIED, T. & SHI, S. 2006. Accumulated chromosomal instability in murine bone marrow mesenchymal stem cells leads to malignant transformation. *Stem Cells,* 24**,** 1095-103.

MORETTA, A., BOTTINO, C., VITALE, M., PENDE, D., CANTONI, C., MINGARI, M. C., BIASSONI, R. & MORETTA, L. 2001. Activating receptors and coreceptors involved in human natural killer cell-mediated cytolysis. *Annu Rev Immunol,* 19**,** 197-223.

MORIKAWA, S., MABUCHI, Y., KUBOTA, Y., NAGAI, Y., NIIBE, K., HIRATSU, E., SUZUKI, S., MIYAUCHI-HARA, C., NAGOSHI, N., SUNABORI, T., SHIMMURA, S., MIYAWAKI, A., NAKAGAWA, T., SUDA, T., OKANO, H. & MATSUZAKI, Y. 2009a. Prospective identification, isolation, and systemic transplantation of multipotent mesenchymal stem cells in murine bone marrow. *J Exp Med,* 206**,** 2483-96.

MORIKAWA, S., MABUCHI, Y., NIIBE, K., SUZUKI, S., NAGOSHI, N., SUNABORI, T., SHIMMURA, S., NAGAI, Y., NAKAGAWA, T., OKANO, H. & MATSUZAKI, Y. 2009b. Development of mesenchymal stem cells partially originate from the neural crest. *Biochem Biophys Res Commun,* 379**,** 1114-9.

MUGURUMA, Y., YAHATA, T., MIYATAKE, H., SATO, T., UNO, T., ITOH, J., KATO, S., ITO, M., HOTTA, T. & ANDO, K. 2006. Reconstitution of the functional human hematopoietic microenvironment derived from human mesenchymal stem cells in the murine bone marrow compartment. *Blood,* 107**,** 1878-87.

NADRI, S. & SOLEIMANI, M. 2007. Isolation murine mesenchymal stem cells by positive selection. *In Vitro Cell Dev Biol Anim,* 43**,** 276-82.

NADRI, S., SOLEIMANI, M., HOSSENI, R. H., MASSUMI, M., ATASHI, A. & IZADPANAH, R. 2007. An efficient method for isolation of murine bone marrow mesenchymal stem cells. *Int J Dev Biol,* 51**,** 723-9.

NAKASHIMA, K., ZHOU, X., KUNKEL, G., ZHANG, Z., DENG, J. M., BEHRINGER, R. R. & DE CROMBRUGGHE, B. 2002. The novel zinc finger-containing transcription factor osterix is required for osteoblast differentiation and bone formation. *Cell,* 108**,** 17-29.

NAUTA, A. J., KRUISSELBRINK, A. B., LURVINK, E., WILLEMZE, R. & FIBBE, W. E. 2006. Mesenchymal stem cells inhibit generation and function of both CD34+-derived and monocyte-derived dendritic cells. *J Immunol,* 177**,** 2080-7.

NEJADNIK, H., HUI, J. H., FENG CHOONG, E. P., TAI, B. C. & LEE, E. H. 2010. Autologous bone marrow-derived mesenchymal stem cells versus autologous chondrocyte implantation: an observational cohort study. *The American journal of sports medicine,* 38**,** 1110-6.

NEMETH, K., LEELAHAVANICHKUL, A., YUEN, P. S., MAYER, B., PARMELEE, A., DOI, K., ROBEY, P. G., LEELAHAVANICHKUL, K., KOLLER, B. H., BROWN, J. M., HU, X., JELINEK, I., STAR, R. A. & MEZEY, E. 2009. Bone marrow stromal cells attenuate sepsis via prostaglandin E(2)-dependent reprogramming of host macrophages to increase their interleukin-10 production. *Nat Med,* 15**,** 42-9.

NG, F., BOUCHER, S., KOH, S., SASTRY, K. S., CHASE, L., LAKSHMIPATHY, U., CHOONG, C., YANG, Z., VEMURI, M. C., RAO, M. S. & TANAVDE, V. 2008. PDGF, TGF-beta, and FGF signaling is important for differentiation and growth of mesenchymal stem cells (MSCs): transcriptional profiling can identify markers and signaling pathways important in differentiation of MSCs into adipogenic, chondrogenic, and osteogenic lineages. *Blood,* 112**,** 295-307.

NG, L. J., WHEATLEY, S., MUSCAT, G. E., CONWAY-CAMPBELL, J., BOWLES, J., WRIGHT, E., BELL, D. M., TAM, P. P., CHEAH, K. S. & KOOPMAN, P. 1997. SOX9 binds DNA, activates transcription, and coexpresses with type II collagen during chondrogenesis in the mouse. *Dev Biol,* 183**,** 108-21.

NG, S. Y., YOSHIDA, T., ZHANG, J. & GEORGOPOULOS, K. 2009. Genome-wide lineage-specific transcriptional networks underscore Ikaros-dependent lymphoid priming in hematopoietic stem cells. *Immunity,* 30**,** 493-507.

NING, H., YANG, F., JIANG, M., HU, L., FENG, K., ZHANG, J., YU, Z., LI, B., XU, C., LI, Y., WANG, J., HU, J., LOU, X. & CHEN, H. 2008. The correlation between cotransplantation of mesenchymal stem cells and higher recurrence rate in hematologic malignancy patients: outcome of a pilot clinical study. *Leukemia,* 22**,** 593-9.

NOMBELA-ARRIETA, C., RITZ, J. & SILBERSTEIN, L. E. 2011. The elusive nature and function of mesenchymal stem cells. *Nat Rev Mol Cell Biol,* 12**,** 126-31.

OLSEN, B. R., REGINATO, A. M. & WANG, W. 2000. Bone development. *Annu Rev Cell Dev Biol,* 16**,** 191-220.

OO, Y. H., HUBSCHER, S. G. & ADAMS, D. H. 2010. Autoimmune hepatitis: new paradigms in the pathogenesis, diagnosis, and management. *Hepatology international,* 4**,** 475-93.

ORLIC, D., KAJSTURA, J., CHIMENTI, S., JAKONIUK, I., ANDERSON, S. M., LI, B., PICKEL, J., MCKAY, R., NADAL-GINARD, B., BODINE, D. M., LERI, A. & ANVERSA, P. 2001. Bone marrow cells regenerate infarcted myocardium. *Nature,* 410**,** 701-5.

ORTIZ, L. A., DUTREIL, M., FATTMAN, C., PANDEY, A. C., TORRES, G., GO, K. & PHINNEY, D. G. 2007. Interleukin 1 receptor antagonist mediates the antiinflammatory and antifibrotic effect of mesenchymal stem cells during lung injury. *Proc Natl Acad Sci U S A,* 104**,** 11002-7.

OSDOBY, P. & CAPLAN, A. I. 1979. Osteogenesis in cultures of limb mesenchymal cells. *Dev Biol,* 73**,** 84-102.

PARKER, R., ARMSTRONG, M. J., CORBETT, C., ROWE, I. A. & HOULIHAN, D. D. 2013. Systematic review: pentoxifylline for the treatment of severe alcoholic hepatitis. *Alimentary pharmacology & therapeutics,* 37**,** 845-54.

PARKIN, J. & COHEN, B. 2001. An overview of the immune system. *Lancet,* 357**,** 1777-89.

PEAT, G., MCCARNEY, R. & CROFT, P. 2001. Knee pain and osteoarthritis in older adults: a review of community burden and current use of primary health care. *Annals of the rheumatic diseases,* 60**,** 91-7.

PEISTER, A., MELLAD, J. A., LARSON, B. L., HALL, B. M., GIBSON, L. F. & PROCKOP, D. J. 2004. Adult stem cells from bone marrow (MSCs) isolated from different strains of inbred mice vary in surface epitopes, rates of proliferation, and differentiation potential. *Blood,* 103**,** 1662-8.

PEK, Y. S., WAN, A. C. & YING, J. Y. 2010. The effect of matrix stiffness on mesenchymal stem cell differentiation in a 3D thixotropic gel. *Biomaterials,* 31**,** 385-91.

PELTTARI, K., STECK, E. & RICHTER, W. 2008. The use of mesenchymal stem cells for chondrogenesis. *Injury,* 39 Suppl 1**,** S58-65.

PETERSEN, B. E., BOWEN, W. C., PATRENE, K. D., MARS, W. M., SULLIVAN, A. K., MURASE, N., BOGGS, S. S., GREENBERGER, J. S. & GOFF, J. P. 1999. Bone marrow as a potential source of hepatic oval cells. *Science,* 284**,** 1168-70.

PHINNEY, D. G., KOPEN, G., ISAACSON, R. L. & PROCKOP, D. J. 1999. Plastic adherent stromal cells from the bone marrow of commonly used strains of inbred mice: variations in yield, growth, and differentiation. *J Cell Biochem,* 72**,** 570-85.

PINHO, S., LACOMBE, J., HANOUN, M., MIZOGUCHI, T., BRUNS, I., KUNISAKI, Y. & FRENETTE, P. S. 2013. PDGFRalpha and CD51 mark human Nestin+ sphere-forming mesenchymal stem cells capable of hematopoietic progenitor cell expansion. *The Journal of experimental medicine,* 210**,** 1351-67.

PITTENGER, M. F., MACKAY, A. M., BECK, S. C., JAISWAL, R. K., DOUGLAS, R., MOSCA, J. D., MOORMAN, M. A., SIMONETTI, D. W., CRAIG, S. & MARSHAK, D. R. 1999. Multilineage potential of adult human mesenchymal stem cells. *Science,* 284**,** 143-7.

PROCKOP, D. J. & OH, J. Y. 2012. Mesenchymal stem/stromal cells (MSCs): role as guardians of inflammation. *Molecular therapy : the journal of the American Society of Gene Therapy,* 20**,** 14-20.

QUIRICI, N., SOLIGO, D., BOSSOLASCO, P., SERVIDA, F., LUMINI, C. & DELILIERS, G. L. 2002. Isolation of bone marrow mesenchymal stem cells by anti-nerve growth factor receptor antibodies. *Exp Hematol,* 30**,** 783-91.

RAFF, T., VAN DER GIET, M., ENDEMANN, D., WIEDERHOLT, T. & PAUL, M. 1997. Design and testing of beta-actin primers for RT-PCR that do not co-amplify processed pseudogenes. *Biotechniques,* 23**,** 456-60.

RAFFAGHELLO, L., BIANCHI, G., BERTOLOTTO, M., MONTECUCCO, F., BUSCA, A., DALLEGRI, F., OTTONELLO, L. & PISTOIA, V. 2008. Human mesenchymal stem cells inhibit neutrophil apoptosis: a model for neutrophil preservation in the bone marrow niche. *Stem Cells,* 26**,** 151-62.

RASMUSSON, I., RINGDEN, O., SUNDBERG, B. & LE BLANC, K. 2003. Mesenchymal stem cells inhibit the formation of cytotoxic T lymphocytes, but not activated cytotoxic T lymphocytes or natural killer cells. *Transplantation,* 76**,** 1208-13.

REN, G., ZHANG, L., ZHAO, X., XU, G., ZHANG, Y., ROBERTS, A. I., ZHAO, R. C. & SHI, Y. 2008. Mesenchymal stem cell-mediated immunosuppression occurs via concerted action of chemokines and nitric oxide. *Cell Stem Cell,* 2**,** 141-50.

REN, H., CAO, Y., ZHAO, Q., LI, J., ZHOU, C., LIAO, L., JIA, M., CAI, H., HAN, Z. C., YANG, R., CHEN, G. & ZHAO, R. C. 2006. Proliferation and differentiation of bone marrow stromal cells under hypoxic conditions. *Biochemical and biophysical research communications,* 347**,** 12-21.

RIOUX, J. D. & ABBAS, A. K. 2005. Paths to understanding the genetic basis of autoimmune disease. *Nature,* 435**,** 584-9.

ROBLEDO, R. F., RAJAN, L., LI, X. & LUFKIN, T. 2002. The Dlx5 and Dlx6 homeobox genes are essential for craniofacial, axial, and appendicular skeletal development. *Genes Dev,* 16**,** 1089-101.

RODEHEFFER, M. S., BIRSOY, K. & FRIEDMAN, J. M. 2008. Identification of white adipocyte progenitor cells in vivo. *Cell,* 135**,** 240-9.

ROMBOUTS, W. J. & PLOEMACHER, R. E. 2003. Primary murine MSC show highly efficient homing to the bone marrow but lose homing ability following culture. *Leukemia,* 17**,** 160-70.

ROSEN, E. D. & MACDOUGALD, O. A. 2006. Adipocyte differentiation from the inside out. *Nat Rev Mol Cell Biol,* 7**,** 885-96.

ROSLAND, G. V., SVENDSEN, A., TORSVIK, A., SOBALA, E., MCCORMACK, E., IMMERVOLL, H., MYSLIWIETZ, J., TONN, J. C., GOLDBRUNNER, R., LONNING, P. E., BJERKVIG, R. & SCHICHOR, C. 2009. Long-term cultures of bone marrow-derived human mesenchymal stem cells frequently undergo spontaneous malignant transformation. *Cancer research,* 69**,** 5331-9.

RUSSO, F. P., ALISON, M. R., BIGGER, B. W., AMOFAH, E., FLOROU, A., AMIN, F., BOU-GHARIOS, G., JEFFERY, R., IREDALE, J. P. & FORBES, S. J.

2006. The bone marrow functionally contributes to liver fibrosis. *Gastroenterology,* 130**,** 1807-21.

RYAN, J. M., BARRY, F., MURPHY, J. M. & MAHON, B. P. 2007. Interferon-gamma does not break, but promotes the immunosuppressive capacity of adult human mesenchymal stem cells. *Clinical and experimental immunology,* 149**,** 353-63.

SACCHETTI, B., FUNARI, A., MICHIENZI, S., DI CESARE, S., PIERSANTI, S., SAGGIO, I., TAGLIAFICO, E., FERRARI, S., ROBEY, P. G., RIMINUCCI, M. & BIANCO, P. 2007. Self-renewing osteoprogenitors in bone marrow sinusoids can organize a hematopoietic microenvironment. *Cell,* 131**,** 324-36.

SAJIC, M., HUNT, D. P., LEE, W., COMPSTON, D. A., SCHWEIMER, J. V., GREGSON, N. A., CHANDRAN, S. & SMITH, K. J. 2012. Mesenchymal stem cells lack efficacy in the treatment of experimental autoimmune neuritis despite in vitro inhibition of T-cell proliferation. *PLoS One,* 7**,** e30708.

SALLUSTO, F., LENIG, D., FORSTER, R., LIPP, M. & LANZAVECCHIA, A. 1999. Two subsets of memory T lymphocytes with distinct homing potentials and effector functions. *Nature,* 401**,** 708-12.

SALVAT, C., PIGENET, A., HUMBERT, L., BERENBAUM, F. & THIRION, S. 2005. Immature murine articular chondrocytes in primary culture: a new tool for investigating cartilage. *Osteoarthritis and Cartilage,* 13**,** 243-249.

SAMPATH, T. K. & REDDI, A. H. 1981. Dissociative extraction and reconstitution of extracellular matrix components involved in local bone differentiation. *Proc Natl Acad Sci U S A,* 78**,** 7599-603.

SATO, K., OZAKI, K., OH, I., MEGURO, A., HATANAKA, K., NAGAI, T., MUROI, K. & OZAWA, K. 2007. Nitric oxide plays a critical role in suppression of T-cell proliferation by mesenchymal stem cells. *Blood,* 109**,** 228-34.

SATOKATA, I., MA, L., OHSHIMA, H., BEI, M., WOO, I., NISHIZAWA, K., MAEDA, T., TAKANO, Y., UCHIYAMA, M., HEANEY, S., PETERS, H., TANG, Z., MAXSON, R. & MAAS, R. 2000. Msx2 deficiency in mice causes pleiotropic defects in bone growth and ectodermal organ formation. *Nat Genet,* 24**,** 391-5.

SCHMID-SCHONBEIN, G. W. 1990. Microlymphatics and lymph flow. *Physiological reviews,* 70**,** 987-1028.

SCHROEDER, M. A. & DIPERSIO, J. F. 2011. Mouse models of graft-versus-host disease: advances and limitations. *Dis Model Mech,* 4**,** 318-33.

SEGHATOLESLAMI, M. R., ROMAN-BLAS, J. A., RAINVILLE, A. M., MODARESSI, R., DANIELSON, K. G. & TUAN, R. S. 2003. Progression of chondrogenesis in C3H10T1/2 cells is associated with prolonged and tight regulation of ERK1/2. *J Cell Biochem,* 88**,** 1129-44.

SEKIYA, I., LARSON, B. L., VUORISTO, J. T., REGER, R. L. & PROCKOP, D. J. 2005. Comparison of effect of BMP-2, -4, and -6 on in vitro cartilage formation of human adult stem cells from bone marrow stroma. *Cell and tissue research,* 320**,** 269-76.

SELMANI, Z., NAJI, A., ZIDI, I., FAVIER, B., GAIFFE, E., OBERT, L., BORG, C., SAAS, P., TIBERGHIEN, P., ROUAS-FREISS, N., CAROSELLA, E. D. & DESCHASEAUX, F. 2008. Human leukocyte antigen-G5 secretion by human mesenchymal stem cells is required to suppress T lymphocyte and natural killer function and to induce CD4+CD25highFOXP3+ regulatory T cells. *Stem Cells,* 26**,** 212-22.

SHI, Y., SU, J., ROBERTS, A. I., SHOU, P., RABSON, A. B. & REN, G. 2012. How mesenchymal stem cells interact with tissue immune responses. *Trends in immunology,* 33**,** 136-43.

SHOSHANI, O., MASSALHA, H., SHANI, N., KAGAN, S., RAVID, O., MADAR, S., TRAKHTENBROT, L., LESHKOWITZ, D., RECHAVI, G. & ZIPORI, D. 2012.

Polyploidization of murine mesenchymal cells is associated with suppression of the long noncoding RNA H19 and reduced tumorigenicity. *Cancer Res,* 72**,** 6403-13.

SILLENCE, D. O., SENN, A. & DANKS, D. M. 1979. Genetic heterogeneity in osteogenesis imperfecta. *Journal of medical genetics,* 16**,** 101-16.

SIMMONS, P. J. & TOROK-STORB, B. 1991. Identification of stromal cell precursors in human bone marrow by a novel monoclonal antibody, STRO-1. *Blood,* 78**,** 55-62.

SMELTER, E. & HOCHBERG, M. C. 2013. New treatments for osteoarthritis. *Current opinion in rheumatology,* 25**,** 310-6.

SOLEIMANI, M. & NADRI, S. 2009. A protocol for isolation and culture of mesenchymal stem cells from mouse bone marrow. *Nature Protocols,* 4**,** 102-6.

SPAGGIARI, G. M., CAPOBIANCO, A., BECCHETTI, S., MINGARI, M. C. & MORETTA, L. 2006. Mesenchymal stem cell-natural killer cell interactions: evidence that activated NK cells are capable of killing MSCs, whereas MSCs can inhibit IL-2-induced NK-cell proliferation. *Blood,* 107**,** 1484-90.

STAPPENBECK, T. S. & MIYOSHI, H. 2009. The role of stromal stem cells in tissue regeneration and wound repair. *Science,* 324**,** 1666-9.

SUDRES, M., NOROL, F., TRENADO, A., GREGOIRE, S., CHARLOTTE, F., LEVACHER, B., LATAILLADE, J. J., BOURIN, P., HOLY, X., VERNANT, J. P., KLATZMANN, D. & COHEN, J. L. 2006. Bone marrow mesenchymal stem cells suppress lymphocyte proliferation in vitro but fail to prevent graft-versus-host disease in mice. *Journal of immunology,* 176**,** 7761-7.

SUH, J. M., GAO, X., MCKAY, J., MCKAY, R., SALO, Z. & GRAFF, J. M. 2006. Hedgehog signaling plays a conserved role in inhibiting fat formation. *Cell Metab,* 3**,** 25-34.

TAKASHIMA, Y., ERA, T., NAKAO, K., KONDO, S., KASUGA, M., SMITH, A. G. & NISHIKAWA, S. 2007. Neuroepithelial cells supply an initial transient wave of MSC differentiation. *Cell,* 129**,** 1377-88.

TAKEDA, K., KAISHO, T. & AKIRA, S. 2003. Toll-like receptors. *Annual review of immunology,* 21**,** 335-76.

TANG, Q. Q., OTTO, T. C. & LANE, M. D. 2004. Commitment of C3H10T1/2 pluripotent stem cells to the adipocyte lineage. *Proc Natl Acad Sci U S A,* 101**,** 9607-11.

TANG, W., ZEVE, D., SUH, J. M., BOSNAKOVSKI, D., KYBA, M., HAMMER, R. E., TALLQUIST, M. D. & GRAFF, J. M. 2008. White fat progenitor cells reside in the adipose vasculature. *Science,* 322**,** 583-6.

TAO, X. R., LI, W. L., SU, J., JIN, C. X., WANG, X. M., LI, J. X., HU, J. K., XIANG, Z. H., LAU, J. T. & HU, Y. P. 2009. Clonal mesenchymal stem cells derived from human bone marrow can differentiate into hepatocyte-like cells in injured livers of SCID mice. *Journal of cellular biochemistry,* 108**,** 693-704.

THANKAMONY, S. P. & SACKSTEIN, R. 2011. Enforced hematopoietic cell E- and L-selectin ligand (HCELL) expression primes transendothelial migration of human mesenchymal stem cells. *Proceedings of the National Academy of Sciences of the United States of America,* 108**,** 2258-63.

TICKLE, C. 2003. Patterning systems--from one end of the limb to the other. *Dev Cell,* 4**,** 449-58.

TOLAR, J., NAUTA, A. J., OSBORN, M. J., PANOSKALTSIS MORTARI, A., MCELMURRY, R. T., BELL, S., XIA, L., ZHOU, N., RIDDLE, M., SCHROEDER, T. M., WESTENDORF, J. J., MCIVOR, R. S., HOGENDOORN, P. C., SZUHAI, K., OSETH, L., HIRSCH, B., YANT, S. R., KAY, M. A., PEISTER, A., PROCKOP, D. J., FIBBE, W. E. & BLAZAR, B. R. 2007. Sarcoma derived from cultured mesenchymal stem cells. *Stem Cells,* 25**,** 371-9.

TOMCHUCK, S. L., ZWEZDARYK, K. J., COFFELT, S. B., WATERMAN, R. S., DANKA, E. S. & SCANDURRO, A. B. 2008. Toll-like receptors on human mesenchymal stem cells drive their migration and immunomodulating responses. *Stem Cells,* 26**,** 99-107.

TONG, Q., TSAI, J., TAN, G., DALGIN, G. & HOTAMISLIGIL, G. S. 2005. Interaction between GATA and the C/EBP family of transcription factors is critical in GATA-mediated suppression of adipocyte differentiation. *Mol Cell Biol,* 25**,** 706-15.

TONTONOZ, P., HU, E. & SPIEGELMAN, B. M. 1994. Stimulation of adipogenesis in fibroblasts by PPAR gamma 2, a lipid-activated transcription factor. *Cell,* 79**,** 1147-56.

TONTONOZ, P. & SPIEGELMAN, B. M. 2008. Fat and beyond: the diverse biology of PPARgamma. *Annual review of biochemistry,* 77**,** 289-312.

TORMIN, A., LI, O., BRUNE, J. C., WALSH, S., SCHUTZ, B., EHINGER, M., DITZEL, N., KASSEM, M. & SCHEDING, S. 2011. CD146 expression on primary nonhematopoietic bone marrow stem cells is correlated with in situ localization. *Blood,* 117**,** 5067-77.

UCCELLI, A., MORETTA, L. & PISTOIA, V. 2008. Mesenchymal stem cells in health and disease. *Nat Rev Immunol,* 8**,** 726-36.

VAN VLASSELAER, P., FALLA, N., SNOECK, H. & MATHIEU, E. 1994. Characterization and purification of osteogenic cells from murine bone marrow by two-color cell sorting using anti-Sca-1 monoclonal antibody and wheat germ agglutinin. *Blood,* 84**,** 753-63.

VILLENA, J. A., KIM, K. H. & SUL, H. S. 2002. Pref-1 and ADSF/resistin: two secreted factors inhibiting adipose tissue development. *Horm Metab Res,* 34**,** 664-70.

VOGEL, G. 2013. Trachea transplants test the limits. *Science,* 340**,** 266-8.

VON ANDRIAN, U. H. & MEMPEL, T. R. 2003. Homing and cellular traffic in lymph nodes. *Nature reviews. Immunology,* 3**,** 867-78.

WAGNER, T., WIRTH, J., MEYER, J., ZABEL, B., HELD, M., ZIMMER, J., PASANTES, J., BRICARELLI, F. D., KEUTEL, J., HUSTERT, E., WOLF, U., TOMMERUP, N., SCHEMPP, W. & SCHERER, G. 1994. Autosomal sex reversal and campomelic dysplasia are caused by mutations in and around the SRY-related gene SOX9. *Cell,* 79**,** 1111-20.

WAGNER, W., HORN, P., CASTOLDI, M., DIEHLMANN, A., BORK, S., SAFFRICH, R., BENES, V., BLAKE, J., PFISTER, S., ECKSTEIN, V. & HO, A. D. 2008. Replicative senescence of mesenchymal stem cells: a continuous and organized process. *PLoS One,* 3**,** e2213.

WAKITANI, S., NAWATA, M., TENSHO, K., OKABE, T., MACHIDA, H. & OHGUSHI, H. 2007. Repair of articular cartilage defects in the patello-femoral joint with autologous bone marrow mesenchymal cell transplantation: three case reports involving nine defects in five knees. *Journal of tissue engineering and regenerative medicine,* 1**,** 74-9.

WAN, M. & CAO, X. 2005. BMP signaling in skeletal development. *Biochem Biophys Res Commun,* 328**,** 651-7.

WANG, E. A., ISRAEL, D. I., KELLY, S. & LUXENBERG, D. P. 1993. Bone morphogenetic protein-2 causes commitment and differentiation in C3H10T1/2 and 3T3 cells. *Growth Factors,* 9**,** 57-71.

WATERMAN, R. S., TOMCHUCK, S. L., HENKLE, S. L. & BETANCOURT, A. M. 2010. A new mesenchymal stem cell (MSC) paradigm: polarization into a pro-inflammatory MSC1 or an Immunosuppressive MSC2 phenotype. *PLoS One,* 5**,** e10088.

WIEST, R. & GARCIA-TSAO, G. 2005. Bacterial translocation (BT) in cirrhosis. *Hepatology,* 41**,** 422-33.

WILLIAMS, A. J. & BARRY, R. E. 1987. Free radical generation by neutrophils: a potential mechanism of cellular injury in acute alcoholic hepatitis. *Gut,* 28**,** 1157-61.

WILSON, A. & TRUMPP, A. 2006. Bone-marrow haematopoietic-stem-cell niches. *Nat Rev Immunol,* 6**,** 93-106.

WRIGHT, E., HARGRAVE, M. R., CHRISTIANSEN, J., COOPER, L., KUN, J., EVANS, T., GANGADHARAN, U., GREENFIELD, A. & KOOPMAN, P. 1995. The Sry-related gene Sox9 is expressed during chondrogenesis in mouse embryos. *Nature genetics,* 9**,** 15-20.

YAMACHIKA, E., TSUJIGIWA, H., MATSUBARA, M., HIRATA, Y., KITA, K., TAKABATAKE, K., MIZUKAWA, N., KANEDA, Y., NAGATSUKA, H. & IIDA, S. 2012. Basic fibroblast growth factor supports expansion of mouse compact bone-derived mesenchymal stem cells (MSCs) and regeneration of bone from MSC in vivo. *Journal of molecular histology,* 43**,** 223-33.

YAMAZAKI, S., EMA, H., KARLSSON, G., YAMAGUCHI, T., MIYOSHI, H., SHIODA, S., TAKETO, M. M., KARLSSON, S., IWAMA, A. & NAKAUCHI, H. 2011. Nonmyelinating Schwann cells maintain hematopoietic stem cell hibernation in the bone marrow niche. *Cell,* 147**,** 1146-58.

YEN, B. L., HUANG, H. I., CHIEN, C. C., JUI, H. Y., KO, B. S., YAO, M., SHUN, C. T., YEN, M. L., LEE, M. C. & CHEN, Y. C. 2005. Isolation of multipotent cells from human term placenta. *Stem Cells,* 23**,** 3-9.

YOON, B. S., OVCHINNIKOV, D. A., YOSHII, I., MISHINA, Y., BEHRINGER, R. R. & LYONS, K. M. 2005. Bmpr1a and Bmpr1b have overlapping functions and are essential for chondrogenesis in vivo. *Proc Natl Acad Sci U S A,* 102**,** 5062-7.

YOSHIDA, C. A., FURUICHI, T., FUJITA, T., FUKUYAMA, R., KANATANI, N., KOBAYASHI, S., SATAKE, M., TAKADA, K. & KOMORI, T. 2002. Core-binding factor beta interacts with Runx2 and is required for skeletal development. *Nat Genet,* 32**,** 633-8.

ZAPPIA, E., CASAZZA, S., PEDEMONTE, E., BENVENUTO, F., BONANNI, I., GERDONI, E., GIUNTI, D., CERAVOLO, A., CAZZANTI, F., FRASSONI, F., MANCARDI, G. & UCCELLI, A. 2005. Mesenchymal stem cells ameliorate experimental autoimmune encephalomyelitis inducing T-cell anergy. *Blood,* 106**,** 1755-61.

ZHAO, L. & HANTASH, B. M. 2011. TGF-beta1 regulates differentiation of bone marrow mesenchymal stem cells. *Vitamins and hormones,* 87**,** 127-41.

ZHAO, X. J., DONG, Q., BINDAS, J., PIGANELLI, J. D., MAGILL, A., REISER, J. & KOLLS, J. K. 2008. TRIF and IRF-3 binding to the TNF promoter results in macrophage TNF dysregulation and steatosis induced by chronic ethanol. *Journal of immunology,* 181**,** 3049-56.

ZHOU, Y. F., BOSCH-MARCE, M., OKUYAMA, H., KRISHNAMACHARY, B., KIMURA, H., ZHANG, L., HUSO, D. L. & SEMENZA, G. L. 2006. Spontaneous transformation of cultured mouse bone marrow-derived stromal cells. *Cancer Res,* 66**,** 10849-54.

ZHU, H., GUO, Z.-K., JIANG, X.-X., LI, H., WANG, X.-Y., YAO, H.-Y., ZHANG, Y. & MAO, N. 2010. A protocol for isolation and culture of mesenchymal stem cells from mouse compact bone. *Nature Protocols,* 5**,** 550-60.

ZVAIFLER, N. J., MARINOVA-MUTAFCHIEVA, L., ADAMS, G., EDWARDS, C. J., MOSS, J., BURGER, J. A. & MAINI, R. N. 2000. Mesenchymal precursor cells in the blood of normal individuals. *Arthritis research,* 2**,** 477-88.

**APPENDIX 1-** List of genes that were significantly up or down regulated in the treatment groups compared to SM

| GeneID | Symbol | Description | FGF Fold.Change | PDGF Fold.Change | TGFb Fold.Change |
|---|---|---|---|---|---|
| 11450 | Adipoq | adiponectin, C1Q and collagen domain containing | 27.50 | 11.66 | -3.22 |
| 11647 | Alpl | alkaline phosphatase, liver/bone/kidney | -3.08 | -5.69 | -20.04 |
| 11754 | Aoc3 | amine oxidase, copper containing 3 | 2.17 | 1.15 | -3.86 |
| 11770 | Fabp4 | fatty acid binding protein 4, adipocyte | 8.85 | 4.80 | -2.24 |
| 11799 | Birc5 | baculoviral IAP repeat-containing 5 | 1.51 | 1.71 | 1.17 |
| 11816 | Apoe | apolipoprotein E | 3.32 | 1.95 | -1.43 |
| 11832 | Aqp7 | aquaporin 7 | 27.09 | 10.20 | -1.74 |
| 12156 | Bmp2 | bone morphogenetic protein 2 | 33.49 | 2.93 | 2.89 |
| 12159 | Bmp4 | bone morphogenetic protein 4 | -20.15 | -8.20 | -3.99 |
| 12161 | Bmp6 | bone morphogenetic protein 6 | -2.44 | -1.15 | -1.39 |
| 12167 | Bmpr1b | bone morphogenetic protein receptor, type 1B | -2.66 | 1.10 | 2.46 |
| 12182 | Bst1 | bone marrow stromal cell antigen 1 | -10.85 | -7.09 | -10.06 |
| 12484 | Cd24a | CD24a antigen | 1.52 | 1.32 | -1.76 |
| 12606 | Cebpa | CCAAT/enhancer binding protein (C/EBP), alpha | 2.55 | 1.70 | -3.33 |
| 12609 | Cebpd | CCAAT/enhancer binding protein (C/EBP), delta | -1.72 | -1.92 | -1.38 |
| 12813 | Col10a1 | collagen, type X, | 1.06 | 4.16 | -2.23 |

| | | | | | |
|---|---|---|---|---|---|
| | | alpha 1 | | | |
| 12814 | Col11a1 | collagen, type XI, alpha 1 | -2.55 | -2.33 | 2.44 |
| 12834 | Col6a2 | collagen, type VI, alpha 2 | 1.10 | 1.07 | -1.94 |
| 12842 | Col1a1 | collagen, type I, alpha 1 | -6.28 | -2.27 | 1.20 |
| 12843 | Col1a2 | collagen, type I, alpha 2 | -3.23 | -1.68 | 1.28 |
| 12845 | Comp | cartilage oligomeric matrix protein | -4.54 | -2.63 | -3.19 |
| 13380 | Dkk1 | dickkopf homolog 1 (Xenopus laevis) | 1.55 | 1.13 | 1.10 |
| 13386 | Dlk1 | delta-like 1 homolog (Drosophila) | 11.07 | 5.09 | -2.06 |
| 13395 | Dlx5 | distal-less homeobox 5 | -2.76 | -1.63 | -1.40 |
| 13805 | Eng | endoglin | -1.93 | -1.61 | -1.06 |
| 13865 | Nr2f1 | nuclear receptor subfamily 2, group F, member 1 | 4.31 | 1.47 | 1.20 |
| 14164 | Fgf1 | fibroblast growth factor 1 | 1.60 | 1.39 | 1.30 |
| 14165 | Fgf10 | fibroblast growth factor 10 | 2.16 | 3.00 | -4.98 |
| 14183 | Fgfr2 | fibroblast growth factor receptor 2 | -4.12 | -2.63 | -6.97 |
| 14184 | Fgfr3 | fibroblast growth factor receptor 3 | -1.47 | -1.54 | -1.66 |
| 14461 | Gata2 | GATA binding protein 2 | 1.56 | 1.38 | -1.11 |
| 14462 | Gata3 | GATA binding protein 3 | 1.28 | 2.15 | 1.09 |
| 14465 | Gata6 | GATA binding protein 6 | 1.90 | 2.05 | 1.56 |
| 14555 | Gpd1 | glycerol-3-phosphate dehydrogenase 1 (soluble) | 25.26 | 5.75 | -1.32 |
| 15398 | Hoxa13 | homeobox A13 | -1.73 | -1.18 | -1.46 |
| 15402 | Hoxa5 | homeobox A5 | 1.92 | 1.09 | -1.10 |
| 15891 | Ibsp | integrin binding sialoprotein | -5.15 | -4.28 | -5.37 |
| 16000 | Igf1 | insulin-like growth factor 1 | -4.63 | -6.59 | -1.64 |
| 16173 | Il18 | interleukin 18 | -1.32 | -1.51 | -1.81 |
| 16193 | Il6 | interleukin 6 | -19.29 | -5.78 | -2.95 |
| 16878 | Lif | leukemia inhibitory factor | -1.17 | -1.22 | 5.93 |
| 16880 | Lifr | leukemia inhibitory factor receptor | -2.01 | -2.44 | -3.29 |
| 16956 | Lpl | lipoprotein lipase | 2.76 | 1.69 | -27.46 |

| | | | | | |
|---|---|---|---|---|---|
| 16973 | Lrp5 | low density lipoprotein receptor-related protein 5 | 1.65 | -1.14 | -1.25 |
| 17258 | Mef2a | myocyte enhancer factor 2A | 1.11 | -1.03 | -1.53 |
| 17260 | Mef2c | myocyte enhancer factor 2C | -1.14 | 1.38 | -1.98 |
| 17311 | Kitl | kit ligand | -1.07 | 1.45 | -10.27 |
| 17470 | Cd200 | CD200 antigen | 5.67 | 1.07 | 5.63 |
| 18295 | Ogn | osteoglycin | -6.13 | -1.30 | -1.42 |
| 18595 | Pdgfra | platelet derived growth factor receptor, alpha polypeptide | 1.62 | 1.79 | -1.50 |
| 18596 | Pdgfrb | platelet derived growth factor receptor, beta polypeptide | -1.77 | -1.33 | 1.17 |
| 19016 | Pparg | peroxisome proliferator activated receptor gamma | 4.53 | 2.97 | -3.24 |
| 19228 | Pth1r | parathyroid hormone 1 receptor | -1.65 | -2.36 | -1.44 |
| 20181 | Rxra | retinoid X receptor alpha | 1.24 | 1.03 | -1.53 |
| 20319 | Sfrp2 | secreted frizzled-related protein 2 | -79.67 | -7.34 | -89.78 |
| 20429 | Shox2 | short stature homeobox 2 | 1.14 | 1.15 | 1.53 |
| 20674 | Sox2 | SRY-box containing gene 2 | 7.39 | 1.16 | 1.19 |
| 20678 | Sox5 | SRY-box containing gene 5 | 4.56 | 3.28 | 1.05 |
| 20750 | Spp1 | secreted phosphoprotein 1 | 1.73 | 1.57 | 1.49 |
| 20787 | Srebf1 | sterol regulatory element binding transcription factor 1 | 2.47 | 1.12 | 1.25 |
| 21418 | Tfap2a | transcription factor AP-2, alpha | 1.98 | 1.50 | 1.12 |
| 21812 | Tgfbr1 | transforming growth factor, beta receptor I | 1.42 | -1.25 | -1.60 |
| 21813 | Tgfbr2 | transforming growth factor, beta receptor II | -1.62 | -1.34 | 1.05 |
| 21814 | Tgfbr3 | transforming growth factor, beta receptor III | 1.34 | 1.28 | -2.43 |
| 22402 | Wisp1 | WNT1 inducible signaling | -9.65 | -5.13 | 2.25 |

| | | | | | |
|---|---|---|---|---|---|
| | | pathway protein 1 | | | |
| 22403 | Wisp2 | WNT1 inducible signaling pathway protein 2 | -6.24 | -2.12 | -1.65 |
| 22413 | Wnt2 | wingless-related MMTV integration site 2 | -3.37 | -1.65 | -3.19 |
| 23959 | Nt5e | 5' nucleotidase, ecto | 2.19 | 1.13 | 7.95 |
| 24059 | Slco2a1 | solute carrier organic anion transporter family, member 2a1 | 2.03 | 4.87 | -1.24 |
| 27279 | Tnfrsf12a | tumor necrosis factor receptor superfamily, member 12a | -1.25 | 1.45 | 1.87 |
| 71436 | Flrt3 | fibronectin leucine rich transmembrane protein 3 | 2.50 | -1.62 | 1.15 |
| 77037 | Mrap | melanocortin 2 receptor accessory protein | 2.36 | 1.13 | 1.11 |
| 103968 | Plin1 | perilipin 1 | 24.26 | 8.11 | -1.23 |
| 116701 | Fgfrl1 | fibroblast growth factor receptor-like 1 | 1.54 | -1.02 | -1.64 |
| 121021 | Cspg4 | chondroitin sulfate proteoglycan 4 | 1.56 | 2.54 | 2.91 |
| 211323 | Nrg1 | neuregulin 1 | -4.77 | -2.26 | 1.63 |
| 235320 | Zbtb16 | zinc finger and BTB domain containing 16 | 2.32 | 1.71 | -1.05 |

**APPENDIX 2 –** Published manuscripts in relation to the PhD

Mabuchi Y, Morikawa S, Harada S, Niibe K, Suzuki S, Renault-Mihara F, Houlihan DD, Akazawa C, Okano H, Matsuzaki Y. LNGFR$^{+}$THY-1$^{+}$VCAM-1$^{hi+}$ Cells Reveal Functionally Distinct Subpopulations in Mesenchymal Stem Cells. **Stem Cell Reports**. **2013** [online 11 July 2013].

Mabuchi Y, Houlihan DD, Akazawa C, Okano H, Matsuzaki Y. Prospective isolation of murine and human bone marrow mesenchymal stem cells based on surface markers. **Stem Cells Int. 2013**;2013:507301.

Houlihan DD, Mabuchi Y, Morikawa S, Niibe K, Araki D, Suzuki S, Okano H, Matsuzaki Y. Isolation of mouse mesenchymal stem cells on the basis of expression of Sca-1 and PDGFR-α. **Nat Protoc. 2012**;7(12):2103-11.

Houlihan DD, Hopkins LJ, Suresh SX, Armstrong MJ, Newsome PN. Autologous bone marrow mesenchymal stem cell transplantation in liver failure patients caused by hepatitis B: short-term and long-term outcomes. **Hepatology. 2011**;54(5):1891-2. Letter.

Houlihan DD, Newsome PN. Critical review of clinical trials of bone marrow stem cells in liver disease. **Gastroenterology. 2008**;135(2):438-50. Review.